Nondeterministic Linear Static Finite Element Analysis: An Interval Approach

A Thesis
Presented to
The Academic Faculty

by

Hao Zhang

In Partial Fulfillment
of the Requirements for the Degree
Doctor of Philosophy

School of Civil and Environmental Engineering
Georgia Institute of Technology
December 2005

Nondeterministic Linear Static Finite Element Analysis: An Interval Approach

Approved by:

Dr. Rafi L. Muhanna, Advisor
School of Civil and Environmental Engineering
Georgia Institute of Technology

Dr. Donald White
School of Civil and Environmental Engineering
Georgia Institute of Technology

Dr. Rami Haj-Ali
School of Civil and Environmental Engineering
Georgia Institute of Technology

Dr. Kenneth Will
School of Civil and Environmental Engineering
Georgia Institute of Technology

Dr. Dewey Hodges
School of Aerospace Engineering
Georgia Institute of Technology

Dr. Abdul Hamid Zureick
School of Civil and Environmental Engineering
Georgia Institute of Technology

Date Approved: August 18, 2005

To my parents

and to Yan Jiang

ACKNOWLEDGEMENTS

First and foremost, I would like to express my deep gratitude to my advisor, Dr. Rafi Muhanna, for the many hours of excellent guidance, for providing me with excellent facilities, and for ensuring financial support throughout my Ph.D. studies. It is his support that has been the key to my academic and personal growth over the past four years. I am grateful to him for his contributions, not just to this thesis, but also to making me a better researcher and a better person.

I also wish to thank the other faculty of Georgia Institute of Technology, most notably my committee members, Dr. Dewey Hodges, Dr. Donald White, Dr. Kenneth Will, Dr. Abdul Hamid Zureick and Dr. Rami Haj-Ali, for their suggestions on my thesis and valuable time serving as my advisory committee. I would also like to thank Dr. Robert Mullen in Case Western Reserve University for his valuable comments on my thesis. I am also grateful to Dr. Andrzej Pownuk, Silesian University of Technology, for providing me the program of sensitivity analysis method. I am also grateful to Jillison Parks for proofreading my thesis.

I am indebted to many of my colleagues and friends, especially Mingfang He, Ruiting Wu, Tianyi Yi, Min Pei and Quangwang Li for providing a constant source of encouragement and support, and for being there for me at all times.

Finally, I would like to thank my parents and wife for their help, encouragement and prayers through all these years. I dedicate my work to them.

TABLE OF CONTENTS

LIST OF TABLES

LIST OF FIGURES

SUMMARY

This thesis presents a nontraditional treatment for uncertainties in the material, geometry, and load parameters in linear static finite element analysis (FEA) for mechanics problems. Uncertainties are introduced as bounded possible values (intervals). FEA with interval parameters (interval FEA, IFEA) estimates the range of the system response based on the bounds of the system parameters. The obtained results should be accurate and efficiently computed. Toward this end, a rigorous interval FEA is developed and implemented.

In this study, interval arithmetic is used in the formulation to guarantee an enclosure for the response range. The major difficulty associated with interval computation is the dependence problem, which results in severe overestimation of the system response ranges. Particular attention in the development of the present method is given to control the dependence problem for sharp results. The developed method is based on an Element-By-Element (EBE) technique. By using the EBE technique, the interval parameters can be handled more efficiently to control the dependence problem. The penalty method and the Lagrange multiplier method are used to impose the necessary constraints for compatibility and equilibrium. The resulting structural equations comprise a system of parametric linear interval equations. The standard fixed point iteration is modified, enhanced, and used to solve the interval equations accurately and efficiently. The newly developed dependence control algorithm ensures the convergence of the fixed point iteration even for problems with relatively large uncertainties. Further, special algorithms have been developed to calculate sharp results for stress and element nodal force. The present method is generally applicable

to linear static interval FEA, regardless of element type.

Numerical examples are presented to demonstrate the capabilities of the developed method. It is illustrated that the present method yields accurate results which are guaranteed to enclose the true response ranges in all the problems considered, including those with a large number of interval variables (e.g., more than 250). The scalability of the present method is also illustrated. In addition to its accuracy, rigorousness and scalability, the efficiency of the present method is also significantly superior to previous methods such as the combinatorial, the sensitivity analysis, and the Monte Carlo sampling method.

CHAPTER 1

INTRODUCTION

In recent years, there has been an increased interest in the modeling and analysis of engineered systems under uncertainties. The interest stems from the fact that numerous sources of uncertainties exist in reality and arise in the modeling and analysis process. Some of these uncertainties stem from factors that are inherently random (or aleatory). Others arise from a lack of knowledge (or epistemic). Computational solid and structural mechanics, for example, entails uncertainties in the geometry, material and load parameters as well as in the model itself and in the analysis procedure. As an inevitable consequence of these uncertainties, the responses of the mechanical system, such as displacement, stress and vibration frequencies, will always exhibit some degree of uncertainty. Even though significant effort may be needed to incorporate uncertainties into the modeling and analysis process, this results in providing useful information that can aid in decision making.

Probabilistic modeling and statistical analysis is well-established for uncertainty modeling and uncertainty propagation. This approach can describe uncertainty arising from stochastic disturbance. In addition, a number of non-probabilistic approaches have been proposed recently, including fuzzy set theory and possibility theory (Zadeh, 1965; **?**), interval approach (Moore, 1966), Dempster-Shafer theory of evidence (Dempster, 1967; Shafer, 1976), random set theory (Kendall, 1974), probability bounds approach (Berleant, 1993; Ferson and Ginzburg, 1996; Ferson et al., 2003), imprecise probabilities (Walley, 1991), convex model (Ben-Haim and Elishakoff, 1990), and others. The growing interest in non-probabilistic approaches originated from criticism of the credibility of probabilistic approach when data is insufficient. It is

argued that the non-probabilistic approaches could be more appropriate in modeling certain types of nondeterministic information, resulting in a better representation of the simulated physical behavior.

In this thesis, interval approach is used to describe the parameter uncertainties of structures. The uncertainty is assumed to be unknown but bounded, and it has lower and upper bounds without assigning a probability structure.

The finite element analysis (FEA) is currently the dominant tool for analysis of structural behavior. This thesis studies the FEA of structures with interval parameters. Such an analysis is referred to as *Interval FEA* (IFEA). The objective of interval FEA is to obtain a rigorous sharp enclosure (outer bounds) for the ranges of structural responses. The interval FEA provides a treatment for problems where

1. no information can be defined beyond lower and upper bounds for system parameters;

2. rapid analysis of the response ranges are desired.

It is the aim of this thesis to develop an efficient computational framework for FEA of structures with interval parameters. The attention is restricted to the static analysis of linear elastic structures only.

As an introduction, this chapter describes the necessary background information to put into context the research conducted in this thesis. First, a classification of uncertainties is presented. Then, the probabilistic approach, fuzzy set theory and interval approach are discussed. This is followed by an introduction of FEA of structures with interval parameters. Finally, the chapter is concluded with the objectives and organization of the thesis.

1.1 Aleatory and Epistemic Uncertainty

There are various ways in which the types of uncertainty might be classified. It is common in engineering practice to distinguish between "aleatory" uncertainty and "epistemic" uncertainty (e.g., Melchers, 1999; Ferson and Ginzburg, 1996; Paté-Cornell, 1996; Helton and Burmaster, 1996; Hora, 1996).

Aleatory uncertainty refers to underlying, intrinsic variabilities of physical quantities. It is not due to a lack of knowledge and cannot be reduced. Aleatory uncertainty is also termed as type A uncertainty, stochastic uncertainty, variability, irreducible uncertainty, or objective uncertainty. Ideally, objective information on both the range and the likelihood of the quantity within this range is available. Aleatory uncertainty is generally quantified by a probability or frequency distribution when sufficient information is available to estimate the distribution.

Epistemic uncertainty refers to uncertainty which results from the lack of knowledge or incomplete information. In contrast with aleatory uncertainty, epistemic uncertainty might be reduced with additional data or information, or better modeling and better parameter estimation. It is also termed as type B uncertainty, ignorance, incertitude, reducible uncertainty or subjective uncertainty. The fundamental cause of epistemic uncertainty is incomplete knowledge. Sources of incomplete information, including vagueness, nonspecificity, and dissonance, are summarized in Table 1.1 (Klier and Folger, 1998). Examples of epistemic uncertainty are:

- statistical uncertainty due to lack of sufficient data,
- a range of possible values of a physical quantity provided by expert opinion,
- model uncertainty due to limited understanding of complex physical processes.

Table 1.1: Incomplete information definitions (Klier and Folger, 1998).

Type	Definition
Vagueness	The information that is imprecisely defined, unclear, or indistinct (characteristic of communication by language).
Nonspecificity	The variety of alternatives in a given situation that are all possible, i.e., not specified.
Dissonance	The existence of totally or partially conflicting evidence.

1.2 Approaches for Representation of Uncertainty

The distinction between epistemic uncertainty and aleatory uncertainty is important when determining how each should be described mathematically and propagated through the analysis. While probabilistic approach is widely accepted to represent aleatory uncertainty, the use of probabilistic approach for representation of epistemic uncertainty often raises debate (Elishakoff, 1995; Ben-Haim, 1994; Ferson and Ginzburg, 1996; Ferson, 1996; Ferson et al., 2004). Many researchers argue that because epistemic uncertainty has a different nature, it should be represented using non-probabilistic approaches such as the fuzzy set theory (Zadeh, 1965), interval approach (Moore, 1966), convex model (Ben-Haim and Elishakoff, 1990), Dempster-Shafer evidence theory (Dempster, 1967; Shafer, 1976), imprecise probabilities (Walley, 1991), and so on. Among these non-probabilistic approaches, the fuzzy set theory and the interval approach have been applied in the area of computational mechanics for analysis of structures under uncertainties. In the following sections, the probabilistic approach and its limitations are discussed. Also, the Fuzzy set theory and the interval approach are introduced.

1.2.1 Probabilistic approach

In the probabilistic approach, uncertainties are described by random variables, uncertain time dependent functions are represented by stochastic processes, and uncertain

spatial properties are modeled by random fields. The main objective of the probability analysis is the determination of the reliability of the system. Herein, reliability is defined as the probability that the system will adequately perform its intended mission over a given period of time. The commonly used techniques for uncertainty propagation include Monte Carlo and Latin Hypercube sampling methods, first-order and second-order reliability methods (FORM and SORM, respectively) and the response surface method. The probabilistic approach is well developed and is described in many texts (e.g., Ang and Tang, 1975; Melchers, 1999; Hayter, 2002).

It is widely accepted that the probabilistic approach is most appropriate to describe aleatory uncertainty when sufficient experimental data are available. More often, the necessary data are simply lacking or limited. In this case, the analyst provides subjective information about the input probability distribution. This is sometimes referred to as a *subjective* probability or *Bayesian* probability. For example, it is common to assume a uniform distribution if only a range of possible values for an uncertainty is available, but no likelihood information of the quantity within this range is available. This practice identifies ignorance of likelihood with equality of probabilities. In this context, the Bayesian approach can be used to amend and improve the estimates when more data become available. Before receiving additional information, however, the Bayesian approach remains a subjective representation of uncertainty.

It often raises the debate as to whether probabilistic approach can deliver the reliability when there is a lack of sufficient experimental data to validate the assumptions made regarding the joint probability functions of random variables involved. Elishakoff (1995) studied the effect of human error in constructing a probabilistic model. It has been shown that a small error in probabilistic data may lead to a large errors in estimating reliability (Elishakoff, 1995; Ben-Haim, 1994). As Elishakoff (1995) notes, "In modern probabilistic codes and in most, if not all, studies the necessary

probabilistic information on uncertain quantities is assumed rather than appropriately substantiated through statistical analysis of extensive experimental data. After numerous assumptions are made, some new numerical approaches, often sophisticated ones, are tested on simple examples. On the other hand the accuracy of the experimental data (if at all present) is not discussed."

It is also argued that probability theory cannot handle situations when the information is nonspecific, ambiguous, or conflicting (Walley, 1991; Ferson and Ginzburg, 1996; Sentz and Ferson, 2002; Oberkampf and Helton, 2005). Freudenthal (1972), who was one of the pioneers of probabilistic approaches in engineering, states that "...ignorance of variation does not make such variation random". This statement means uncertainty does not always equal randomness, and should not always be treated as though it were variability.

1.2.2 Fuzzy set theory

The concept of fuzzy set and fuzzy logic were introduced by Zadeh (1965) to mathematically represent uncertainties due to vagueness rather than randomness.

A fuzzy set is a generalization to classical set to allow elements to take partial membership in vague concepts. Consider a universe of discourse X (i.e., a universal set X that covers a definite range of objects) with elements x. The crisp set A of X is defined by the characteristic function $\mu_A(x)$ of A, where

$$\mu_A(x) = \begin{cases} 1 & \text{for} \quad x \in A, \\ 0 & \text{for} \quad x \notin A. \end{cases} \tag{1.1}$$

That is, the characteristic function associated with A is a mapping that can be expressed by

$$\mu_A(x) : X \rightarrow 0, 1. \tag{1.2}$$

A fuzzy set B over the universe of discourse X is defined by an analogous membership function $\mu_B(x)$, $\mu_B(x) : X \rightarrow [0,\ 1]$. The membership function maps the

members of the universe into the interval [0, 1] as

$$\mu_B(x) = \begin{cases} 1 & \text{if } \ x \in B, \\ 0 & \text{if } \ x \notin B, \\ p, \ 0 < p < 1 & \text{if } \ x \text{ partly in } B. \end{cases} \tag{1.3}$$

$\mu_B(x) = 1$ if x is completely in B, $\mu_B(x) = 0$ if x is completely outside B, and $0 < \mu_B(x) < 1$ if x is partly in B. The function $\mu_B(x)$ represents the degree of membership, or membership value, of an element x in the fuzzy set B. For example, given the measured value of a parameter, the membership function gives the "degree of membership" that the parameter is "small" or "large." The value of the membership function is referred to as "possibility." The possibility in fuzzy sets should not be equated with the statistical concept of probability. Fuzzy membership represents similarities of objects to imprecisely defined properties, while probability describes information about relative frequencies.

Many types of functions can be used for membership functions in fuzzy sets, but *triangular* or *trapezoidal* shaped membership functions are the most common because they are easier to represent. The triangular membership function, illustrated in Fig. 1.1, is

$$\mu(x) = \begin{cases} \dfrac{x-a}{b-a}, & \text{if } a \le x \le b, \\ \dfrac{c-x}{c-b}, & \text{if } b < x \le c, \\ 0, & \text{otherwise}, \end{cases} \tag{1.4}$$

and the trapezoidal membership function (Fig. 1.2) is

$$\mu(x) = \begin{cases} \dfrac{x-a}{b-a}, & \text{if } a \le x < b, \\ 1, & \text{if } b \le x \le c, \\ \dfrac{x-d}{c-d}, & \text{if } c < x \le d, \\ 0, & \text{if } x < a \text{ or } x > d. \end{cases} \tag{1.5}$$

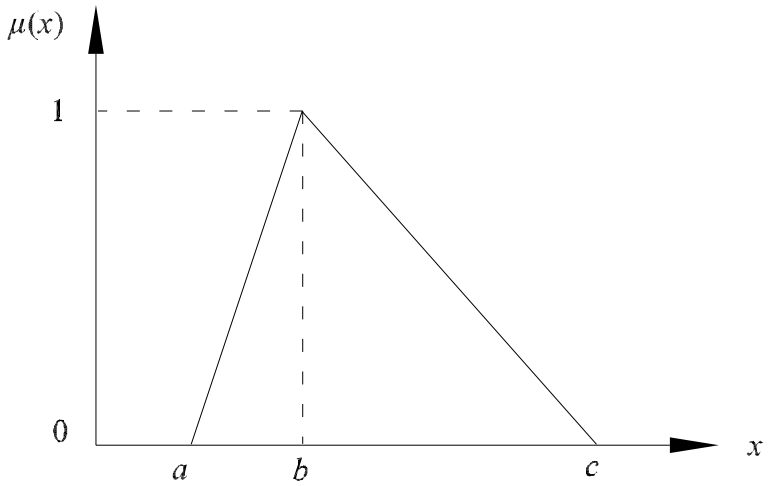

Figure 1.1: Fuzzy set: triangular membership function.

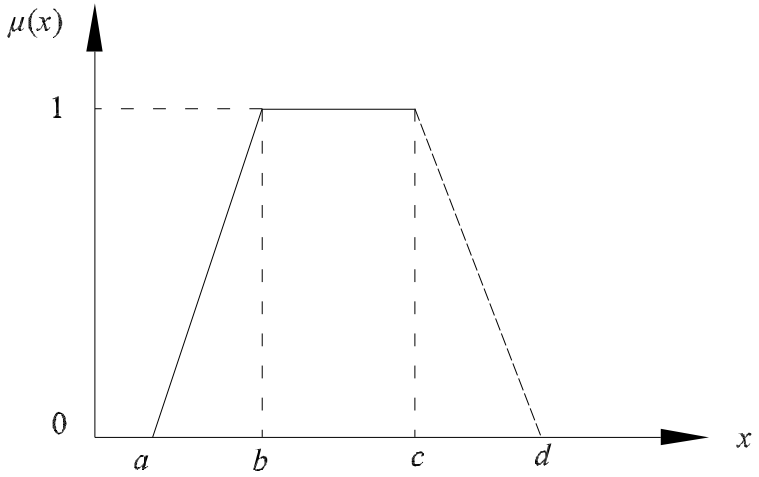

Figure 1.2: Fuzzy set: trapezoidal membership function.

In fuzzy analysis, all uncertainties are described by fuzzy sets. Various methods for fuzzification of uncertain parameters have been reported in the literature, including intuition, inference, rank ordering, neural networks, genetic algorithm, inductive reasoning, soft partitioning, meta rules and fuzzy statistics. A comprehensive review of these methods can be found in Ross (1995). Once the uncertainties are expressed

as fuzzy sets, fuzzy arithmetic is used to compute the fuzzy response quantity. Information about fuzzy arithmetic can be found in series of books and publications such as Kaufman and Gupta (1991) and Bojadziev and Bojadziev (1995).

Fuzzy sets and fuzzy logic have found extensive applications in control problems and artificial intelligence (AI) (Yen et al., 1995; Yen, 1999), but its use for uncertainty modeling within the context of computational mechanics is a relatively new area of research. Rao and Chen (1998), Muhanna and Mullen (1999), Möller et al. (2000), Akpan et al. (2001a), and Akpan et al. (2001b) studied linear static problems with fuzzy material properties and fuzzy loads. Gersem et al. (2004) analyzed the dynamic behavior of structures with fuzzy parameters. Möller et al. (1999) studied structural safety assessment by using fuzzy set theory. Non-stochastic uncertainty and subjective estimates of objective values by experts were taken into account.

1.2.3 Interval approach

In many cases, only a range of possible values for a non-deterministic quantity is available, but no further information about which values are more likely to occur is available. In this situation, a uniform distribution is often used in probability theory. As such, the lack of knowledge is filled by *subjective* information assumed by the analyst, expressed in the form of uniform distribution. Ferson and Ginzburg (1996) demonstrated how the probabilistic approach can yield incorrect results in this case. Many argue that in this situation, the uncertainty is best represented by the information as provided to us; that is, by the interval itself (Ferson and Ginzburg, 1996; Joslyn and Ferson, 2004).

In the interval approach, an uncertain quantity is assumed to be unknown but bounded, and it has lower and upper bounds (endpoints) without assigning a probability structure. Therefore, the interval representation of an uncertain quantity $\boldsymbol{x}$ is

given by

$$\boldsymbol{x} = [\underline{x},\ \overline{x}] \tag{1.6}$$

where $\underline{x}$ and $\overline{x}$ are the lower and upper bounds of the uncertain quantity respectively.

The interval approach concept can be directly attributed to Moore (1966). Moore's purpose for introducing intervals was to provide a treatment of rounding errors and truncation errors in finite precision arithmetic. For example, in a computer with five significant digits, the number $\sqrt{2}$ can be represented using an interval $\sqrt{2} \in [1.4142, 1.4143]$. Thus the rounding error is enclosed in the interval. Besides bounding the effects of rounding errors, interval arithmetic can probe the behavior of functions efficiently and reliably over whole sets of arguments at once. By its nature, interval arithmetic yields rigorous enclosures for the range of operations and functions. The results are intervals in which the exact results *must* lie. This characteristic has made interval arithmetic useful in scientific computing, including

- Bounding the effects of rounding errors and truncation errors (Moore, 1966, 1979);
- Bounding the range of functions (Moore, 1966, 1979; Hansen and Walster, 2003; Neumaier, 1990);
- Bounding the error term in Taylor's theorem (Neumaier, 1990);
- Bounding the results of Monte Carlo simulations in reliability analysis (Tonon, 2004);
- Computing rigorous bounds on the solution of ordinary and partial differential equations (Moore, 1979; Plum, 2001; Jackson and Nedialkov, 2002).
- Global optimization (Hansen and Walster, 2003);
- Solving nonlinear systems (Neumaier, 1990; Hansen and Walster, 2003)

– construct rigorous bounds around an approximate solution, in which an actual solution must lie,

– exhaustively search a region to find all roots of a nonlinear system.

Interval arithmetic has been successfully applied to many applications. These include reliable modeling and optimization for chemical engineering (Bogle et al., 2004), estimating the performance of financial trading systems (Matthews et al., 1990), calculating validated reliability bounds (Tonon, 2004), computer-assisted proofs in mathematical physics (Lanford, 1984), solving interval constraints in computer-aided design (Wang, 2004), existence verification and construction of robust controller (Nataraj and Tharewal, 2004), and others. More information about applications for interval arithmetic is found in Corliss (1990), Corliss and Kearfott (1999), Kearfott (1996), Muhanna and Mullen (2004).

Starting in the mid-nineties, the interval approach has been used to describe parameter uncertainty in engineering systems. The interval approach provides a simple, elegant, and computationally efficient way to represent the uncertainties with only range information. For example, the thickness of a plate is subject to manufacturing tolerance, and is given as $h \pm \delta$ or in an interval form as $[h - \delta, h + \delta] = [\underline{h}, \overline{h}]$. In the case of the distributed live load, if it is known to range from 2.2 kN/m^2 to 2.6 kN/m^2, it can be represented as an interval [2.2, 2.6] kN/m^2. The load may be a constant the value of which is not precisely known, or it may vary according to some *unknown* distribution with known bounds in [2.2, 2.6] kN/m^2. Experimental data, measurements, statistical analysis and expert knowledge represent information for defining bounds on the possible ranges of such quantities (Ferson et al., 2003; Ferson and Hajagos, 2004; Ferson et al., 2004). Care should be taken not to interpret the interval quantity as the absolute assurance in the physical quantity. It merely represents the values the analyst considers possible at the time the analysis is performed.

Interval analysis provides rigorous bounds on system responses based on the

bounds of the input parameters. Interval arithmetic has been developed for computations involving interval quantities. A review of interval arithmetic is found in Chapter 2.

If sufficient probabilistic information is available, the use of the interval approach to describe uncertainties only gives the bounds of the responses, and the additional likelihood information about the responses is lost. In this situation, probabilistic approach is generally preferred. However, since interval analysis usually requires much less computation than a probability analysis such as Monte Carlo simulation, it might still be valuable to use the interval approach to perform a rapid analysis of the response ranges. Another practical application of the interval approach is in the study of the sensitivity of the system behavior with respect to changes in input parameters. The system behavior over the entire interval range of parameter variation can be studied by interval analysis (Muhanna and Mullen, 2004).

Another motivation for using the interval approach in this research work is that interval analysis is intimately connected with the analysis of other uncertainty approaches, such as fuzzy set theory, random set theory, convex modeling, Dempster-Shafer structure and probability-bounds approach. Analysis of these uncertainty models and interval analysis are mutually relevant. For example, a fuzzy number can be formed from a continuum of intervals corresponding to α levels. This being the case, the mathematical analysis associated with fuzzy set theory can be performed as interval analysis on different α levels (Kaufman and Gupta, 1991; Muhanna and Mullen, 1995, 1999). A Dempster-Shafer structure with interval focal elements can be viewed as a collection of pairs, each consisting of an interval and a probability mass; thus the mathematical analysis of Dempster-Shafer structures can be built up using a series of interval analysis on the Cartesian product of the interval focal elements. Therefore, the interval FEA developed in this research work can also be applied to the FEA for the problems with fuzzy set parameters or Dempster-Shafer structures.

1.3 Uncertainties and Errors in Finite Element Analysis

The numerical method most frequently used to capture the behavior of complicated engineering systems appears to be the finite element analysis (FEA), also called the finite element method (FEM). It has been used extensively in many engineering applications such as stress analysis, heat transfer, magnetic fields, fluid flows and other fields.

FEA is a method for numerical solution of the governing partial differential equations of field problems posed over a domain Ω. In FEA, this domain is replaced by the union $\cup$ of subdomains Ω^e called finite elements, or simply *elements*. Elements are connected at points called *nodes*. The particular arrangement of elements is called a *mesh*. The field quantity is locally (piecewise) approximated over each element by an interpolation formula expressed in terms of the nodal values of the field quantity. The assemblage of elements represents a discrete analog of the original domain, and the associated system of algebraic equations represents a numerical analog of the mathematical model of the problem being analyzed (Reddy, 1993). The solution for nodal quantities, when combined with the assumed field in any given element, completely determines the spatial variation of the field in that element (Cook et al., 2002). These are the two most important concepts of FEA: discretization of the domain and approximation of the field quantity using its nodal values. A brief review of FEA is found in Sec. 3.1. Many excellent texts on FEA are available in the literature (e.g., Gallagher, 1975; Zienkiewicz, 1977; Reddy, 1993; Bathe, 1996; Cook et al., 2002).

The accuracy of FEA is affected by errors and uncertainties, which may be related to the numerical tool itself (discretization, element formulation, equation solver) or to the physics of the problem. The possible sources of uncertainties and errors in FEA include model uncertainty, discretization error, parameter uncertainty and rounding

error (Cook et al., 2002; Bathe, 1996; Oberkampf et al., 2002; Muhanna and Mullen, 2004). The definitions of these uncertainty and errors are summarized in Table 1.2 and presented in the following sections.

Table 1.2: Uncertainty and errors in FEA.

Type	Definition/Explanation
Model uncertainty	Associated with the appropriateness of the mathematical model to describe the physical system.
Discretization error	Associated with the conversion of the mathematical model into the computational framework.
Parameter uncertainty	Arises because of the inexact knowledge of the input parameters for the analysis.
Rounding error	Numerical errors introduced by the nature of computer finite precision arithmetic.

1.3.1 Model uncertainty

The first step in FEA selects a mathematical model to represent the physical system being analyzed. The actual problem is simplified and idealized, and is described by an accepted mathematical formulation such as the theory of elasticity, or thin-plate theory, or equations of heat conduction, and so on. The uncertainty about how well the mathematical model represents the true behavior of the real physical system is termed *model uncertainty*. Model uncertainty is a form of epistemic uncertainty. Typical model uncertainties in FEA are:

- the idealization of the boundary conditions
- the use of plane model rather than three-dimensional model
- the use of linear model rather than nonlinear model
- the use of time-independent model rather than dynamic model

1.3.2 Discretization error

The established mathematical model is represented by an FE discretization. This involves selecting a mesh and elements. The computed solution of the FE model is in general only an approximation of the exact solution of the mathematical model, and the discrepancy is called *discretization error*. FEA solution is influenced by a variety of factors, such as the number of elements used, the nature of element shape functions, integration rules used, and other formulation details of particular elements.

1.3.3 Parameter uncertainty

Parameter uncertainty arises because the precise data needed for the analysis is not available. This type of uncertainty is sometimes called *parametric uncertainty* or *data uncertainty*. In FEA, the parameter uncertainty may exist in the geometrical, material or loading data. Parameter uncertainty may result from a lack of knowledge (epistemic uncertainty), an inherent variability (aleatory uncertainty) in the parameters, or both.

1.3.4 Rounding error

FEA solution is limited in accuracy by the finite precision of computer arithmetic. When arithmetic operations are performed on floating point numbers, the exact result will not, in general, be representable as a floating point number. The exact result will be rounded to the nearest floating point number, and this loss of information is referred to as *rounding error*. To avoid possibly serious rounding errors, FEA typically requires 12 to 14 digits per word (Cook et al., 2002). A more fundamental approach, however, is to use interval arithmetic. As introduced in Sec. 1.2.3, interval arithmetic can rigorously bound the rounding error.

1.4 Nondeterministic FEA: An Interval Approach

This thesis concentrates on the study of parameter uncertainty in FEA. The study of model uncertainty and discretization error is beyond the scope of this work. Incorporating parameter uncertainty in FEA requires a nondeterministic FEA. If the uncertainty is described within the framework of probability theory, the stochastic FEA can be used. In the stochastic FEA, the random filed is discretized into a set of correlated random variables. The problem is to estimate up to the second moments of the system response. Various methods for stochastic FEA are proposed in the literature, including Monte Carlo simulation, the weighted integral method, perturbation method, Neumann series expansion method, improved Neumann expansion, spectral based method, and others (Ghanem and Spanos, 1991; Haldar and Mahadevan, 2000). Comprehensive reviews of the stochastic FEA are found in Matthies et al. (1997) and Keese (2003). A state-of-the-art report on computational stochastic mechanics is provided by Schuëller (1997) with contributions from many authors.

More recently, a number of nondeterministic FEA based on non-probabilistic uncertainty modeling have been investigated, including interval FEA and fuzzy FEA. In interval FEA, the uncertain parameters are described by intervals. Hence, the response of the system will be a function of the interval parameters and therefore vary in an interval. The objective of interval FEA is to estimate the range of the system response (displacement, stress, etc.) based on the bounds of the input parameters.

The fuzzy FEA is based on the fuzzy representation of the uncertain parameters, and it is basically an extension of interval FEA, that is, the analysis can be broken down into a series of interval FEA (Mullen and Muhanna, 1996; Rao and Chen, 1998; Kulpa et al., 1998; Muhanna and Mullen, 1999; Akpan et al., 2001a,b; Gersem et al., 2004). For this reason, the fuzzy FEA is also "interval-based" FEA.

The mid-nineties can be considered the period when the main activities for uncertainty treatment in a form of intervals began in the area of computational mechanics

and when the efforts for development of interval FEA commenced. Since then, interval FEA has become an active area of research and has been studied in a number of specific research domains:

- Static structural analysis (e.g., Koyluoglu et al., 1995; Muhanna and Mullen, 1995; Mullen and Muhanna, 1996; Rao and Berke, 1997; Rao and Chen, 1998; Koyluoglu and Elishakoff, 1998; Mullen and Muhanna, 1999; Muhanna and Mullen, 2001; Möller et al., 2000; Pantelides and Ganzerli, 2001; Akpan et al., 2001a,b; Chen et al., 2002; Popova et al., 2003; Zhang and Muhanna, 2004; Pownuk, 2004a; Rao and Liu, 2004)

- Dynamic analysis (e.g., Chen and Rao, 1997; Moens and Vandepitte, 2002; Dessombz et al., 2001; Modares et al., 2004)

- Geotechnical engineering (e.g., Fetz et al., 1999; Tonon et al., 2000; Peschl and Schweiger, 2003; Hall et al., 2004)

- Heat transfer problem (Jasiński and Pownuk, 2000; Pereira et al., 2004, e.g.,)

A review of the commonly used methods for interval FEA is presented in Chapter 3.

1.5 Objective

The primary objective of this study is to develop an efficient computational framework for linear static FEA of structures with interval parameters. Particular attention is given to obtaining rigorous, sharp and efficiently computed bounds on the ranges of the structural responses. Overestimation in results due to dependence in interval computation is to be addressed. The developed interval FEA will satisfy the following requirements:

- *Rigorousness.* If the exact bounds of the responses ranges are not achievable, the approximate bounds should be guaranteed to contain the exact ranges of the responses, That is, enclosures are obtained.

- *Sharpness.* Given the rigorousness condition is satisfied, the obtained bounds of the response range should be tight enough to be practically useful. That is, the bounds are not overly conservative.

- *Computational efficiency.* The method should be computationally efficient compared with the existing interval finite element methods.

- *Scalability.* The accuracy of the method does not deteriorate with the increase of the problem scale.

1.6 Thesis Organization

This chapter addresses the background of FEA of structures with interval parameters. The objective is summarized. The remaining contents of the thesis are organized in the following manner.

Chapter 2 presents the fundamentals of interval arithmetic relevant to the work in this thesis. The properties of interval arithmetic are discussed. The concept of linear interval equations is presented. Particular attention is given to the dependence problem in interval arithmetic, which results in overestimation in the solution. In Chapter 3 a review of the existing solution techniques for linear elastic static interval FEA is provided. The merits and limitations of each method are discussed, and an argument is made for an alternative method that can yield rigorous, accurate, and efficiently computed results. Chapter 4 presents the developed interval FE formulation. The techniques used are discussed in detail. Chapter 5 presents numerical studies using the computational framework developed in Chapter 4. The rigorousness, accuracy, scalability and computational efficiency of the present interval FEA is studied. Chapter 6 summarizes the main findings of the study and presents suggestions for further work.

CHAPTER 2

INTERVAL ARITHMETIC

This chapter presents a review of (real) interval arithmetic relevant to the work in this thesis. The properties of intervals and interval arithmetic are discussed. The concept of linear interval equations is presented. Information about other aspects of interval arithmetic, such as nonlinear interval equations and global optimization using interval analysis, can be found in series of books and publications such as Moore (1966), Moore (1979), Alefeld and Herzberger (1983), Neumaier (1990), Jaulin et al. (2001), and Hansen and Walster (2003).

2.1 Notation

In this thesis, boldface will denote interval quantities (interval number, interval vector, interval matrix). All interval quantities are implicitly real interval quantities. Non-boldface will denote real (deterministic) quantities. For an interval quantity $\boldsymbol{x}$ or $\boldsymbol{A}$, the notation x and A is used to denote a generic (arbitrary) element $x \in \boldsymbol{x}$ and $A \in \boldsymbol{A}$.

2.2 Interval Number

A (real) interval is a nonempty set of real numbers

$$\boldsymbol{x} = [\underline{x},\ \overline{x}] = \{x \in \mathbb{R} | \underline{x} \leq x \leq \overline{x}\}, \tag{2.1}$$

where $\underline{x}$ and $\overline{x}$ are the lower and upper bounds (endpoints) of the interval number $\boldsymbol{x}$, respectively. x is a generic (arbitrary) element in the interval $\boldsymbol{x}$. $\mathbb{R}$ denotes the set of all real numbers. If $\boldsymbol{x}$ is a more complex expression, the lower bound and the upper

bound are also written as

$$\underline{x} \equiv \inf(\boldsymbol{x}), \quad \overline{x} \equiv \sup(\boldsymbol{x}). \tag{2.2}$$

The set of all intervals is denoted by $\mathbb{IR}$. To represent an unknown number as an approximation plus/minus an error bound, the *midpoint* $\check{x}$ of an interval $\boldsymbol{x}$, is introduced as

$$\check{x} \equiv \mathrm{mid}(\boldsymbol{x}) = \frac{\underline{x} + \overline{x}}{2}, \tag{2.3}$$

and the *radius* of $\boldsymbol{x}$ is defined as

$$\mathrm{rad}(\boldsymbol{x}) = \frac{\overline{x} - \underline{x}}{2}. \tag{2.4}$$

Hence $\boldsymbol{x}$ can be represented as

$$\boldsymbol{x} = [\check{x} - \mathrm{rad}(\boldsymbol{x}),\ \check{x} + \mathrm{rad}(\boldsymbol{x})]. \tag{2.5}$$

In many cases, the midpoint $\check{x}$ is seen as the "nominal" value of the uncertain variable.

If an interval has zero radius it is called *thin* (*degenerated*) interval. A thin interval contains only one real number. A *thick* interval has a radius greater than zero. If $\check{x} \neq 0$, $\boldsymbol{x}$ can be decomposed into two parts, the deterministic (midpoint) part $\check{x}$ and the interval part $(1 + \boldsymbol{\delta})$:

$$\boldsymbol{x} = \check{x}(1 + \boldsymbol{\delta}), \tag{2.6}$$

where

$$\boldsymbol{\delta} = \frac{\boldsymbol{x}}{\check{x}} - 1 = \begin{cases} [-\mathrm{rad}(\boldsymbol{x})/\check{x},\ \mathrm{rad}(\boldsymbol{x})/\check{x}], & \text{for } \check{x} > 0, \\ [\mathrm{rad}(\boldsymbol{x})/\check{x},\ -\mathrm{rad}(\boldsymbol{x})/\check{x}], & \text{for } \check{x} < 0. \end{cases} \tag{2.7}$$

$\boldsymbol{\delta}$ is a zero-midpoint interval, and it is referred to as the *interval multiplier* of $\boldsymbol{x}$. $\boldsymbol{\delta}$ is a measurement of the fluctuation of $\boldsymbol{x}$ with respect to its midpoint $\check{x}$. In this thesis, if an interval $\boldsymbol{x}$ is said to have 2% uncertainty (with respect to its midpoint), it suggests $\boldsymbol{\delta} = [-0.01, 0.01]$, and $\boldsymbol{x} = \check{x}(1 + [-0.01, 0.01])$.

The *width* of an interval $\boldsymbol{x}$ is

$$\mathrm{wid}(\boldsymbol{x}) = 2\mathrm{rad}(\boldsymbol{x}) = \overline{x} - \underline{x}. \tag{2.8}$$

The *interior* of an interval $\boldsymbol{x}$ is defined as

$$\text{int}(\boldsymbol{x}) = \{x \in \mathbb{R} \mid \underline{x} < x < \overline{x}\}. \tag{2.9}$$

The *absolute value* or the *magnitude* of an interval is defined as

$$|\boldsymbol{x}| = \text{mag}(\boldsymbol{x}) = \max\{|\underline{x}|, |\overline{x}|\}, \tag{2.10}$$

and the *mignitude* of $\boldsymbol{x}$ is defined as

$$\text{mig}(\boldsymbol{x}) = \begin{cases} \min\{|\underline{x}|, |\overline{x}|\}, & \text{if } 0 \notin \boldsymbol{x} \\ 0 & \text{otherwise.} \end{cases} \tag{2.11}$$

An interval $\boldsymbol{x}$ is a *subset* of an interval $\boldsymbol{y}$, denoted by $\boldsymbol{x} \subseteq \boldsymbol{y}$, if and only if $\underline{y} \leq \underline{x}$ and $\overline{y} \geq \overline{x}$.

If S is a nonempty bounded subset of $\mathbb{R}$ we denote by

$$\Diamond S := [\inf(S), \sup(S)] \tag{2.12}$$

the *hull* of S, i.e., the narrowest interval enclosing S.

The four *elementary operations* of real arithmetic, namely addition (+), subtraction (-), multiplication ($\times$) and division ($\div$) can be extended to intervals. Operations $\circ \in \{+, -, \times, \div\}$ over intervals are defined by the general rule

$$\boldsymbol{x} \circ \boldsymbol{y} = \{x \circ y \mid x \in \boldsymbol{x},\ y \in \boldsymbol{y}\}. \tag{2.13}$$

It is easy to see that the set of all possible results for $x \in \boldsymbol{x}$ and $y \in \boldsymbol{y}$ forms a closed interval (for 0 not in a denominator interval), and the endpoints can be calculated by

$$\boldsymbol{x} \circ \boldsymbol{y} = [\min\ (x \circ y),\ \max\ (x \circ y)] \quad \text{for } \circ \in \{+, -, \times, \div\}. \tag{2.14}$$

By noting monotonicity properties of operations (Neumaier, 1990), the lower and upper bounds of $\boldsymbol{x} \circ \boldsymbol{y}$ can be determined from the four possible endpoints $\underline{x} \circ \underline{y}$, $\underline{x} \circ \overline{y}$, $\overline{x} \circ \underline{y}$, and $\overline{x} \circ \overline{y}$. For addition and subtraction,

$$\boldsymbol{x} + \boldsymbol{y} = [\underline{x} + \underline{y},\ \overline{x} + \overline{y}],$$

$$\boldsymbol{x} - \boldsymbol{y} = [\underline{x} - \overline{y},\ \overline{x} - \underline{y}].$$

For multiplication and division, the result depends on the signs of $\boldsymbol{x}$ and $\boldsymbol{y}$ as displayed in Tables 2.1 and 2.2 (Neumaier, 1990).

Table 2.1: Interval multiplication $\boldsymbol{xy}$.

	if $\underline{y} \geq 0$ and $\overline{y} \geq 0$	if $\underline{y} < 0 < \overline{y}$	if $\underline{y} \leq 0$ and $\overline{y} \leq 0$
if $\underline{x} \geq 0$ and $\overline{x} \geq 0$	$[\underline{x}\underline{y}, \overline{x}\overline{y}]$	$[\overline{x}\underline{y}, \overline{x}\overline{y}]$	$[\overline{x}\underline{y}, \underline{x}\overline{y}]$
if $\underline{x} < 0 < \overline{x}$	$[\underline{x}\overline{y}, \overline{x}\overline{y}]$	$[\min(\underline{x}\overline{y}, \overline{x}\underline{y}),\ \max(\underline{x}\underline{y}, \overline{x}\overline{y})]$	$[\overline{x}\underline{y}, \underline{x}\underline{y}]$
if $\underline{x} \leq 0$ and $\overline{x} \leq 0$	$[\underline{x}\overline{y}, \overline{x}\underline{y}]$	$[\underline{x}\overline{y}, \underline{x}\underline{y}]$	$[\overline{x}\overline{y}, \underline{x}\underline{y}]$

Table 2.2: Interval division $\boldsymbol{x} \div \boldsymbol{y}$ $(0 \notin \boldsymbol{y})$.

	if $\underline{y} > 0$ and $\overline{y} > 0$	if $\underline{y} < 0 < \overline{y}$
if $\underline{x} \geq 0$ and $\overline{x} \geq 0$	$[\underline{x}/\overline{y}, \overline{x}/\underline{y}]$	$[\overline{x}/\overline{y}, \underline{x}/\underline{y}]$
if $\underline{x} < 0 < \overline{x}$	$[\underline{x}/\underline{y}, \overline{x}/\underline{y}]$	$[\overline{x}/\overline{y}, \underline{x}/\overline{y}]$
if $\underline{x} \leq 0$ and $\overline{x} \leq 0$	$[\underline{x}/\underline{y}, \overline{x}/\overline{y}]$	$[\overline{x}/\underline{y}, \underline{x}/\overline{y}]$

It can also be seen that the only case where more than two real operations are necessary is the multiplication with both operands containing 0. In all other cases the two pairs of operands yielding the lower and upper bound can be determined immediately or by case distinctions. Hence, the theoretical overhead for most operations is a factor of 2. However, if interval supports are implemented directly in the hardware, zero penalties will be implied (Sun microsystems, 2002).

The following examples illustrate the elementary interval operations:

$$[1,2] + [3,4] = [4,6], \qquad 2/[1,2] = [1,2],$$
$$[2,5] - [0,2] = [0,5], \qquad [1,2] \times [3,4] = [3,8],$$
$$[-1,2]([2,3] + [-4,5]) = [-1,2][-2,8] = [-8,16],$$
$$[-1,2][2,3] + [-1,2][-4,5] = [-3,6] + [-8,10] = [-11,16].$$

2.3 Interval Arithmetic Expression

An *interval function* is an interval-valued function of one or more interval arguments. Thus, an interval function maps the value of one or more interval arguments onto an interval. Consider a real-valued function $f(x_1, \ldots, x_n)$, if an interval-valued function $\boldsymbol{f}(\boldsymbol{x}_1, \ldots, \boldsymbol{x}_n)$ has the property

$$\boldsymbol{f}(x_1, \ldots, x_n) = f(x_1, \ldots, x_n) \quad \text{for real arguments,}$$

then $\boldsymbol{f}$ is called an *interval extension* of f (Moore, 1966). In particular, the *natural interval extension* of f is obtained by replacing each real variable x_i by an interval variable $\boldsymbol{x}_i$ and each real operation by its corresponding interval arithmetic operation.

If the function $\boldsymbol{f}(\boldsymbol{x}_1, \ldots, \boldsymbol{x}_n)$ is an expression with a finite number of intervals $\boldsymbol{x}_1, \ldots, \boldsymbol{x}_n$ and interval operations $(+, -, \times, \div)$, then it satisfies the fundamental property of *inclusion isotonicity* (Moore, 1966):
if

$$\boldsymbol{x}_1 \subseteq \boldsymbol{y}_1, \ldots, \boldsymbol{x}_n \subseteq \boldsymbol{y}_n,$$

then

$$\boldsymbol{f}(\boldsymbol{x}_1, \ldots, \boldsymbol{x}_n) \subseteq \boldsymbol{f}(\boldsymbol{y}_1, \ldots, \boldsymbol{y}_n)$$

A remarkable property of inclusion isotonicity is that the range of a function can be rigorously estimated by its interval extension function (Moore, 1966):

$$\{f(x_1, \ldots, x_n) \mid x_1 \in \boldsymbol{x}_1, \ldots, x_n \in \boldsymbol{x}_n\} \subseteq \boldsymbol{f}(\boldsymbol{x}_1, \ldots, \boldsymbol{x}_n). \tag{2.15}$$

That means $\boldsymbol{f}(\boldsymbol{x}_1, \ldots, \boldsymbol{x}_n)$ contains the range of values of $f(x_1, \ldots, x_n)$ for all $x_i \in \boldsymbol{x}_i$ $(i = 1, \ldots, n)$. For example, consider the function $f(x_1, x_2) = x_1 + x_2$, with $x_1 \in [1, 2]$ and $x_2 \in [2, 3]$. The bounds of the range of f can be obtained by evaluating its natural interval extension function

$$\boldsymbol{f} = \boldsymbol{x}_1 + \boldsymbol{x}_2 = [1, 2] + [2, 3] = [3, 5].$$

2.4 Dependence Problem

According to Eq. (2.15), the interval evaluation $\boldsymbol{f}(\boldsymbol{x})$ generally does not provide the exact range of f, but only an enclosure (outer bound). Clearly, it is desirable to obtain a sharp enclosure. Unfortunately, in some cases the bounds provided by interval arithmetic tend to be too conservative: the bounds produced are often much wider than the true range of the corresponding quantities, often to the point of uselessness. Consider the arithmetic expression $f(x) = x^2 - x$, with $x \in [-1, 1]$. The attempt to find the range of f over the interval $[-1, 1]$ by evaluating the natural interval extension function gives the result

$$\boldsymbol{f}(\boldsymbol{x}) = \boldsymbol{x}^2 - \boldsymbol{x} = [-1, 1]^2 - [-1, 1] = [0, 1] - [-1, 1] = [-1, 2].$$

Since $\{f(x) = x^2 - x = (x - 0.5)^2 - 0.25 \mid x \in [-1, 1]\} = [-0.25, 2]$, the range given by the interval function $\boldsymbol{f}$ contains the exact range, but it overestimates the lower bound from -0.25 to -1. In general, each occurrence of a given interval variable in an interval computation is treated as a *different, independent* variable. After the subexpression $\boldsymbol{x}^2$ is computed, interval arithmetic does not recognize that the value of $\boldsymbol{x}^2$ is strongly related to the value of $\boldsymbol{x}$. Interval arithmetic implicitly makes the assumption that all intervals are independent, namely it treats $\boldsymbol{x}^2 - \boldsymbol{x}$ as if evaluating $\boldsymbol{x}_1^2 - \boldsymbol{x}_2$, with $\boldsymbol{x}_1 = [-1, 1]$ and $\boldsymbol{x}_2 = [-1, 1]$. This causes widening of the computed result and makes it difficult to compute the sharp enclosure for complicated interval expressions.

This unwanted extra interval width is referred to as *overestimation* due to *dependence problem*, or simply *dependence* (Moore, 1966; Neumaier, 1990; Hansen and Walster, 2003). In general, the dependence problem arises when some interval variables occur more than once in the computation. For expressions in which all variables occur only once, the dependence problem is absent and the exact range of the function is obtained (Moore, 1966).

In some cases it is possible to reduce the number of occurrences of each variable to avoid the dependence problem. In the foregoing example, the function f can be transformed to $g(x) = (x-0.5)^2 - 0.25$, which is equivalent to $f(x)$ in real arithmetic. Since x only occurs once in $g(x)$, the interval evaluation of g gives the exact range of the expression,

$$\boldsymbol{g} = (\boldsymbol{x} - 0.5)^2 - 0.25 = [-1.5, 0.5]^2 - 0.25 = [0, 2.25] - 0.25 = [-0.25, 2].$$

Due to dependence problem, only some of the algebraic laws, valid for real numbers, remain strictly valid for interval arithmetic; other laws only hold in a weaker form. There are two general rules for the algebraic properties of interval operations (Neumaier, 1990):

1. Two arithmetic expressions which are equivalent in real arithmetic are equivalent in interval arithmetic when every variable occurs only once on each side. For example, the following laws hold for $\boldsymbol{a}, \boldsymbol{b}, \boldsymbol{c} \in \mathbb{IR}$:

$$\boldsymbol{a} + \boldsymbol{b} = \boldsymbol{b} + \boldsymbol{a}, \quad \boldsymbol{ab} = \boldsymbol{ba},$$
$$(\boldsymbol{a} + \boldsymbol{b}) \pm \boldsymbol{c} = \boldsymbol{a} + (\boldsymbol{b} \pm \boldsymbol{c}), \quad (\boldsymbol{ab})\boldsymbol{c} = \boldsymbol{a}(\boldsymbol{bc}).$$

2. If f, g are two arithmetic expressions which are equivalent in real arithmetic, then the interval extension function $\boldsymbol{f} \subseteq \boldsymbol{g}$ holds if every variable occurs only once in f. For example, if $\boldsymbol{a}, \boldsymbol{b}, \boldsymbol{c} \in \mathbb{IR}$, then

$$\boldsymbol{a}(\boldsymbol{b} \pm \boldsymbol{c}) \subseteq \boldsymbol{ab} \pm \boldsymbol{ac}, \quad (\boldsymbol{a} \pm \boldsymbol{b})\boldsymbol{c} \subseteq \boldsymbol{ac} \pm \boldsymbol{bc}, \quad \text{(subdistributivity)}$$
$$\boldsymbol{a} - \boldsymbol{b} \subseteq (\boldsymbol{a} + \boldsymbol{c}) - (\boldsymbol{b} + \boldsymbol{c}), \quad \boldsymbol{a}/\boldsymbol{b} \subseteq (\boldsymbol{ac})/(\boldsymbol{bc}), \quad \text{(subcancellation)}$$
$$0 \in \boldsymbol{a} - \boldsymbol{a}, \quad 1 \in \boldsymbol{a}/\boldsymbol{a}. \quad \text{(subcancellation)}$$

The dependence problem causes the failure of the distributivity law and the cancellation law, and makes it difficult to compute sharp results for complicated interval analysis. The success of an interval analysis largely depends on the reduction of the dependence.

2.5 Interval Vectors and Interval Matrices

An interval matrix $\boldsymbol{A} \in \mathbb{IR}^{m\times n}$ is a matrix whose entries $\boldsymbol{A}_{jk} = [\underline{A}_{jk}, \overline{A}_{jk}]$ are intervals, and it is interpreted as the set of all real matrices $A \in \mathbb{R}^{m\times n}$ with $A_{jk} \in \boldsymbol{A}_{jk}$, for $j = 1, \ldots, m,\ k = 1, \ldots, n$. $\mathbb{R}^{m\times n}$ denotes the set of all $m \times n$ real matrices. $\mathbb{IR}^{m\times n}$ denotes the set of all $m \times n$ interval matrices. The lower bound, upper bound, midpoint, interior, and absolute value of an interval matrix are defined componentwise, respectively:

$$\underline{A} = (\underline{A}_{jk}), \tag{2.16}$$

$$\overline{A} = (\overline{A}_{jk}), \tag{2.17}$$

$$\check{A} = (\check{A}_{jk}), \tag{2.18}$$

$$\mathrm{int}(\boldsymbol{A}) = (\mathrm{int}(\boldsymbol{A}_{jk})), \tag{2.19}$$

$$|\boldsymbol{A}| = (|\boldsymbol{A}_{jk}|). \tag{2.20}$$

An $n \times 1$ interval matrix is an interval vector, denoted by $\mathbb{IR}^n$. The set of vectors with n real components is denoted by $\mathbb{R}^n$. An interval vector is also referred to as a *box*. Fig. 2.1 shows a two-component interval vector $\boldsymbol{x} = ([1, 3],\ [1, 2])^T$.

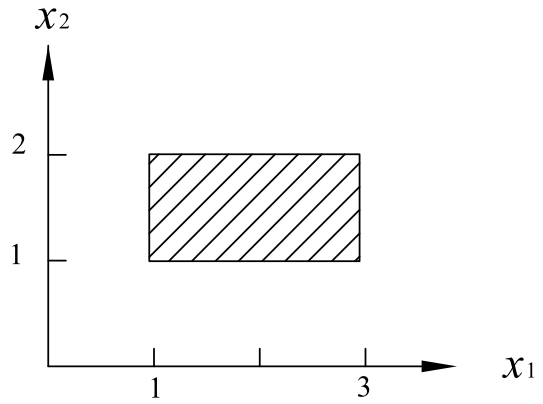

Figure 2.1: The interval vector $\boldsymbol{x} = ([1, 3],\ [1, 2])^T$.

Operations on interval matrices are extended naturally from the corresponding

real matrices operations. For instance, if $\boldsymbol{A} \in \mathbb{IR}^{n\times n}$, $\boldsymbol{B} \in \mathbb{IR}^{n\times n}$, and $\boldsymbol{x} \in \mathbb{IR}^{n}$, then

$$\boldsymbol{A} + \boldsymbol{B} = (\boldsymbol{A}_{ij} + \boldsymbol{B}_{ij})_{1\leqslant i\leqslant n, 1\leqslant j\leqslant n} \tag{2.21}$$

$$\boldsymbol{A} * \boldsymbol{B} = \left(\sum_{k=1}^{n} \boldsymbol{A}_{ik} * \boldsymbol{B}_{kj}\right)_{1\leqslant i\leqslant n, 1\leqslant j\leqslant n} \tag{2.22}$$

$$\boldsymbol{A} * \boldsymbol{x} = \left(\sum_{j=1}^{n} \boldsymbol{A}_{ij} * \boldsymbol{x}_{j}\right)_{1\leqslant i\leqslant n} \tag{2.23}$$

Algebraic properties of interval matrix operations are provided in Neumaier (1990), Apostolatos and Kulisch (1968), and Mayer (1970).

It is noticeable that due to the nature of interval arithmetic, some algebraic laws valid for real matrix operations only hold in a weaker form in the interval matrix operations. For example (Neumaier, 1990), let

$$A = \begin{pmatrix} 1 & 1 \\ 0 & 1 \end{pmatrix}, \quad B = \begin{pmatrix} 1 & 0 \\ -1 & 1 \end{pmatrix}, \quad \boldsymbol{C} = \begin{pmatrix} [-1,1] & 0 \\ 0 & [-1,1] \end{pmatrix}.$$

Then

$$(AB)\boldsymbol{C} = \begin{pmatrix} 0 & 1 \\ -1 & 1 \end{pmatrix} \begin{pmatrix} [-1,1] & 0 \\ 0 & [-1,1] \end{pmatrix} = \begin{pmatrix} 0 & [-1,1] \\ [-1,1] & [-1,1] \end{pmatrix},$$

and

$$A(B\boldsymbol{C}) = \begin{pmatrix} 1 & 1 \\ 0 & 1 \end{pmatrix} \begin{pmatrix} [-1,1] & 0 \\ [-1,1] & [-1,1] \end{pmatrix} = \begin{pmatrix} [-2,2] & [-1,1] \\ [-1,1] & [-1,1] \end{pmatrix}.$$

It can be seen $(AB)\boldsymbol{C} \neq A(B\boldsymbol{C})$, i.e., the associative law fails. We have $(AB)\boldsymbol{C} \subseteq A(B\boldsymbol{C})$.

The following weaker algebraic laws can be presented (Neumaier, 1990):

Proposition 2.1 (Neumaier 1990)

$$
\begin{aligned}
(AB)\boldsymbol{C} &\subseteq A(B\boldsymbol{C}) \quad \text{for } A \in \mathbb{R}^{m\times n}, B \in \mathbb{R}^{n\times p}, \boldsymbol{C} \in \mathbb{IR}^{p\times q} \\
(A\boldsymbol{B})\boldsymbol{C} &\subseteq A(\boldsymbol{BC}) \quad \text{for } A \in \mathbb{R}^{m\times n}, \boldsymbol{B} \in \mathbb{IR}^{n\times p}, \boldsymbol{C} \in \mathbb{IR}^{p\times q} \\
\boldsymbol{A}(BC) &\subseteq (\boldsymbol{AB})C \quad \text{for } \boldsymbol{A} \in \mathbb{IR}^{m\times n}, \boldsymbol{B} \in \mathbb{IR}^{n\times p}, C \in \mathbb{R}^{p\times q} \\
A(\boldsymbol{B}C) &= (A\boldsymbol{B})C \quad \text{for } A \in \mathbb{R}^{m\times n}, \boldsymbol{B} \in \mathbb{IR}^{n\times p}, C \in \mathbb{R}^{p\times q} \\
\boldsymbol{A}(\alpha\boldsymbol{B}) &= \alpha(\boldsymbol{AB}) \quad \text{for all } \alpha \in \mathbb{R}, \boldsymbol{A} \in \mathbb{IR}^{m\times n}, \boldsymbol{B} \in \mathbb{IR}^{n\times p}.
\end{aligned}
$$

In general, for computations involving both real and interval quantities, it is desirable to delay the interval operations to yield a sharper result. This is very much in the spirit of Wilkinson (1971), who wrote "In general it is the best in algebraic computations to leave the use of interval arithmetic as late as possible..."

2.6 Linear Interval Equations

Linear systems of equations are a fundamental part of scientific calculations. In this section we introduce the concept of linear interval equations. A linear interval equation with coefficient matrix $\boldsymbol{A} \in \mathbb{IR}^{n\times n}$ and right-hand side vector $\boldsymbol{b} \in \mathbb{IR}^n$ is defined as the family of linear equations

$$Ax = b \quad (A \in \boldsymbol{A},\ b \in \boldsymbol{b}). \tag{2.24}$$

Thus a linear interval equation represents systems of equations in which the coefficients are unknown numbers ranging in certain intervals. The solution set of (2.24) is given by:

$$\Sigma(\boldsymbol{A}, \boldsymbol{b}) = \{x \in \mathbb{R}^n \mid \exists A \in \boldsymbol{A},\ \exists b \in \boldsymbol{b} : Ax = b\}. \tag{2.25}$$

In order to guarantee that the solution set $\Sigma(\boldsymbol{A}, \boldsymbol{b})$ is bounded, it is required that the matrix $\boldsymbol{A}$ be *regular*; i.e., that every matrix $A \in \boldsymbol{A}$ is nonsingular. In general, the solution set $\Sigma(\boldsymbol{A}, \boldsymbol{b})$ has a very complicated shape and is expensive to compute (Neumaier, 1990). If $\boldsymbol{A} \in \mathbb{IR}^{n\times n}$ is a regular square interval matrix, then the solution

set is bounded, and the hull of the solution set is defined as the narrowest interval vector containing $\Sigma(\boldsymbol{A}, \boldsymbol{b})$, denoted as

$$\boldsymbol{A}^H\boldsymbol{b} = \Diamond\Sigma(\boldsymbol{A}, \boldsymbol{b}). \tag{2.26}$$

For each $A \in \boldsymbol{A}$, $b \in \boldsymbol{b}$, the equation $Ax = b$ has a unique solution $x = A^{-1}b$ so that $\boldsymbol{A}^H\boldsymbol{b}$ can be expressed as

$$\boldsymbol{A}^H\boldsymbol{b} = \Diamond\{A^{-1}b|\ A \in \boldsymbol{A}, b \in \boldsymbol{b}\}. \tag{2.27}$$

However, computing the hull of the solution set for the general case is NP-hard (Rohn, 1995). In practice, the solution of interest is bounding the hull of the solution set; i.e., seeking an interval vector $\boldsymbol{x}$ containing $\boldsymbol{A}^H\boldsymbol{b}$, while still sharp enough to be practically useful:

$$\boldsymbol{A}^H\boldsymbol{b}\ \subseteq \boldsymbol{x}. \tag{2.28}$$

$\boldsymbol{x}$ is referred to as the enclosure of the solution set. Obviously $\boldsymbol{x}$ is not unique, but a sharper enclosure is desirable. If the enclosure is too conservative, it may not provide any useful information. In this thesis, the "solution of an interval equation" is defined as "the enclosure of the solution set," and the "exact solution" is "the hull of the solution set."

In some cases an inner bound $\boldsymbol{y}$ of the hull of the solution set is also desirable so that

$$\boldsymbol{y}\ \subseteq \boldsymbol{A}^H\boldsymbol{b}\ \subseteq \boldsymbol{x}. \tag{2.29}$$

The commonly used methods of solving a linear interval equation include interval Gauss elimination, interval Gauss-Seidel iteration, and fixed point iteration, discussed in Sec. 4.2.5.

The concept of the solution set, the hull of the solution set and the enclosure of the solution set is illustrated in the following example (Neumaier, 1990)

$$\boldsymbol{A} = \begin{pmatrix} 2 & [-1,0] \\ [-1,0] & 2 \end{pmatrix}, \quad b = \begin{pmatrix} 1.2 \\ -1.2 \end{pmatrix}.$$

Then $\boldsymbol{A}$ represents any real matrix A of the form

$$A = \begin{pmatrix} 2 & -\alpha \\ -\beta & 2 \end{pmatrix}$$

with $\alpha,\ \beta \in [0,1]$. By Cramer's rule, the analytical solution of $Ax = b$ is

$$x = \begin{pmatrix} 1.2(2-\alpha)/(4-\alpha\beta) \\ 1.2(\beta-2)/(4-\alpha\beta) \end{pmatrix}.$$

The solution set is shown in Fig. 2.2. The four vertices for the solution set are (0.3, -0.6), (0.6, -0.6), (0.6, -0.3) and (0.4, -0.4), from which can be seen that the hull of the solution set is

$$\boldsymbol{A}^H b = \begin{pmatrix} [0.3, 0.6] \\ [-0.6, -0.3] \end{pmatrix}.$$

To obtain an enclosure of the solution set, the above example was solved in Matlab using the fixed point iteration routine of the Matlab interval arithmetic toolbox b4m (Zemke, 1998). The enclosure given by b4m is

$$\boldsymbol{x} = \begin{pmatrix} [0.2398, 0.7202] \\ [-0.7202, -0.2398] \end{pmatrix},$$

and is shown in Fig. 2.2. As expected, the numerically obtained enclosure $\boldsymbol{x}$ is wider than the hull of the solution set $\boldsymbol{A}^H b$.

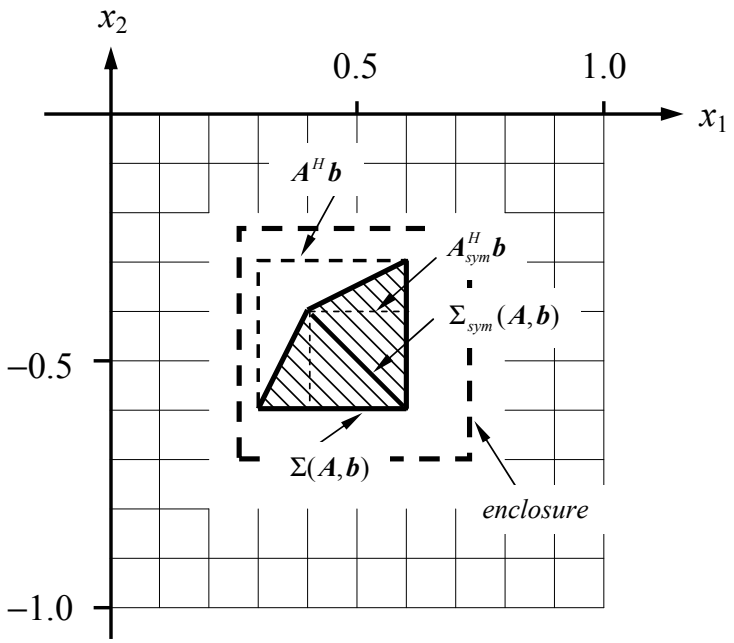

Figure 2.2: Solution set, hull of the solution set, and enclosure of the solution set for linear interval equation (general case and symmetric case).

In the above example, no dependence between the interval coefficients in $\boldsymbol{A}$ are considered. Both coefficients α and β are assumed to vary independently between their bounds. This type of linear interval equation is referred to as *non-parametric* linear interval equation. In many applications, however, certain dependence exists between interval coefficients of the interval matrix, resulting in the *parametric* linear interval equation. For instance, assume that the interval matrix $\boldsymbol{A}$ in Eq. (2.30) stands for *symmetric* matrices

$$A = \begin{pmatrix} 2 & -\alpha \\ -\alpha & 2 \end{pmatrix},$$

with $\alpha \in [0, 1]$. In this case, the solution set is

$$\Sigma_{sym}(\boldsymbol{A},\, \boldsymbol{b}) = \{x \in \mathbb{R}^n \mid \exists A \in \boldsymbol{A},\ \exists b \in \boldsymbol{b} : Ax = b \text{ with } A^T = A\}.$$

The analytical solution of $A_{sym}x = b$ is

$$x = \begin{pmatrix} 1.2(2-\alpha)/(4-\alpha^2) \\ 1.2(\alpha-2)/(4-\alpha^2) \end{pmatrix}.$$

According to the above analytical solution, the solution set $\Sigma_{sym}(\boldsymbol{A}, \boldsymbol{b})$ is a heavy line indicated in Fig. 2.2, and the hull of the solution set is

$$\boldsymbol{A}^H_{sym} b = \begin{pmatrix} [0.4, 0.6] \\ [-0.6, -0.4] \end{pmatrix}.$$

Clearly,

$$\boldsymbol{A}^H_{sym} b \subseteq \boldsymbol{A}^H b,$$

that is, the hull of the symmetric case is narrower than the hull of the previous general case. This example illustrates the importance of accounting for the dependence when solving for a sharp enclosure of linear interval equations with dependent coefficients.

2.7 Interval Compilers and Programming Environments

There is an increasing amount of software support for interval computations. Researchers have developed such software packages in various programming environments, such as C, C++, Fortran 77, Fortran 90, Pascal, Matlab, Maple, Mathematica and others. This section introduces some available software tools for interval arithmetic. More information about interval software and languages can be found at:
`http://www.cs.utep.edu/interval-comp/main.html`

2.7.1 C/C++ and Fortran

2.7.1.1 Sun Microsystems products

Sun Microsystems, Inc. currently offers both language and hardware support for computing with intervals. Interval arithmetic is intrinsically supported in the Sun Forte™

Fortran 95 compiler and C++ compilers. The regular basic arithmetic operations, intrinsic functions, and logical operations have been extended to intervals.

Hardware support for interval arithmetic is provided in Sun's UltraSPARC III processors with the "Set Interval Arithmetic Mode" (SIAM) instructions. Implementing interval-specific hardware instructions for the basic arithmetic operations $(+, -, \times, \div)$ will eliminate the existing performance deficit in the time required to compute interval versus floating-point expressions (Sun microsystems, 2002).

2.7.1.2 PROFIL/BIAS

PROFIL (Knüppel, 1994b) is a C++ class library supporting the most commonly needed interval arithmetic and real matrix operations. The supported data types are INT (integer), REAL, INTERVAL, vectors and matrices of these types, and complex numbers. PROFIL is based on BIAS (Basic Interval Arithmetic Subroutines), a package which aims to do for interval arithmetic what BLAS (Basic Linear Algebra Subprograms, Dongarra et al. (1988)) has done for non-interval arithmetic; i.e., provide an interface for basic vector and matrix operations with specific and fast implementations for various architectures. The difference between the two is that all interval operations of PROFIL are independent of the internal representation and implementation of the interval types.

The PROFIL/BIAS library includes various scalar interval, vector, integer vector, matrix, interval matrix, and integer matrix operations. It also contains a large selection of standard functions; e.g., trigonometric and log functions, absolute value, etc., as well as utility functions for finding matrix inverses, transposes, identities as well as some interval vector functions. There are also linear system solvers which compute the enclosures of solution sets. There is a procedure for using Fortran library functions with the library, and multiple precision arithmetic is also possible. An extension package called PROFEXT is available which contains miscellaneous functions, test

matrices, subroutines for local minimization, general linear singly linked lists, automatic differentiation subroutines, sample programs, and instructions on how to adapt the library to non-supported architectures.

2.7.1.3 C-XSC

C-XSC (Klatte et al., 1993) is a C++ class library for eXtended Scientific Computing. C-XSC provides the data types of real, interval, complex, and complex interval. For the scalar data types, vector and matrix types are also available. C-XSC contains the appropriate arithmetic and relational operators and mathematical standard functions. The standard functions for the data types interval and complex interval provide range inclusions which are sharp bounds.

2.7.1.4 INTLIB

INTLIB (Kearfott et al., 1994) is a portable interval arithmetic library written in Fortran 77. Functionalities of INTLIB include: elementary interval arithmetic such as interval addition, subtraction, multiplication, division; interval standard functions such as exponential, logarithmic, trigonometric, inverse trigonometric, and other functions; utility and error-printing functions: data conversion, midpoint, width, absolute value, and others; and interval set operations: union, intersection, subset, superset, and others. INTLIB is portable to any commonly used platform. It is freely available through the Internet. Based on INTLIB, a Fortran 90 library for interval arithmetic has been published by Kearfott (1995).

2.7.1.5 GlobSol

GlobSol (Global Solutions) is a public domain package written in Fortran 90 that includes an interval as a user defined data type. GlobSol was designed primarily to be a global optimization package. It finds all rigorously verified solutions to constrained and unconstrained global optimization problems. It also finds all rigorously verified

solutions to algebraic systems of equations. The features of GlobSol includes:

- self-contained interval arithmetic based on INTLIB,
- automatic differentiation based on operator overloading,
- an advanced combination of techniques including constraint propagation, an innovative method of finding approximate feasible points, epsilon inflation in verification, set complementation techniques to avoid large clusters of boxes, and a careful consideration of stopping criteria and tolerance.

GlobSol is freely available through the Internet at: `http://www.mscs.mu.edu/~globsol`

2.7.2 Matlab

2.7.2.1 b4m

b4m (Zemke, 1998) is a free interval arithmetic toolbox for Matlab. It has been tested under Matlab 5.1, Matlab 5.2 and Matlab 5.3 with Windows and Unix systems. The toolbox b4m has been designed

- to use the ANSI C interval arithmetic library BIAS (Knüppel, 1994a) in an interactive way and
- to add interval arithmetic operations and inclusion algorithms to the standard floating point environment Matlab.

The toolbox b4m consists of a new data type interval and of arithmetical operations between arguments of type double and interval. The elementary operations are performed using BIAS developed by Knüppel (1994a). The toolbox b4m tries to combine the efficiency of BIAS and the ease of use of Matlab. The interface between BIAS and Matlab is implemented Mex-files. The user interface consists of ordinary M-files.

2.7.2.2 INTLAB

INTLAB (Rump, 2002; Hargreaves, 2002) is a Matlab toolbox for interval arithmetic. It is comprised of

- interval arithmetic for real and complex data including scalars, vectors, matrices, and sparse matrices;
- automatic differentiation
  - gradients to solve systems of nonlinear equations,
  - Hessians for global optimization;
- rigorous interval standard functions;
- rigorous input and output;
- multiple precision interval arithmetic.

INTLAB is written entirely in Matlab code to assure best portability. INTLAB also makes extensive use of BLAS (Basic Linear Algebra Subprograms, Dongarra et al. (1988)) to assure fast computing time, comparable to pure floating point arithmetic.

2.7.3 Maple

intpak and intpakX (Krämer and Geulig, 2001) are interval packages for Maple. The package intpak is comprised of the following features:

- interval data type as basic data type for interval computations, accompanied by functions for interval construction and conversion,
- basic arithmetic operations,
- basic interval functions (root and power, exponential function and logarithm, trigonometric functions).

The package intpakX is based on intpak. It introduced a wide range of additional features:

- interval Newton method,
- range enclosure for real-valued functions of one or two real variables,
- graphic output for the implemented methods.

The package intpakX is distributed as a share library with Maple.

CHAPTER 3

INTERVAL FEA: LITERATURE REVIEW

This chapter presents a review of the commonly used methods for linear static interval finite element analysis. The merits and limitations of each method are discussed.

3.1 Deterministic FEA

We start with the brief review of the deterministic finite element method. In this section, Einstein's summation convention over repeated indices is enforced for the equations expressed in index notation.

Consider a body of quasistatic linearly elastic material. The governing differential equations of equilibrium for this problem are

$$\sigma_{ij,j} + F_i = 0, \tag{3.1}$$

with some essential boundary conditions and natural boundary conditions.
In Eq. (3.1), σ_{ij} is the stress tensor and F_i is the body force. The natural boundary conditions involve surface tractions

$$\phi_i = \sigma_{ij} n_j \quad \text{on } \Gamma \tag{3.2}$$

where ϕ is the traction force acting on a surface with outward unit normal n, and Γ is the surface on which traction forces are prescribed. Some concentrated loads p_c may also be applied on the boundary.

The linearized strain-displacement relations are

$$\varepsilon_{ij} = \frac{1}{2}(\tilde{u}_{i,j} + \tilde{u}_{j,i}) \tag{3.3}$$

where ε_{ij} is the strain tensor, and $\tilde{u}_i$ represents the displacement, where a tilde is used to distinguish the "exact" displacement field from the nodal displacements in finite element analysis.

Finite element formulation can be obtained using variational methods or weighted residual methods (Gallagher, 1975; Zienkiewicz, 1977; Bathe, 1996; Cook et al., 2002). In solid mechanics, the principle of stationary potential energy is often used. The principle of stationary potential energy states that (Cook et al., 2002) "Among all admissible configurations of a conservative system, those that satisfy the equations of equilibrium make the potential energy Π stationary with respect to small admissible variations of displacement". According to the principle of stationary potential energy, one has

$$\Pi = \int_\Omega \frac{1}{2}\sigma^T\varepsilon \; dV - \int_\Omega \tilde{u}^T F \; dV - \int_\Gamma \tilde{u}^T\phi \; dS - u^T p_c, \tag{3.4}$$

$$\delta\Pi = 0. \tag{3.5}$$

Eq. (3.4) is the total potential energy written in matrix form. Eqs. (3.4) and (3.5) can be seen as the variational formulation (weak form) of the governing differential equations of equilibrium (strong form).

For linear elastic conditions, the stress-strain relations can be stated in matrix form as

$$\sigma = C(\varepsilon - \varepsilon_0) + \sigma_0 \tag{3.6}$$

where C is the elasticity matrix, ε_0 and σ_0 are initial strains and initial stresses, respectively. Substitution of Eq. (3.6) into Eq. (3.5) gives

$$\Pi = \int_\Omega \left(\frac{1}{2}\varepsilon^T C\varepsilon - \varepsilon^T C\varepsilon_0 + \varepsilon^T\sigma_0\right) dV - \int_\Omega \tilde{u}^T F \; dV - \int_\Gamma \tilde{u}^T\phi \; dS - u^T p_c, \tag{3.7}$$

In FEA the domain Ω is discretized into subdomains Ω^e (elements). The boundary of Ω^e is denoted as Γ^e. Thus Eq. (3.7) is broken into element contributions and

becomes

$$\Pi = \sum_{i=1}^{N_e} \int_{\Omega^e} \left(\frac{1}{2} \varepsilon^T C \varepsilon - \varepsilon^T C \varepsilon_0 + \varepsilon^T \sigma_0 \right) dV - \sum_{i=1}^{N_e} \int_{\Omega^e} \tilde{u}^T F \, dV - \sum_{i=1}^{N_e} \int_{\Gamma^e} \tilde{u}^T \phi \, dS - u^T p_c \tag{3.8}$$

in which N_e is the number of elements.

In the displacement-based finite element method, the displacements $\tilde{u}$ within element i are interpolated from element nodal displacement vector $(u_e)_i$ by

$$\tilde{u} = N(u_e)_i \tag{3.9}$$

where N is the shape function matrix.

The strain is determined from the displacement field according to the strain-displacement relations in Eq. (3.3). For the interpolated displacement field, the strain is obtained from the nodal displacement u as

$$\varepsilon = Bu \tag{3.10}$$

where B is the strain-displacement matrix. Substitution of Eqs. (3.9) and (3.10) into Eq. (3.8) yields

$$\Pi = \frac{1}{2} \sum_{i=1}^{N_e} (u_e)_i^T k_i (u_e)_i - \sum_{i=1}^{N_e} (u_e)_i^T (p_e)_i - u^T p_c \tag{3.11}$$

in which k_i and $(p_e)_i$ are respectively the stiffness matrix and load vector of i-th element:

$$k_i = \int_{\Omega^e} B^T C B \, dV, \tag{3.12}$$

$$p_e = \int_{\Omega^e} N^T F \, dV + \int_{\Gamma^e} N^T \phi \, dS + \int_{\Omega^e} B^T C \varepsilon_0 \, dV - \int_{\Omega^e} B^T \sigma_0 \, dV. \tag{3.13}$$

To express Eq. (3.11) as a function of the structure nodal displacement u, the element nodal displacement $(u_e)_i$ is written as

$$(u_e)_i = L_i u \tag{3.14}$$

where the matrix L_i is referred to as element Boolean connectivity matrix. L_i contains only zeros and ones, and it has size n_i by n where n_i is the number of degrees of freedom (d.o.f.) in element i and n is the total number of d.o.f. in the structure.

Substitution of Eq. (3.14) into Eq. (3.11) provides

$$\Pi = \frac{1}{2}u^T \left(\sum_{i=1}^{N_e} L_i^T k_i L_i \right) u - u^T \sum_{i=1}^{N_e} L_i^T (p_e)_i - u^T p_c \tag{3.15}$$

Making Π stationary with respect to u gives the structural equations

$$\left(\sum_{i=1}^{N_e} L_i^T k_i L_i \right) u = p_c + \sum_{i=1}^{N_e} L_i^T (p_e)_i \tag{3.16}$$

or

$$Ku = p. \tag{3.17}$$

where K is the structure stiffness matrix,

$$K = \sum_{i=1}^{N_e} L_i^T k_i L_i. \tag{3.18}$$

The structure load vector p is composed of two parts:

$$p = p_c + p_b, \tag{3.19}$$

in which p_c = externally applied concentrated loads on structure nodes, p_b = nodal load contributions from all elements, and is obtained as

$$p_b = \sum_{i=1}^{N_e} L_i^T (p_e)_i \tag{3.20}$$

Eq. (3.17) is solved for the system nodal displacement u. For stresses in each element, they can be recovered from Eq. (3.6) with $\varepsilon = Bu$.

3.2 Interval FEA

Interval FEA, as the name suggests, can be viewed as an extension to the foregoing deterministic FEA. The main difference is that in interval FEA, some system parameters are intervals, such as the modulus of elasticity, cross-sectional area, or loads.

Both the stiffness matrix K and the load vector p may contain the interval parameters. Hence, the response of the system will be a function of interval parameters and therefore varies in an interval range itself. The problem herein is to estimate the range of the system response, which may include nodal displacements, element stresses and/or strains.

If the only interval parameter is the applied load, the problem becomes easier as the system matrix K does not involve intervals and the exact range of the system responses can be obtained without difficulties. Mullen and Muhanna (1999) developed an interval arithmetic based algorithm for this purpose. The structural responses under worst case load patterns are obtained efficiently. Based on the work of Mullen and Muhanna (1999), Saxena (2003) studied all possible load patterns for large and complicated structures. Pantelides and Ganzerli (2001) used the superposition method to solve linear elastic problems with interval load. The results were compared with the one obtained using the interval method of Mullen and Muhanna (1999). The comparison showed both methods yielded the exact solution. However, the superposition method is less efficient, especially for problems with a large number of interval loads.

Another special case is the analysis of statically determinate structures (truss, beam and frame) with interval stiffness. In this case, the structural internal forces are independent of the structural stiffness. Although the structural stiffness is uncertain, the structural internal forces do not change with the stiffness. This characteristic has been exploited in Muhanna and Mullen (2001) to analyze statically determinate structures with interval stiffness. The Lagrange multiplier method was used, and the exact range of displacement was obtained.

More difficult, however, is the general case when both the stiffness matrix $\boldsymbol{K}$ and the load vector $\boldsymbol{p}$ involve intervals. In such a case, the exact range of the system response is difficult to obtain. In practice, the solution of interest is to estimate an outer bound of the true response range.

This chapter summarizes the commonly used methods for linear static interval FEA, including closed-form solution, combinatorial method, perturbation method, sensitivity analysis method, optimization method, and Monte Carlo sampling method.

3.2.1 Closed-form solution

In this method, the problem is solved analytically, and the expressions of the responses are obtained. The expressions are converted to interval expressions by replacing each real parameter α_i by the interval parameter $\boldsymbol{\alpha}_i$, and evaluating them using interval arithmetic. If any interval parameter occurs more than once in the expressions, there is possible overestimation in the result due to the dependence problem. In such a case, the analyst should reformulate the expressions to reduce the number of occurrences of the same interval parameters, when possible.

This method was used in Rao and Berke (1997), Kulpa et al. (1998), Muhanna and Mullen (2001), Corliss et al. (2004) for linear static structural analysis. The closed form solution is only possible in very simple problems; therefore, this method does not provide a sufficiently general methodology for the interval FEA.

3.2.2 Combinatorial method

If $f(\alpha_1, \ldots, \alpha_m)$ denotes a monotonic function of the parameters within the intervals $\boldsymbol{\alpha}_1, \ldots, \boldsymbol{\alpha}_m$, the range of f can be determined by considering all possible combinations of the bounds of the interval parameters. Let the interval parameters $\boldsymbol{\alpha}_i$ be denoted as an interval number as

$$\boldsymbol{\alpha}_i = [\underline{\alpha_i},\ \overline{\alpha}_i] = [\alpha_i^{(1)},\ \alpha_i^{(2)}].$$

Introducing all possible combinations of the bounds of the interval parameters into analysis:

$$\begin{aligned} &f_r = f(\alpha_1^{(i)}, \alpha_2^{(j)}, \ldots, \alpha_m^{(s)}), \\ &i = 1,\ 2;\ j = 1,\ 2;\ \ldots\ s = 1,\ 2;\ r = 1, 2, \ldots, 2^m \end{aligned} \tag{3.21}$$

where f_r denotes the value of f for a particular combination of the bounds of the intervals $\boldsymbol{\alpha}_1, \ldots, \boldsymbol{\alpha}_m$. The range of function f can be represented as an interval number as

$$[\underline{f},\ \overline{f}] = \left[\min_{r=1,2,\ldots,2^m}(f_r)\ ,\ \max_{r=1,2,\ldots,2^m}(f_r) \right]. \tag{3.22}$$

The primary advantage of this method is that it is straightforward to apply to interval FEA. Any existing deterministic finite element code can be used for the calculations in Eq. (3.21). The combinatorial method was used in Muhanna and Mullen (1995), Rao and Berke (1997), Ganzerli and Pantelides (1999) for linear static structural analysis. However, it must be noted that the combinatorial method gives exact response range only if the system response is monotonic with respect to each parameter in its interval range. For the general case of FEA when the stiffness matrix involves intervals, the monotonicity is not guaranteed (McWilliam, 2000), and the interval obtained in Eq. (3.22) is only an inner bound of the true response range. Further, this method has exponential complexity. The computational cost increases exponentially with the number of interval parameters. For m interval parameters, there are 2^m combinations for which the deterministic FEA has to be performed. The exponential complexity limits the applicability of the combinatorial method to rather small systems.

It is worthwhile to point out that the hull of a general non-parametric linear interval equation $\boldsymbol{A}\boldsymbol{x} = \boldsymbol{b}$ can be obtained by solving for all possible combinations of the upper and lower bounds of the interval coefficients of the matrix $\boldsymbol{A}$ and vector $\boldsymbol{b}$ (Kulpa et al., 1998). However, this method is not applicable to interval FEA. Firstly, this algorithm is of exponential complexity. Consider a linear interval system of equations with an interval coefficient matrix $\boldsymbol{A} \in \mathbb{IR}^{n\times n}$ and an interval right-hand vector $\boldsymbol{b} \in \mathbb{IR}^n$. When all coefficients in $\boldsymbol{A}$ and $\boldsymbol{b}$ are intervals, the algorithm must solve 2^{n^2+n} linear systems of n equations; hence, its practical value is small. Secondly, this algorithm assumes all coefficients in $\boldsymbol{A}$ are independent. However, the coefficients of the interval stiffness matrix are dependent on each other through the

interval parameters. As a consequence of not accounting for dependence, this method computes excessively conservative bounds of the response range.

3.2.3 Perturbation method

The basic idea behind perturbation method is to calculate the changes to the responses that takes place when a *small* change (perturbation) is made to the original system. Consider the equilibrium equations that arise in the static finite element analysis

$$K_0 u_0 = p_0 \tag{3.23}$$

where K_0 is the nominal (unperturbed) stiffness matrix of the finite element assemblage, p_0 is the nominal load vector, and u_0 is the nominal displacement vector. When the input parameters have small changes, the stiffness matrix and load vector will change to $K_0 + \Delta K$ and $p_0 + \Delta p$. ΔK and Δp denote the small changes to the structure stiffness matrix and load vector, respectively. According to Chen (1999), the perturbed system can be written as

$$(K_0 + \Delta K)(u_0 + \Delta u) = p_0 + \Delta p. \tag{3.24}$$

Expanding Eq. (3.24) gives

$$K_0 u_0 + K_0 \Delta u + \Delta K u_0 + \Delta K \Delta u = p_0 + \Delta p. \tag{3.25}$$

Neglecting the higher order part $\Delta K \Delta u$ and using Eq. (3.23), one fines that

$$\Delta u \approx K_0^{-1}(\Delta p - \Delta K u_0). \tag{3.26}$$

Then the displacement of the perturbed system can be approximated by

$$u = u_0 + \Delta u \approx u_0 + K_0^{-1}(\Delta p - \Delta K u_0). \tag{3.27}$$

Qiu and Elishakoff (1998) used the first-order perturbation method and interval arithmetic to determine the bounds of static displacements of structures under interval

modulus of elasticity and interval loads. This method does not consider the dependence that exists between the interval coefficients of the stiffness matrix and load vector, therefore, the obtained result is overly conservative. To handle the dependence problem, a perturbation method incorporated with Taylor series expansion was used in the work of McWilliam (2000) for analysis of truss structures with interval cross-sectional area and interval load. Assume there are m uncertain parameters in the system, where the i-th uncertain parameter is denoted by α_i and its nominal value by α_{0i}. ΔK and Δp are expressed as a first-order Taylor series

$$\Delta K = \sum_{i=1}^{m} (\alpha_i - \alpha_{0i}) \frac{\partial K}{\partial \alpha_i}\Big|_{\alpha_i = \alpha_{0i}} \tag{3.28}$$

$$\Delta p = \sum_{i=1}^{m} (\alpha_i - \alpha_{0i}) \frac{\partial p}{\partial \alpha_i}\Big|_{\alpha_i = \alpha_{0i}} \tag{3.29}$$

Substitution of Eqs. (3.28) and (3.29) into (3.26) gives

$$\Delta u = \sum_{i=1}^{m} \lambda^{(i)} (\alpha_i - \alpha_{0i}) \tag{3.30}$$

where $\lambda^{(i)}$ is a vector such that

$$K_0 \lambda^{(i)} = \left(\frac{\partial p}{\partial \alpha_i}\Big|_{\alpha_i = \alpha_{0i}} - \frac{\partial K}{\partial \alpha_i}\Big|_{\alpha_i = \alpha_{0i}} u_0\right). \tag{3.31}$$

Eq. (3.30) is linear in terms of $(\alpha_i - \alpha_{0i})$. Thus the upper and lower bounds for Δu_j are obtained as

$$\overline{(\Delta u_j)} = \sum_{i=1}^{m} \lambda_j^{(i)} (b_{ij} - \alpha_{0i}), \tag{3.32}$$

$$\underline{(\Delta u_j)} = \sum_{i=1}^{m} \lambda_j^{(i)} (c_{ij} - \alpha_{0i}), \tag{3.33}$$

respectively, where

$$b_{ij} = \begin{cases} \overline{\alpha}_i & \text{if } \lambda_j^{(i)} \geq 0, \\ \underline{\alpha}_i & \text{if } \lambda_j^{(i)} < 0, \end{cases} \tag{3.34}$$

$$c_{ij} = \begin{cases} \overline{\alpha}_i & \text{if } \lambda_j^{(i)} < 0, \\ \underline{\alpha}_i & \text{if } \lambda_j^{(i)} \geq 0. \end{cases} \tag{3.35}$$

This method uses the concept of interval to describe uncertainty, but all computations are deterministic. A similar first-order perturbation analysis and Taylor series method was also used in Chen and Yang (2000) and Chen et al. (2002) to calculate bounds on static displacements of structures with interval modulus of elasticity and interval cross-sectional area.

The main advantage of the perturbation method is its analytical tractability. The disadvantage is that the bounds obtained by perturbation analysis are not guaranteed to enclose the true response range, since the higher order term is neglected in Eq. (3.26). Moreover, the perturbation method is justified by the assumption that the perturbation is small. As the parameter variations become large, the estimation based on Eqs. (3.32) and (3.33) will become increasingly inaccurate.

3.2.4 Sensitivity analysis method

The sensitivity analysis method determines the bounds of the structural responses based on the obtained knowledge about the monotonicity of the responses with respect to the system parameters. If the displacement u_i is monotonically increasing in the interval $\boldsymbol{\alpha}_j$, then the derivative $\dfrac{\partial u_i}{\partial \alpha_j}$ is always positive. In this case, the maximum of u_i is attained when $\alpha_j = \overline{\alpha}_j$. Similarly, if the response u_i is decreasing in α_j, the maximum of u_i is attained when $\alpha_j = \underline{\alpha_j}$.

Consider the static finite element equation

$$Ku = p. \tag{3.36}$$

Let the system parameters described by a vector $\alpha = (\alpha_1, \ldots, \alpha_m)^T$. The displacement sensitivity with respect to α_j can be obtained as

$$\frac{\partial K}{\partial \alpha_j} u + K \frac{\partial u}{\partial \alpha_j} = \frac{\partial p}{\partial \alpha_j} \tag{3.37}$$

Rearranging (3.37) gives

$$K \frac{\partial u}{\partial \alpha_j} = \frac{\partial p}{\partial \alpha_j} - \frac{\partial K}{\partial \alpha_j} u, \tag{3.38}$$

and

$$\frac{\partial u}{\partial \alpha_j} = K^{-1}\left(\frac{\partial p}{\partial \alpha_j} - \frac{\partial K}{\partial \alpha_j}u\right). \tag{3.39}$$

Eq. (3.39) can be used to evaluate the sensitivity in the vicinity of a point. However, it is very difficult to study the sensitivity over the entire interval ranges of the parameters. Jasiński and Pownuk (2000) proposed an algorithm with an attempt to check the system's monotonicity over the entire interval ranges of the parameters. The algorithm is presented as the following:

Step 1: Compute an enclosure $\boldsymbol{u}$ of the solution set of $\boldsymbol{K}\boldsymbol{u} = \boldsymbol{p}$.

Step 2: Compute an enclosure of the solution set $\sum\left(\boldsymbol{K},\ \frac{\partial \boldsymbol{p}}{\partial \alpha_j} - \frac{\partial \boldsymbol{K}}{\partial \alpha_j}\boldsymbol{u}\right)$,
assign $\frac{\partial u}{\partial \alpha_j}$ = enclosure of $\sum\left(\boldsymbol{K},\ \frac{\partial \boldsymbol{p}}{\partial \alpha_j} - \frac{\partial \boldsymbol{K}}{\partial \alpha_j}\boldsymbol{u}\right)$.

Step 3: If the upper bound of $\frac{\partial u}{\partial \alpha_j}$ is ≤ 0, then $\frac{\partial u}{\partial \alpha_j} \leq 0$ in the whole interval region;
if its lower bound is ≥ 0, then $\frac{\partial u}{\partial \alpha_j} \geq 0$ in the whole interval region.

The above algorithm was applied in Jasiński and Pownuk (2000) for interval FEA of heat transfer in biological tissue. Popova et al. (2003) used the similar algorithm for FEA of simple composite material with interval modulus of elasticity. Although the above algorithm theoretically can be used to check the monotonicity over the entire interval ranges of the parameters, it is very difficult to apply in practice. The algorithm requires the calculation of the enclosures of a series of parametric linear interval equations in Step 1 and Step 2. For m interval parameters, it needs to solve $m+1$ parametric linear interval equations, which is computationally expensive. Moreover, the success of this algorithm relies on the sharpness of the enclosures of the $m+1$ linear interval equations in Step 1 and Step 2. If the enclosures obtained in Step 1 and Step 2 are not sharp, this algorithm may yield an excessively conservative sensitivity $\frac{\partial u}{\partial \alpha_j}$ with negative lower bound and positive upper bound, which does not

provide useful information about the monotonicity property. Therefore this algorithm is of little practical use for interval FEA.

Pownuk (2004a) has introduced the sensitivity analysis to linear static FEA for large scale truss structures with interval stiffness, under the *assumption* that the displacements are monotonic with respect to each parameter in its interval range. The monotonicity is checked at the midpoint of the interval parameter, and is assumed valid over the entire interval. After determination of the monotonicity, the bounds of displacements can be easily computed. In the algorithm of Pownuk (2004a), the derivatives $\dfrac{\partial u_i}{\partial \alpha_j}$ are calculated at the midpoint of the interval parameter to determine the monotonicity. Kreinovich et al. (2004) proposed an algorithm to determine the monotonicity without calculating the derivatives:

Step 1: Use the midpoint value $\check{\alpha}_1, \ldots, \check{\alpha}_m$ of the interval parameter $\boldsymbol{\alpha}_1, \ldots, \boldsymbol{\alpha}_n$, compute the response u_0.

Step 2: For the parameter α_i, modify the input to $\alpha_i' \neq \alpha_i$, and leave other parameter in their midpoints. Compute the response u'. By comparing the values of u_0 and u', it can be determined whether u is increasing or decreasing in α_i. Repeat this step for everey parameter α_i, $i = 1, \ldots, m$.

Step 3: Use the value $\alpha_1^-, \ldots, \alpha_m^-$ to calculate the lower bounds of u, and the value $\alpha_1^+, \ldots, \alpha_m^+$ to calculate the upper bounds of u, where

- for the parameter α_i for which u increases with α_i, $\alpha_i^- = \underline{\alpha}_i$ and $\alpha_i^+ = \overline{\alpha}_i$,
- for the parameter α_i for which u decreases with α_i, $\alpha_i^- = \overline{\alpha}_i$ and $\alpha_i^+ = \underline{\alpha}_i$.

The sensitivity analysis method is justified by the assumption that the response u is monotonic with respect to each parameter in its interval range. As mentioned previously in Sec. 3.2.2, the monotonicity assumption is not always satisfied. In the case when monotonicity is not valid, this method fails to provide a solution enclosure,

but a good inner bound usually can be obtained when the uncertainties are small. Another disadvantage of this method is that it is computationally very expensive for problems with a large number of interval variables (Pownuk, 2004a). The inefficiency of the sensitivity analysis method will also be demonstrated in the example in Sec. 5.4.

3.2.5 Optimization method

Another way to find the bounds of the response is to perform two optimizations to compute the minimal and maximal responses when each parameter α_i is constrained to belong to an interval $\boldsymbol{\alpha}_i$. A number of works have been developed to formulate interval FEA as an optimization problem.

Koyluoglu et al. (1995) analyzed frames with interval bending rigidity and interval loads. The interval element stiffness matrix and interval element load vector were developed. The resulting interval structural equation was solved by the triangle inequality and the linear programming method (Oettli, 1965). Consider the interval system equilibrium equation

$$\boldsymbol{K}\boldsymbol{u} = \boldsymbol{p} \tag{3.40}$$

with $\boldsymbol{K} = [\check{K} - \Delta K, \check{K} + \Delta K]$ and $\boldsymbol{p} = [\check{p} - \Delta p, \check{p} + \Delta p]$, $\boldsymbol{K} \in \mathbb{IR}^{n\times n}$, $\boldsymbol{p} \in \mathbb{IR}^n$, $\Delta K \in \mathbb{R}^{n\times n}$, $\Delta p \in \mathbb{R}^n$. According to Oettli (1965), the satisfaction of the following inequality is necessary and sufficient for u to be in the solution set of Eq. (3.40):

$$|\check{K}u - \check{p}| \leq \Delta K|u| + \Delta p \tag{3.41}$$

which is equivalent to

$$\check{K}u - \Delta K|u| \leq \check{p} + \Delta p, \tag{3.42}$$

and

$$\check{K}u + \Delta K|u| \geq \check{p} - \Delta p. \tag{3.43}$$

Eqs. (3.42) and (3.43) represent a set of $2n$ inequalities. The minimal and maximal values of u can be found by solving the $2n$ coupled linear programming problems.

The above algorithm was also presented in the work of Rao and Berke (1997), Kulpa et al. (1998) for linear static structural problems. The main drawback of this method is that it assumes all interval coefficients in the stiffness matrices vary independently within their bounds. This assumption violates the physics of the problem. The coefficients of $\boldsymbol{K}$ are dependent on each other through the parameter vector $\boldsymbol{\alpha}$. As a consequence of not accounting for dependence, this method computes overly conservative results. In the frame example given in Koyluoglu et al. (1995), only one element possesses interval bending rigidity. As the number of interval parameters increase, the overestimation in the results will be more serious.

Koyluoglu and Elishakoff (1998) introduced a comparison of stochastic FEA and interval FEA applied to a shear frame exhibiting uncertain bending rigidity. For the interval model, the bounds of the displacement were computed from optimizations. No detail information was provided about the optimization method used in this work. As in his previous work (Koyluoglu et al., 1995), dependence was not taken into account in the interval stiffness matrix.

Rao and Chen (1998) developed a Taguchi-oriented search algorithm with an attempt to find the optimum settings of the parameters which yield min/max responses. In one of the examples they showed that 64 operations were needed to obtain the solution, where 128 operations are required by the combinatorial method. That shows the inefficiency of the algorithm, especially in large size problems; and the accuracy of the result is limited to narrow interval parameters only.

Möller et al. (2000) developed an optimization algorithm combining evolution strategy, the gradient method and Monte-Carlo method. The optimization algorithm was applied to both static and dynamic linear/nonlinear structural analysis. The accuracy of the method is not clear since the exact solution was not presented in the paper.

A response surface methodology was used in the work of Akpan et al. (2001b).

The mapping of input parameters to output responses in FEA was approximated by a simple response surface function. Combinatorial optimization was performed on the response surface function to determine the combination of the variables that result in the min/max responses. Validation of the response surface function was not presented in that paper.

Although theoretically interval FEA can be formulated as an optimization problem, the implementation turns out to be far from trivial in general. Firstly, it requires an efficient and robust optimization algorithm. In most FE problems the objective function is nonlinear and complicated, so that often only an approximate solution is achievable. The obtained solution is not always a *global* optimum. Secondly, the optimization method is computationally expensive. For each response quantity, usually two optimization problems have to be solved to find the minimal and maximal values. Therefore, the optimization method is best suited for small problems with a limited number of uncertain parameters.

3.2.6 Monte Carlo sampling method

The Monte Carlo sampling method involves sampling from the intervals of input parameters with hope that the samples will fall sufficiently close to the values giving extremal system responses. If the number of samples is large enough, the lower and upper bounds of the solution set of the simulations could be a good approximation for the actual response range. Since the interval parameters do not have probability information, a probability distribution over the interval should be assumed for the sampling purpose. The distribution can be chosen arbitrarily. In practice, a uniform distribution over the interval is often chosen for convenience. The algorithm for Monte Carlo sampling method is summarized as the following:

Step 1: For j from 1 to N:

- for i from 1 to m, run a random number generator using a uniform distribution on the interval $[\underline{\alpha}_i, \overline{\alpha}_i]$ and store the result in $\alpha_i^{(j)}$;
- using $\alpha_1^{(j)}, \ldots, \alpha_m^{(j)}$, run the deterministic FEA and store the result in $u^{(j)}$.

Step 2: The lower and upper bounds are obtained as:

- $\underline{u} = \min(u^{(1)}, \ldots, u^{(N)})$,
- $\overline{u} = \max(u^{(1)}, \ldots, u^{(N)})$.

In the above algorithm, N is the number of samples, and m is the number of interval parameters. The Monte Carlo sampling method has been used in Koyluoglu et al. (1995), Dessombz et al. (2001), and Kulpa et al. (1998) for the evaluation of alternative methods. The advantage of the Monte Carlo sampling is its convenience to implement. All computations are deterministic. The accuracy is improved with the increase of the number of samples. The disadvantage of this method is its computational inefficiency: it requires a large number of deterministic analysis. Moreover, by its nature, Monte Carlo method samples only a finite number of scenarios, thus the obtained bounds are always inner bounds of the response ranges.

3.3 Need for Alternative Interval FEA

The above review shows that there are still many limitations in the prior works of interval FEA. Most methods, such as the combinatorial method, sensitivity analysis method and Monte Carlo sampling do not guarantee to bound the true response ranges. Only inner bounds are obtained by these methods. On the other hand, a few methods (e.g., Koyluoglu et al., 1995; Jasiński and Pownuk, 2000; Popova et al., 2003) can obtain outer bounds of the response ranges, but the results tend to be excessively conservative with the increase of problem complexity. Another limitation is the computational cost. The methods such as combinatorial method and sensitivity analysis method are computationally very expensive. Therefore,thus there is a need

for a computationally efficient method for interval FEA that is capable of accounting for uncertain parameters and yielding rigorous and sharp bounds on the ranges of the structural responses. It is the aim of this thesis to develop an interval FEA addressing the following requirements:

- *Rigorousness.* If the exact range of the system responses are not achievable, the approximate solution should be guaranteed to enclose the exact ranges of the responses; i.e., an outer bound is obtained.

- *Sharpness.* Given the rigorousness condition is satisfied, the obtained solution should be tight enough to be practically useful; that is, the solution should not be excessively conservative.

- *Computational efficiency.* The interval FEA should be computationally efficient compared with previous works.

- *Scalability.* The accuracy of the interval FEA does not deteriorate with the increase of the problem scale and complexity.

CHAPTER 4

INTERVAL FEA: DEVELOPMENT AND IMPLEMENTATION

As seen in the previous chapter, one of the major limitations of existing methods for FEA with interval parameters is that the obtained result is not guaranteed to enclose the exact response range. Although intervals are used to describe uncertainties, most existing methods for interval FEA do not, or just in some certain steps, use interval arithmetic for computations. In Chapter 2 it was noted that interval arithmetic guarantees to produce an enclosure (outer bound) for the range of a function over whole sets of arguments. This characteristic of interval arithmetic motivates us to develop an interval FEA using interval arithmetic. This methodology can be referred to as "interval arithmetic FEA."

Conceptually, the interval arithmetic FEA consists of the same computational procedures as the deterministic FEA: (1) formulation of element matrices, (2) assembly of elements into a structure matrix, (3) application of loads and boundary conditions, and (4) solution of structural equations. The main difference between the interval arithmetic FEA and the deterministic FEA is that, in the former, some parameters are uncertain and described by intervals, such as material parameters, cross-sectional geometry and load parameters. Hence, the response of the structure will be a function of interval parameters and varies in an interval range itself. The problem herein is to use interval arithmetic to obtain an enclosure for the range of the system response, which may include nodal displacements, element nodal forces and/or stresses. As described in Sec. 2.4, the major challenge of interval computations is to reduce the

overestimation in the results due to the dependence problem, which is peculiar to interval arithmetic. The effectiveness of an interval arithmetic FEA depends to a large degree on the reduction of overestimation. To obtain a sharp result, it is essential to

(a) reduce the occurrences of the same interval variables in the computations, and

(b) place the use of interval arithmetic as late as possible in "mixed" computations (the computations involving both real and interval quantities).

The conventional formulation of FEA, however, is not suitable for the above purposes, as will be demonstrated in Sec. 4.1. New formulation will be developed.

This chapter discusses the development and implementation of the present interval FEA in the context of static linear elastic structural behavior. The concepts of deterministic FEA, such as the derivation of element stiffness matrices and coordinate transformation, are not discussed in detail. Many excellent texts are available for deterministic FEA (e.g., Gallagher, 1975; Zienkiewicz, 1977; Reddy, 1993; Bathe, 1996; Cook et al., 2002).

4.1 Naïve interval arithmetic FEA

A natural idea to implement interval FEA is to convert the deterministic FE formulation by replacing each real parameters with interval parameters and each real operation by its corresponding interval arithmetic operation. This idea is attractive due to its ease of implementation. Unfortunately, such a naïve use of interval arithmetic in FEA (naïve interval FEA) often yields meaningless and overly wide results (Muhanna and Mullen, 1995; Kulpa et al., 1998; Muhanna and Mullen, 2001; Dessombz et al., 2001).

Consider the two-bar structure shown in Fig. 4.1. Only axial displacements are allowed. The structure is subjected to two concentrated loads at node 2 and 3. The

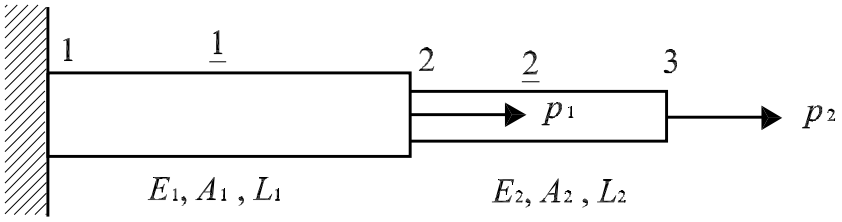

Figure 4.1: Two-bar structure.

cross-sectional area is denoted as A, the modulus of elasticity as E, and the length of the element as L. Subscripts indicate element number. Stiffnesses of the respective elements are k_1 and k_2, where $k_i = E_i A_i / L_i$, $i = 1, 2$. The structural equation for this example is

$$Ku = p \tag{4.1}$$

or

$$\begin{pmatrix} k_1 + k_2 & -k_2 \\ -k_2 & k_2 \end{pmatrix} \begin{pmatrix} u_1 \\ u_2 \end{pmatrix} = \begin{pmatrix} p_1 \\ p_2 \end{pmatrix} \tag{4.2}$$

in which u_1 and u_2 are the axial displacements of node 2 and node 3, respectively. Assume the stiffness terms k_1 and k_2 are uncertain and represented by two interval variables $\boldsymbol{k_1} = [0.95, 1.05]$ and $\boldsymbol{k_2} = [1.9, 2.1]$. The loads are considered deterministic, $p_1 = 0.5$ and $p_2 = 1.0$. Substituting $\boldsymbol{k}_1$ and $\boldsymbol{k}_2$ in Eq. (4.2) gives the interval system equation

$$\begin{pmatrix} [2.85, 3.15] & [-2.1, -1.9] \\ [-2.1, -1.9] & [1.9, 2.1] \end{pmatrix} \begin{pmatrix} \boldsymbol{u_1} \\ \boldsymbol{u_2} \end{pmatrix} = \begin{pmatrix} 0.5 \\ 1 \end{pmatrix}. \tag{4.3}$$

Eq. (4.3) is a linear interval equation. Using the fixed point iteration (see Sec. 4.2.5.4) routine provided in the Matlab interval arithmetic toolbox b4m (1998), $\boldsymbol{u_1}$ and $\boldsymbol{u_2}$

are obtained as:

$$\begin{aligned} \boldsymbol{u_1} &= [-0.0521, 3.0521], \\ \boldsymbol{u_2} &= [0.0983, 3.9017]. \end{aligned}$$

On the other hand, the exact ranges of $\boldsymbol{u}_1$ and $\boldsymbol{u}_2$ can be achieved by solving (4.2) analytically. The inverse of K is

$$K^{-1} = \begin{pmatrix} \dfrac{1}{k_1} & \dfrac{1}{k_1} \\ \dfrac{1}{k_1} & \dfrac{k_1+k_2}{k_1 k_2} \end{pmatrix}.$$

Thus, the displacements are obtained as

$$\boldsymbol{u_1} = \frac{p_1}{\boldsymbol{k_1}} + \frac{p_2}{\boldsymbol{k_1}} = \frac{p_1+p_2}{\boldsymbol{k_1}} = \frac{1.5}{[0.95, 1.05]} = [1.4286, 1.5789],$$

$$\boldsymbol{u_2} = \frac{p_1}{\boldsymbol{k_1}} + \frac{(\boldsymbol{k_1}+\boldsymbol{k_2})p_2}{\boldsymbol{k_1 k_2}} = \frac{p_1+p_2}{\boldsymbol{k_1}} + \frac{p_2}{\boldsymbol{k_2}} = \frac{1.5}{[0.95, 1.05]} + \frac{1}{[1.9, 2.1]} = [1.9048, 2.1053].$$

Note that the above interval expressions are written in such a way that each interval variable only appears once. Therefore, the dependence problem is avoided and the exact ranges of the expressions are obtained.

Clearly, although the bounds obtained by the naïve interval FEA contain the exact range, they are too conservative to provide useful information. The naïve interval FEA could not even get the correct sign for the lower bound of $\boldsymbol{u}_1$. Interval arithmetic implicitly made the assumption that all interval coefficients in the stiffness matrix vary independently between their bounds. For instance, it treats two interval numbers $[-2.1, -1.9]$ in Eq. (4.3) as two independent interval variables that happen to have the same endpoints. From a physical point of view, these two coefficients are $-k_2$ in Eq. (4.2), and they have to take the same value. It is critical to the

formulation of the interval FEA to identify interval numbers that represent a single physical parameter and prevent the widening of results.

4.2 Computational Procedures

In this section we elaborate on the steps that are involved in the present interval finite element analysis. The following techniques have been developed for the analysis:

- Factorization of interval parameters out of the element stiffness matrices.
- Element-By-Element (EBE) technique for element assembly.
- Penalty functions and Lagrange multipliers for imposition of constraint conditions.
- Fixed point iteration for the solution of the interval structural equations.
- Symbolic manipulations of expressions to avoid dependence in interval computations.

These techniques are generally applicable to the interval FEA, regardless of element type. As specific applications, Sec. 4.2.8 discusses frame analysis under interval modulus of elasticity, interval cross-sectional area, interval moment of inertia and interval loads at the same time. Sec. 4.2.9 discusses plane stress and plane strain problems of isotropic material with interval modulus of elasticity and interval loads.

In an interval finite element model, the following two scenarios for parameter variations might be considered: (a) each element has constant parameter variations, but the variations are different from one finite element to another; (b) the parameter variations are constant over a certain subdomain, but are different from one subdomain to another. In this chapter, the first scenario is considered; that is, the parameters are different and independent for each finite element. This is the most general case and the scenario (b) represents a special case.

4.2.1 Interval element stiffness matrix: factorization of interval parameters

For the finite elements based on assumed displacement fields, the element stiffness matrix is given by Eq. (3.12):

$$k = \int B^T C B \, dV$$

in which B is the strain-displacement matrix, and C is the elasticity matrix. For isotropy and plane stress conditions, the elasticity matrix C is

$$C = \frac{E}{1-\mu^2} \begin{pmatrix} 1 & \mu & 0 \\ \mu & 1 & 0 \\ 0 & 0 & (1-\mu)/2 \end{pmatrix}, \tag{4.4}$$

where μ is the Poisson's ratio, and E is the modulus of elasticity. Assume E is uncertain and described by an interval variable $\boldsymbol{E}$. We may write $\boldsymbol{E}$ as

$$\boldsymbol{E} = \check{E}(1 + \boldsymbol{\delta}) \tag{4.5}$$

where $\check{E}$ is the midpoint of $\boldsymbol{E}$, and $\boldsymbol{\delta}$ is the interval multiplier of $\boldsymbol{E}$. $\boldsymbol{\delta}$ is a zero-midpoint interval, and is defined according to Eq. (2.7) as

$$\boldsymbol{\delta} = \frac{\boldsymbol{E}}{\check{E}} - 1 = [-\mathrm{rad}(\boldsymbol{E})/\check{E},\ \mathrm{rad}(\boldsymbol{E})/\check{E}].$$

Applying Eq. (4.5) to Eq. (3.12), an interval element stiffness matrix $\boldsymbol{k}$ is obtained. It can be decomposed into two parts, the deterministic (midpoint) part $\check{k}$ and the interval part $\check{k}\boldsymbol{d}$:

$$\boldsymbol{k} = \check{k}(I + \boldsymbol{d}) \tag{4.6}$$

where I is an identify matrix, and $\boldsymbol{d}$ is an interval diagonal matrix. $\check{k}$ is the deterministic element stiffness matrix evaluated using the midpoint of $\boldsymbol{E}$. $\check{k}$ can be obtained using the conventional finite element formulation. The matrix $\boldsymbol{d}$ is called the interval

multiplier matrix of the element, and it has the form

$$\boldsymbol{d} = \begin{pmatrix} \boldsymbol{\delta} & & \\ & \ddots & \\ & & \boldsymbol{\delta} \end{pmatrix}. \tag{4.7}$$

In this thesis, it is assumed that the interval parameters can be factored out from the element stiffness matrix as in Eq. (4.6). For example, this factorization is possible for isotropic elements with interval modulus of elasticity, plane elements with interval thickness, truss element with interval length, beam element with interval bending rigidity, etc. In the following discussions, it is assumed that the interval parameters involved in the analysis are the modulus of elasticity and loads. Sec. 4.2.8 discusses frame element with interval modulus of elasticity, interval cross-sectional area and interval moment of inertia at the same time. In that case, the factorization of interval parameters can only be carried out in the local coordinate system. Special treatment will be introduced.

4.2.1.1 Example: truss element

As an example, a two-dimensional truss element with interval modulus of elasticity is considered. This element was implemented in the thesis work to analyze the truss structures with interval stiffness and interval loads. We use this comparatively simple element to illustrate the factorization of interval parameters from the element stiffness matrix.

Consider a uniform prismatic elastic truss (bar) element shown in Fig. 4.2. A node is located at each end. The element has a length of L, cross-sectional area A and elastic modulus E. The element has only axial displacement as degrees of freedom at each node.

For this truss element, the element stiffness matrix in the local coordinate system is

Figure 4.2: A truss element and its nodal d.o.f. (degrees of freedom).

$$k' = \begin{pmatrix} \frac{EA}{L} & -\frac{EA}{L} \\ -\frac{EA}{L} & \frac{EA}{L} \end{pmatrix}. \tag{4.8}$$

Assume the modulus of elasticity E is uncertain and described by an interval variable $\boldsymbol{E}$. Eq. (4.5) is used to rewrite $\boldsymbol{E}$ as

$$\boldsymbol{E} = \check{E}(1 + \boldsymbol{\delta}).$$

Substituting Eq. (4.5) in Eq. (4.8) one has

$$\boldsymbol{k}' = \begin{pmatrix} \frac{\check{E}A}{L} & -\frac{\check{E}A}{L} \\ -\frac{\check{E}A}{L} & \frac{\check{E}A}{L} \end{pmatrix} \left(\begin{pmatrix} 1 & 0 \\ 0 & 1 \end{pmatrix} + \begin{pmatrix} \boldsymbol{\delta} & 0 \\ 0 & \boldsymbol{\delta} \end{pmatrix} \right), \tag{4.9}$$

or

$$\boldsymbol{k}' = \check{k}'(I + \boldsymbol{d}) \tag{4.10}$$

For a truss element of arbitrary orientation (Fig. 4.3), it has four d.o.f. (u_1, v_1, u_2, v_2) in the *global* coordinate system. A rotational coordinate transformation has to be applied to $\boldsymbol{k}'$ to obtain the element stiffness matrix $\boldsymbol{k}$ in the global coordinate system:

$$\boldsymbol{k} = T_e^T \boldsymbol{k}' T_e \tag{4.11}$$

in which T_e is the element transformation matrix, and is given by

$$T_e = \begin{pmatrix} c & s & 0 & 0 \\ 0 & 0 & c & s \end{pmatrix}, \tag{4.12}$$

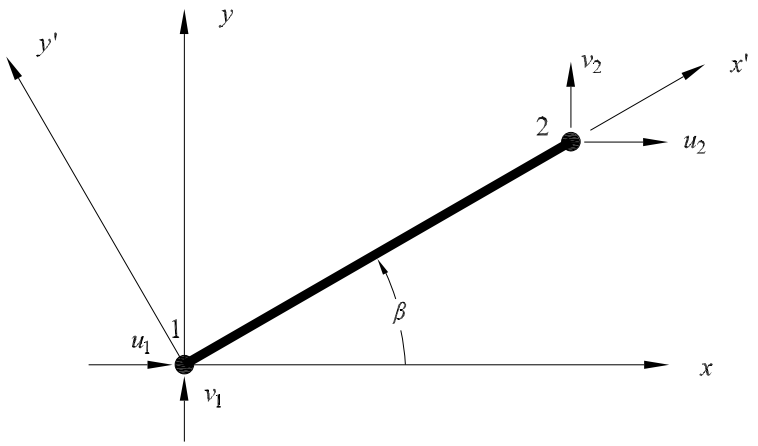

Figure 4.3: A truss element in the global coordinate system xy.

where

$$c = \cos\beta, \quad s = \sin\beta.$$

After the application of coordinate transformation, $\boldsymbol{k}$ is the 4×4 matrix

$$\boldsymbol{k} = \frac{\boldsymbol{E}A}{L} \begin{pmatrix} c^2 & cs & -c^2 & -cs \\ cs & s^2 & -cs & -s^2 \\ -c^2 & -cs & c^2 & cs \\ -cs & -s^2 & cs & s^2 \end{pmatrix}. \tag{4.13}$$

Substituting Eq. (4.5) in Eq. (4.13), $\boldsymbol{k}$ can be expressed as

$$\boldsymbol{k} = \check{k}(I + \boldsymbol{d}), \tag{4.14}$$

where $\check{k}$ is the midpoint of $\boldsymbol{k}$, I is the identity matrix, and $\boldsymbol{d}$ is the interval multiplier matrix, whose diagonal entries are the interval multiplier $\boldsymbol{\delta}$ associated with $\boldsymbol{E}$.

4.2.2 Assembly of elements: Element-By-Element technique

In conventional FEA, the structure stiffness matrix K becomes populated by the addition of stiffness coefficients from elements using Eq. (3.18). This assembly process,

if applied in interval formulation, represents a significant source of dependence. Two stiffness constants, $\boldsymbol{K}_{ij}$ and $\boldsymbol{K}_{mn}$, may have contributions from the same element, thus they are dependent on each other. This dependence cannot be automatically identified by interval arithmetic. It is necessary to track the involvement of each interval variable in the whole computational process. However, the tracking of interval variables in the conventional assembly process is impractical. To overcome this difficulty, an Element-By-Element (EBE) technique is used (Muhanna and Mullen, 2001) for element assembly. The basic idea of the EBE technique is to *detach* the elements so that there are no connections between elements at all, avoiding element coupling in the element assembly procedure. The resulting disjointed structure is referred to as the EBE model of the original structure. As a consequence of detaching elements, a node originally shared by two elements will appear in both elements, but with different node numbering. In this sense, each node belongs to *only* one element in the EBE model.

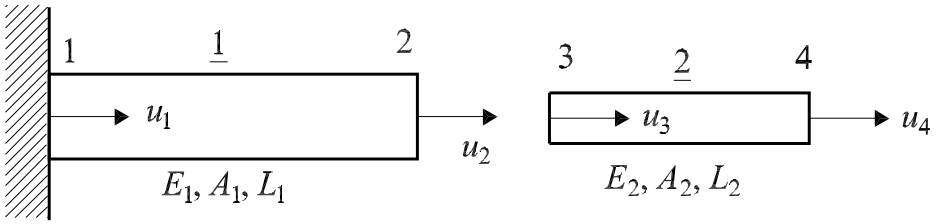

Figure 4.4: Two-bar structure: Element-By-Element model.

The EBE technique may be illustrated using the two-bar structure of Fig. 4.1. The two elements are detached from each other as shown in Fig. 4.4. The node shared by element 1 and 2 now becomes two separate nodes, namely node 2 in element 1 and node 3 in element 2. The axial displacements at nodes are denoted by u_i, $i = 1, \ldots, 4$. For the EBE model in Fig. 4.4, the structure stiffness matrix K is

$$K = \begin{pmatrix} 1 & 0 & 0 & 0 \\ 0 & \dfrac{E_1 A_1}{L_1} & 0 & 0 \\ 0 & 0 & \dfrac{E_2 A_2}{L_2} & -\dfrac{E_2 A_2}{L_2} \\ 0 & 0 & -\dfrac{E_2 A_2}{L_2} & \dfrac{E_2 A_2}{L_2} \end{pmatrix}. \tag{4.15}$$

Note that the boundary condition $u_1 = 0$ has been imposed in K. In general, the structure stiffness matrix K produced by the EBE technique takes a block-diagonal structure,

$$K = \begin{pmatrix} k_1 & & & \\ & k_2 & & \\ & & \ddots & \\ & & & k_{N_e} \end{pmatrix} \tag{4.16}$$

in which each diagonal submatrix is the corresponding element stiffness matrix k_i, $i = 1, \ldots, N_e$, and N_e is the number of elements in the structure.

It is notable that the structure stiffness matrix K given in Eq. (4.16) is singular even after the boundary conditions have been imposed. This is due to the fact that the elements are not connected. To recover the elements' connections and eliminate the singularity of K, proper constraints must be imposed, and the procedure will be introduced in Sec. 4.2.4.

When converting a conventional FE model into its corresponding EBE model, a shared node will appear in different elements, but with different node numbering. Because of the multiple occurrences of the shared nodes, the total number of nodes in the EBE model increases to N_n, N_n = number of nodes per element $\times$ N_e. Correspondingly, the number of d.o.f. in the system increases to n, $n = n_i \times N_e$ where n_i is the d.o.f. per element.

In spite of the increase of the system size, using the EBE technique has the advantage of avoiding element coupling in assembly of elements. This advantage allows factoring out the interval variables from $\boldsymbol{K}$. Substituting Eq. (4.6) in (4.16), the interval structure stiffness matrix $\boldsymbol{K}$ can be written as

$$\boldsymbol{K} = \begin{pmatrix} \boldsymbol{k}_1 & & \\ & \ddots & \\ & & \boldsymbol{k}_{N_e} \end{pmatrix} = \begin{pmatrix} \check{k}_1 & & \\ & \ddots & \\ & & \check{k}_{N_e} \end{pmatrix} \left(I + \begin{pmatrix} \boldsymbol{d}_1 & & \\ & \ddots & \\ & & \boldsymbol{d}_{N_e} \end{pmatrix} \right), \quad (4.17)$$

or

$$\boldsymbol{K} = \check{K}(I + \boldsymbol{D}) \quad (4.18)$$

in which $\boldsymbol{D}$ is called the structure interval multiplier matrix, whose submatrices are $\boldsymbol{d}_i$. Since $\boldsymbol{d}_i$ is interval diagonal matrix, $\boldsymbol{D}$ is also diagonal. Eq. (4.18) suggests that the structure stiffness matrix can be decomposed into two matrices: a real matrix and a diagonal interval matrix. The significance of this decomposition is particularly important for tracking the interval variables in solving the structure system of interval equations, discussed in Sec. 4.2.5.6.

Note that in the matrix $\boldsymbol{D}$, each interval multiplier occurs n_i times. For the example of the EBE two-bar structure, each element has two d.o.f., thus

$$\boldsymbol{D} = \begin{pmatrix} \boldsymbol{d}_1 & & & \\ & \boldsymbol{d}_2 & & \end{pmatrix} = \begin{pmatrix} \boldsymbol{\delta}_1 & & & \\ & \boldsymbol{\delta}_1 & & \\ & & \boldsymbol{\delta}_2 & \\ & & & \boldsymbol{\delta}_2 \end{pmatrix}. \quad (4.19)$$

The multiple occurrences of $\boldsymbol{\delta}$ cause the dependence problem. Later in the formulation, care will be taken to remove this dependence.

4.2.3 Interval loads

In FEA, the structure load vector is composed of two parts:

- external concentrated loads applied directly to structure nodes (p_c in Eq. (3.19)), and
- loads applied to nodes by elements (p_b in Eq. (3.19)).

Both of them could be intervals. This section discusses the calculation of the interval loads $\boldsymbol{p}_c$ and $\boldsymbol{p}_b$ within the context of the EBE model, and the treatment of the dependence problem in interval loads.

4.2.3.1 Externally applied nodal loads: $\boldsymbol{p}_c$

When converting a conventional FE model into its corresponding EBE model, a node originally shared by two elements will appear as two different nodes in the two elements. If there is any externally applied nodal load at the shard node, care should be taken to apply that nodal load properly in the EBE model.

Assume an external concentrated load p_i is applied at the shared node i in the original structure. The shared node i appears in t different elements in the EBE model, with node number $i_1, \ldots, i_t$, respectively. The loads applied at the nodes $i_1, \ldots, i_t$ due to the load p_i are denoted as $p_{i_1}, \ldots, p_{i_t}$, respectively. In the case when p_i is deterministic, $p_{i_1}, \ldots, p_{i_t}$ can be chosen arbitrarily as long as satisfying

$$p_i = \sum_{j=1}^{t} p_{i_j}. \tag{4.20}$$

If p_i is uncertain and varies in an interval $\boldsymbol{p}_i$, one has the interval version of Eq. (4.20):

$$\boldsymbol{p}_i = \sum_{j=1}^{t} \boldsymbol{p}_{i_j}. \tag{4.21}$$

In practice, it is desirable to reduce the number of interval variables in the computation. Therefore, $\boldsymbol{p}_{i_1}, \ldots, \boldsymbol{p}_{i_t}$ are chosen as

$$\begin{aligned} \boldsymbol{p}_{i_1} &= \boldsymbol{p}_i, \\ \boldsymbol{p}_{i_j} &= 0, \quad \text{for } j = 2, \ldots, t \end{aligned} \tag{4.22}$$

That is, the interval load $\boldsymbol{p}_i$ is completely applied at one node, and the remaining nodes have no share of $\boldsymbol{p}_i$.

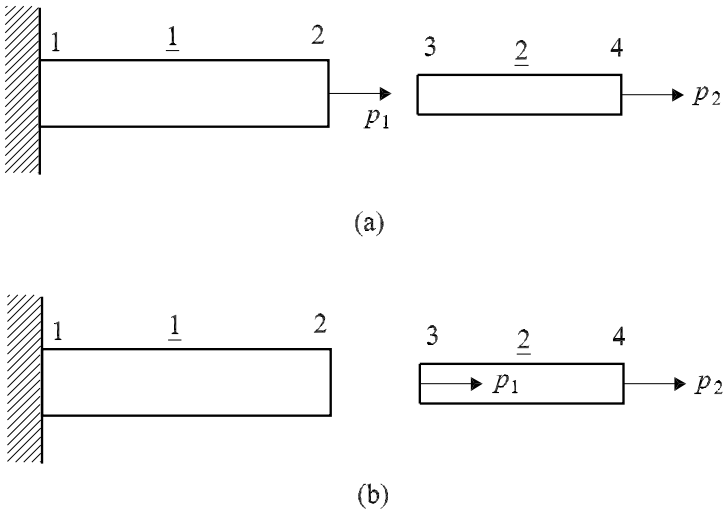

Figure 4.5: EBE model of the two-bar structure (a) p_1 is applied at node 2. (b) p_1 is applied at node 3.

Take the two-bar structure in Fig. 4.1 for example, the concentrated load p_1 is applied at node 2 which is the shared node of element 1 and element 2. In the EBE model of the two-bar structure (Fig. 4.4), the shared node appears in both element 1 and element 2, numbered as node 2 and node 3, respectively. The load p_1 can be applied either at node 2 or node 3, as shown in Fig. 4.5. In the following discussion

of this example, p_1 is applied at node 2. Thus the structure load vector p is

$$p = \begin{pmatrix} 0 \\ p_1 \\ 0 \\ p_2 \end{pmatrix}.$$

4.2.3.2 Nodal loads applied by elements: $\boldsymbol{p}_b$

The load vector p_b is obtained by assembling all element generalized load vectors p_e. In conventional finite element formulation, p_b is given by Eq. (3.20):

$$p_b = \sum_{i=1}^{N_e} L_i^T (p_e)_i.$$

While in the EBE model, p_b has the form

$$p_b = \begin{pmatrix} (p_e)_1 \\ \vdots \\ (p_e)_{N_e} \end{pmatrix} \tag{4.23}$$

in which $(p_e)_i$ is the element load vector of the i-th element, given by Eq. (3.13). It should be noted that dependence problem could occur in the calculation of interval $\boldsymbol{p}_e$. Take the example of a beam element with both ends fixed, the element nodal loads resulting from a uniformly distributed load w are shown in Fig. 4.6. Assuming w is uncertain and represented by an interval variable $\boldsymbol{w}$, the interval element load vector $\boldsymbol{p}_e$ is

$$\boldsymbol{p}_e = \begin{pmatrix} -\boldsymbol{w}L/2 \\ -\boldsymbol{w}L^2/12 \\ -\boldsymbol{w}L/2 \\ \boldsymbol{w}L^2/12 \end{pmatrix}.$$

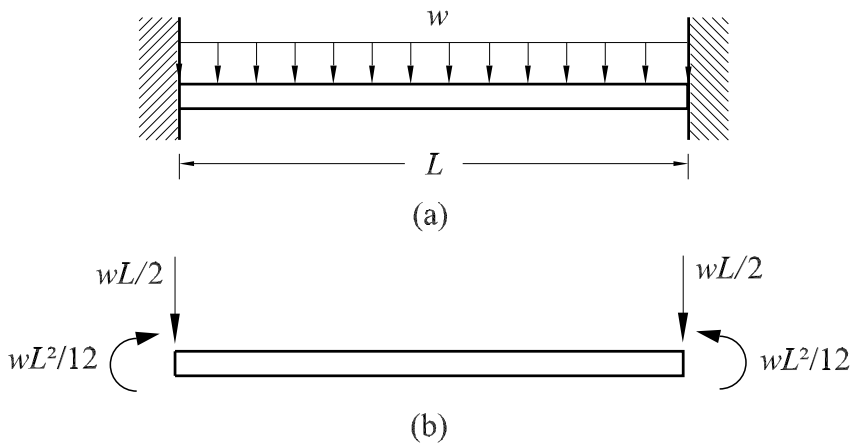

Figure 4.6: Nodal loads for a beam element subjected to uniformly distributed load: (a) actual loading, (b) nodal loads.

It can be seen the components of $\boldsymbol{p}_e$ are related with each other through the parameter $\boldsymbol{w}$. The multiple occurrences of the interval variable $\boldsymbol{w}$ has to be removed from $\boldsymbol{p}_e$ to avoid the overestimation in the computations.

Mullen and Muhanna (1999) considered linear static FEA under interval load. The dependence problem is absent in the developed algorithm and the exact ranges of the response quantities are obtained. In that work, the structure stiffness matrix K is deterministic and is constructed by a conventional element assembly process. The algorithm in Mullen and Muhanna (1999) is modified here to apply within the context of the FEA formulated using the EBE technique.

Consider the case when elements are subjected to interval surface traction. The element load vector due to surface traction is given by

$$\boldsymbol{p}_e = \int N^T \boldsymbol{\phi}(x) dx, \tag{4.24}$$

where N is the shape function, $\boldsymbol{\phi}(x)$ is the applied traction, and is considered to be an interval function. Let $\boldsymbol{\phi}(x)$ on i-th element be given in terms of an m-th order polynomial

$$\boldsymbol{\phi}(x) = \sum_{j=0}^{j=m} \boldsymbol{a}_{ij} x^j. \tag{4.25}$$

The coefficients $\boldsymbol{a}_{ij}$ are intervals, and are expressed as a vector

$$\boldsymbol{F}_i = \begin{pmatrix} \boldsymbol{a}_{i0} \\ \vdots \\ \boldsymbol{a}_{im} \end{pmatrix}. \tag{4.26}$$

Define matrix w_i as

$$w_i = (Q_i^{(0)}, \ldots, Q_i^{(m)}) \tag{4.27}$$

where

$$Q_i^{(j)} = \int N^T x^j dx \tag{4.28}$$

for $j = 0, \ldots, m$. Thus the element load vector $(\boldsymbol{p}_e)_i$ can be expressed as

$$(\boldsymbol{p}_e)_i = \int N^T \boldsymbol{\phi}(x) dx = w_i \boldsymbol{F}_i \ . \tag{4.29}$$

Substituting Eq. (4.29) in (4.23), one has

$$\boldsymbol{p}_b = W \boldsymbol{F}, \tag{4.30}$$

in which W is a deterministic matrix

$$W = \begin{pmatrix} w_1 & & & \\ & w_2 & & \\ & & \ddots & \\ & & & w_{N_e} \end{pmatrix}, \tag{4.31}$$

and $\boldsymbol{F}$ is an interval vector

$$\boldsymbol{F} = \begin{pmatrix} \boldsymbol{F}_1 \\ \boldsymbol{F}_2 \\ \vdots \\ \boldsymbol{F}_{N_e} \end{pmatrix}. \tag{4.32}$$

All interval coefficients of the element surface tractions occur only once in Eq. (4.30). Thus, the dependence problem is eliminated. This treatment is also applicable to interval body force.

4.2.4 Constraints: penalty method and Lagrange multipliers

Because of the fact that the elements are detached in the EBE model, the continuity of the structure is lost, resulting in a singular stiffness matrix K in Eq. (4.16). Also, the EBE model does not automatically satisfy the *compatibility of displacements* at nodes; i.e., a node shared by two elements should have the same displacements when considered as part of either element. Constraints have to be imposed to recover the connections between elements, and to ensure the compatibility of displacements. Two general techniques, namely penalty method and Lagrange multipliers, are used in this thesis to impose constraints.

4.2.4.1 Penalty functions

In steady-state analysis, the variational formulation of a discrete structure model is given in the following form (Gallagher, 1975; Bathe, 1996; Cook et al., 2002)

$$\Pi = \frac{1}{2} u^T K u - u^T p \tag{4.33}$$

with the conditions

$$\frac{\partial \Pi}{\partial u_i} = 0 \quad \text{for all } i \tag{4.34}$$

where Π is the total potential energy. Assume that we want to impose the constraint conditions

$$cu - q = 0 \tag{4.35}$$

where c and q contain constants. Define

$$t = cu - q, \tag{4.36}$$

so that the constraints are satisfied if $t = 0$. The potential energy function Π is augmented by a *penalty function* $\frac{1}{2}t^T\eta t^T$, where η is a diagonal matrix of "penalty numbers" η_i. Therefore

$$\Pi^* = \frac{1}{2}u^T K u - u^T p + \frac{1}{2}t^T \eta t. \tag{4.37}$$

Invoking the stationarity of Π^*, that is $\delta\Pi^* = 0$, results in

$$(K + c^T\eta c)u = p + c^T\eta q \tag{4.38}$$

or

$$(K + Q)u = p + c^T\eta q, \tag{4.39}$$

in which $Q = c^T\eta c$. Considering the constraint conditions in the EBE model takes the form $cu = 0$ and $q = 0$, Eq. (4.39) reduces to

$$(K + Q)u = p \tag{4.40}$$

Q is called a *penalty* matrix. As η grows, u changes in such a way that the constraint equations are more nearly satisfied (Cook et al., 2002). For the interval FEA, the structure stiffness matrix and the load vector are interval quantities, leading to the interval version of Eq. (4.40)

$$(\boldsymbol{K} + Q)\boldsymbol{u} = \boldsymbol{p}. \tag{4.41}$$

Eq. (4.41) defines the structural equation for the interval FEA formulated using the EBE technique and the penalty method. Note that the displacement vector $\boldsymbol{u}$ in the EBE model has the structure

$$\boldsymbol{u} = ((\boldsymbol{u}_e)_1, \ldots, (\boldsymbol{u}_e)_{N_e})^T, \tag{4.42}$$

in which $(\boldsymbol{u}_e)_i$ denotes the nodal displacement vector of i-th element.

The penalty method can be demonstrated using the example of the EBE two-bar structure of Fig. 4.4. Node 2 and node 3 are shared nodes of element 1 and element 2,

thus their displacements should be same in the EBE model. The constraint condition $u_2 = u_3$ implies

$$c = (0 \quad 1 \quad -1 \quad 0),$$

and

$$Q = c^T \eta c = \begin{pmatrix} 0 & 0 & 0 & 0 \\ 0 & \eta & -\eta & 0 \\ 0 & -\eta & \eta & 0 \\ 0 & 0 & 0 & 0 \end{pmatrix}.$$

The structural equation (4.40) becomes

$$\left(\begin{pmatrix} 1 & 0 & 0 & 0 \\ 0 & \frac{E_1 A_1}{L_1} & 0 & 0 \\ 0 & 0 & \frac{E_2 A_2}{L_2} & -\frac{E_2 A_2}{L_2} \\ 0 & 0 & -\frac{E_2 A_2}{L_2} & \frac{E_2 A_2}{L_2} \end{pmatrix} + \begin{pmatrix} 0 & 0 & 0 & 0 \\ 0 & \eta & -\eta & 0 \\ 0 & -\eta & \eta & 0 \\ 0 & 0 & 0 & 0 \end{pmatrix} \right) \cdot \begin{pmatrix} u_1 \\ u_2 \\ u_3 \\ u_4 \end{pmatrix} = \begin{pmatrix} 0 \\ p_1 \\ 0 \\ p_2 \end{pmatrix}$$

The physical interpretation of the penalty method is that a spring of *large* stiffness of η is added to the structure to connect node 2 and node 3, as demonstrated in Fig. 4.7. As η grows, node 2 and node 3 are forced to have the same displacement. Also note that because of the large stiffness of the spring, applying the load p_1 at node 3 will have the same effect as applied at node 2.

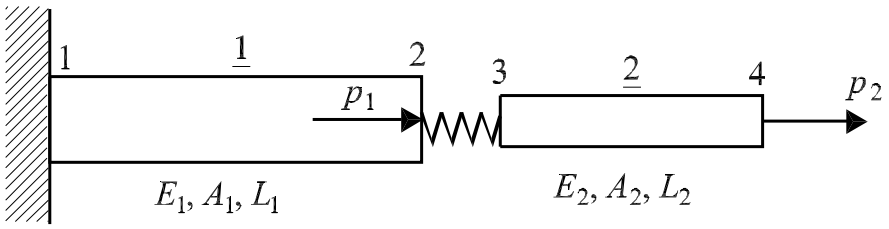

Figure 4.7: Two-bar structure: Element-By-Element model with penalty method.

The advantage of the penalty method is its ease of use. Adding penalty numbers to the structure stiffness matrix is simple and requires no additional equations. However, using the penalty method requires a careful choice of the penalty number. The penalty number should be sufficiently large to fulfill the constraints correctly. On the other hand, as the penalty number increases, the system equation becomes *stiff* and susceptible to *ill-conditioning*. There may be substantial error due to ill-conditioning. Therefore, the penalty number should not be so large as to provoke numerical error. A guideline for choice of the penalty number η is given by Cook et al. (2002):

> "If computer words represent approximately d decimal digits, experience has shown that η should not exceed $10^{d/2}$ if numerical trouble associated with ill-conditioning is to be avoided. Typically $10^{d/2}$ is 10^3 or 10^4 in single precision and 10^6 or 10^7 in double precision."

4.2.4.2 Lagrange multipliers

In the *Lagrange multiplier* method, the left-hand side of the constraint condition $cu - q = 0$ is premultiplied by a row vector λ^T, and added to the right-hand side of potential energy (4.33) to obtain

$$\Pi^{**} = \frac{1}{2}u^T K u - u^T p + \lambda^T (cu - q). \tag{4.43}$$

λ is called the Lagrange multiplier vector for the constraint equation (4.35) (Bathe, 1996; Cook et al., 2002). λ contains as many Lagrange multipliers λ_i as there are constraint equations. Invoking the stationarity of Π^{**}, i.e., $\partial\Pi^{**}/\partial u = 0$ and $\partial\Pi^{**}/\partial\lambda = 0$, one has

$$\begin{pmatrix} K & c^T \\ c & 0 \end{pmatrix} \begin{pmatrix} u \\ \lambda \end{pmatrix} = \begin{pmatrix} p \\ q \end{pmatrix}. \tag{4.44}$$

For the EBE model, $q = 0$ and Eq. (4.44) reduces to

$$\begin{pmatrix} K & c^T \\ c & 0 \end{pmatrix} \begin{pmatrix} u \\ \lambda \end{pmatrix} = \begin{pmatrix} p \\ 0 \end{pmatrix}. \tag{4.45}$$

In the interval FEA, K, u, λ and p become interval quantities, and Eq. (4.45) becomes interval equation

$$\begin{pmatrix} \boldsymbol{K} & c^T \\ c & 0 \end{pmatrix} \begin{pmatrix} \boldsymbol{u} \\ \boldsymbol{\lambda} \end{pmatrix} = \begin{pmatrix} \boldsymbol{p} \\ 0 \end{pmatrix}. \tag{4.46}$$

Eq. (4.46) defines the structural equation for the interval FEA formulated using the EBE technique and Lagrange multipliers.

For the example of the EBE two-bar structure of Fig. 4.4, application of the Lagrange multipliers leads to the structural equation

$$\begin{pmatrix} 1 & 0 & 0 & 0 & 0 \\ 0 & \frac{E_1A_1}{L_1} & 0 & 0 & 1 \\ 0 & 0 & \frac{E_2A_2}{L_2} & -\frac{E_2A_2}{L_2} & -1 \\ 0 & 0 & -\frac{E_2A_2}{L_2} & \frac{E_2A_2}{L_2} & 0 \\ 0 & 1 & -1 & 0 & 0 \end{pmatrix} \cdot \begin{pmatrix} u_1 \\ u_2 \\ u_3 \\ u_4 \\ \lambda \end{pmatrix} = \begin{pmatrix} 0 \\ p_1 \\ 0 \\ p_2 \\ 0 \end{pmatrix}.$$

In the Lagrange multiplier method, λ is introduced as a new set of unknowns in Eq. (4.45). The number of constraints to be imposed in the EBE model is usually very large. Therefore, using Lagrange multipliers will lead to a much larger system than the original system. This makes the Lagrange multiplier method computationally less efficient than the penalty method. For this reason, the penalty method is preferable for the implementation of the present interval FEA.

4.2.5 Solving the linear interval equation

So far we have considered the derivation of the equilibrium equations of an interval finite element system. This included the assemblage of the elements based on the Element-By-Element technique and the imposition of constraints by the penalty method or the Lagrange multipliers. Using the penalty method, the system equilibrium equation is obtained as

$$(\boldsymbol{K} + Q) = \boldsymbol{p}. \tag{4.47}$$

In the case of the Lagrange multipliers being used, the system equation has the form

$$\begin{pmatrix} \boldsymbol{K} & c^T \\ c & 0 \end{pmatrix} \begin{pmatrix} \boldsymbol{u} \\ \boldsymbol{\lambda} \end{pmatrix} = \begin{pmatrix} \boldsymbol{p} \\ 0 \end{pmatrix}. \tag{4.48}$$

Eqs. (4.47) and (4.48) are linear interval equations, and can be represented in a general form

$$\boldsymbol{A}\boldsymbol{x} = \boldsymbol{b}. \tag{4.49}$$

As mentioned in Sec. 2.6, the solution of interest for a linear interval equation is to find a sharp enclosure of its solution set. The overall effectiveness of an interval FEA depends to a large degree on the numerical procedures used for the solution of the interval system equations. The commonly used methods for the solution of linear interval equations include interval Gauss elimination, interval Gauss-Seidel iteration, and fixed point iteration. These methods are presented in the following sections.

4.2.5.1 Preconditioning

To solve a linear interval equation, it is often desirable to transform the original system into a new system with a more tractable coefficient matrix. For the original system $\boldsymbol{A}\boldsymbol{x} = \boldsymbol{b}$, we multiply $\boldsymbol{A}$ and $\boldsymbol{b}$ by a *preconditioning matrix* $R \in \mathbb{R}^{n\times n}$, obtaining a

new system:

$$R\boldsymbol{A}\boldsymbol{x} = R\boldsymbol{b}. \tag{4.50}$$

This is referred to as *preconditioning*. For the preconditioned system, the following theorem can be presented:

Theorem 4.1 (Neumaier, 1990) *Let* $\boldsymbol{A} \in \mathbb{IR}^{n\times n}$ *and* $R \in \mathbb{R}^{n\times n}$. *If* $R\boldsymbol{A}$ *is regular then* $\boldsymbol{A}$ *is regular and*

$$\boldsymbol{A}^H\boldsymbol{b} \subseteq (R\boldsymbol{A})^H(R\boldsymbol{b}). \tag{4.51}$$

Theorem 4.1 states that the hull of the original system is contained in the hull of the preconditioned system. The preconditioning matrix R is usually chosen as $\check{A}^{-1}$, leading to the new system

$$\check{A}^{-1}\boldsymbol{A}\boldsymbol{x} = \check{A}^{-1}\boldsymbol{b}. \tag{4.52}$$

If the interval coefficients of $\boldsymbol{A}$ are not wide, then $\check{A}^{-1}\boldsymbol{A}$ is close to the identity matrix and hence regular. In this case, Eq. (4.52) can be solved with much less overestimation due to the dependence problem than the original system (Neumaier, 1990; Hansen and Walster, 2003).

To use the preconditioning matrix, a considerable amount of work has to be done for computing the midpoint inverse $\check{A}^{-1}$. Unfortunately, in many cases this step is necessary to obtain sharp results (Neumaier, 1990; Hansen and Walster, 2003).

4.2.5.2 Interval Gauss elimination

This algorithm is an interval version of the classic Gauss elimination algorithm known from standard numerical analysis (e.g., Neumaier, 2001; Guan and Lu, 1998). Let us start with a quick review of the class Gauss elimination to motivate its interval version. Starting with the system:

$$\begin{pmatrix} A_{11} & A_{12} & \dots & A_{1n} \\ A_{21} & A_{22} & \dots & A_{1n} \\ \vdots & \vdots & & \vdots \\ A_{n1} & A_{n2} & \dots & A_{nn} \end{pmatrix} \cdot \begin{pmatrix} x_1 \\ x_2 \\ \vdots \\ x_n \end{pmatrix} = \begin{pmatrix} b_1 \\ b_2 \\ \vdots \\ b_n \end{pmatrix}, \tag{4.53}$$

we subtract a suitable multiple of the first row from the other rows such that the subdiagonal entries of the first column becomes zero. If $A_{11} \neq 0$, the multiplication factor for the i-th row is $L_{i1} = A_{i1}/A_{11}$, with $i > 1$. After subtraction, the system is reduced to

$$\begin{pmatrix} A_{11} & A_{12} & \dots & A_{1n} \\ 0 & A_{22}^{(1)} & \dots & A_{1n}^{(1)} \\ \vdots & \vdots & & \vdots \\ 0 & A_{n2}^{(1)} & \dots & A_{nn}^{(1)} \end{pmatrix} \cdot \begin{pmatrix} x_1 \\ x_2 \\ \vdots \\ x_n \end{pmatrix} = \begin{pmatrix} b_1 \\ b_2^{(1)} \\ \vdots \\ b_n^{(1)} \end{pmatrix}, \tag{4.54}$$

in which

$$A_{ik}^{(1)} = A_{ik} - L_{i1}A_{1K} = A_{ik} - A_{i1}A_{11}^{-1}A_{1k} \tag{4.55}$$

$$b_i^{(1)} = b_i - L_{i1}b_1 = b_i - A_{i1}A_{11}^{-1}b_1 \tag{4.56}$$

for $i, k = 2, \dots, n$. After the vector $x^{(1)} = (x_2, \dots, x_n)^T$ are determined from the smaller system $A^{(1)}x^{(1)} = b^{(1)}$, the first variable x_1 is obtained as

$$x_1 = (b_1 - \sum_{k>1} A_{1k}x_k)/A_{11}. \tag{4.57}$$

As long as the corresponding diagonal elements $A_{jj}^{(j-1)}$ remain nonzero, further variables can be eliminated in the same way by

$$\begin{cases} L_{ij} = A_{ij}^{(j-1)}/A_{jj}^{(j-1)}, \\ A_{ik}^{(j)} = A_{ik}^{(j-1)} - L_{ij}A_{jK}^{j-1}, \quad (i, k > j), \\ b_i^{(j)} = b_i^{(j-1)} - L_{ij}b_j^{(j-1)}. \end{cases} \tag{4.58}$$

The variable x_j can then be obtained from $x_{j+1}, \ldots, x_n$ by

$$x_j = (b_j^{(j-1)} - \sum_{k>j} A_{jk}^{(j-1)} x_k)/A_{jj}^{(j-1)}, \text{ for } j = 1, 2, \ldots, n. \tag{4.59}$$

In Eqs. (4.58) and (4.59), $A^{(0)} = A$ and $b^{(0)} = b$.

The multiplication factors L_{ij} $(i > j)$ and the coefficients $U_{jk} = A_{jk}^{(j-1)}$ $(j \leq k)$ in the above formulas can be combined into two triangular matrices

$$L = \begin{pmatrix} 1 & 0 & \ldots & 0 & 0 \\ L_{21} & 1 & \ldots & 0 & 0 \\ L_{31} & L_{32} & \ddots & \vdots & \vdots \\ \vdots & \vdots & & 1 & 0 \\ L_{n1} & L_{n2} & \ldots & L_{nn-1} & 1 \end{pmatrix}, \quad U = \begin{pmatrix} U_{11} & U_{12} & \ldots & & U_{1n} \\ 0 & U_{22} & \ldots & & U_{2n} \\ 0 & 0 & \ddots & & \\ \vdots & \vdots & & \ddots & \vdots \\ 0 & 0 & \ldots & 0 & U_{nn} \end{pmatrix}, \tag{4.60}$$

such that $A = LU$. The coefficients of L and U are calculated from

$$L_{ik} = (A_{ik} - \sum_{j>k} L_{ij} U_{jk})/U_{kk} \quad \text{for } i > k, \tag{4.61}$$

$$U_{ik} = A_{ik} - \sum_{j<i} L_{ij} U_{jk} \quad \text{for } i \leq k. \tag{4.62}$$

Thus, Gauss elimination effectively consists in a decomposition of A into the product of two triangular matrices L and U. The solution of $Ax = b$ is reduced to two triangular systems $Ly = b$ and $Ux = y$, which can be easily solved by forward substitution and backward substitution as follows:

$$y_i = b_i - \sum_{j<i} L_{ij} y_j \quad \text{for } i = 1, \ldots, n, \tag{4.63}$$

$$x_i = (y_i - \sum_{k>i} U_{ik} x_k)/U_{ii} \quad \text{for } i = n, n-1, \ldots, 1. \tag{4.64}$$

For interval case when $\boldsymbol{A} \in \mathbb{IR}^{n \times n}$ and $\boldsymbol{b} \in \mathbb{IR}^n$, Eqs. (4.60) to (4.64) remain valid, provided that the intervals $\boldsymbol{A}_{jj}^{(j-1)} = \boldsymbol{U}_{jj}$ does not contain zero. However, due to the

properties of interval arithmetic (see Sec. 2.4 and 2.5), in general, the product of triangular interval matrices $\boldsymbol{L}$ and $\boldsymbol{U}$ does not equal to $\boldsymbol{A}$. Instead, only the weaker relations are valid:

$$\boldsymbol{A} \subseteq \boldsymbol{LU}, \quad \boldsymbol{Ly} \supseteq \boldsymbol{b}, \quad \boldsymbol{Ux} \supseteq \boldsymbol{y}. \tag{4.65}$$

Hence, the resulting interval vector $\boldsymbol{x}$ is an enclosure of the solution set, i.e., $\Sigma(\boldsymbol{A}, \boldsymbol{b}) \subseteq \boldsymbol{x}$.

Interval Gauss elimination can obtain realistic bounds for certain classes of matrices, such as tridiagonal matrices and M-matrices (Neumaier, 1990). For a general equation $\boldsymbol{Ax} = \boldsymbol{b}$, the interval Gauss elimination should be combined with the preconditioning technique to yield useful results (Neumaier, 1990; Hansen and Walster, 2003). This leads to the preconditioned interval Gauss elimination. The preconditioned interval Gauss elimination can be formulated as follows:

Step 1: Compute the midpoint inverse $\check{A}^{-1}$.

Step 2: Precondition the system with $\check{A}^{-1}$, i.e., calculate $\boldsymbol{A'} = \check{A}^{-1}\boldsymbol{A}$, $\boldsymbol{b'} = \check{A}^{-1}\boldsymbol{b}$.

Step 3: Perform the $\boldsymbol{LU}$ decomposition for $\boldsymbol{A'}$ according to Eqs. (4.61) and (4.62).

Step 4: Solve $\boldsymbol{Ly} = \boldsymbol{b'}$ for $\boldsymbol{y}$ by forward substitution.

Step 5: Solve $\boldsymbol{Ux} = \boldsymbol{y}$ for $\boldsymbol{x}$ by backward substitution.

In interval Gauss elimination, it is required all $\boldsymbol{U}_{ii}$ do not contain zero. In practice, column pivoting can be used to avoid division by zero. Among $\boldsymbol{A}_{jj}^{(j-1)}, \ldots, \boldsymbol{A}_{nj}^{(j-1)}$, the one with the largest mignitude is chosen as the pivot element. Recall the mignitude of an interval $\boldsymbol{x}$ is defined as

$$\operatorname{mig}(\boldsymbol{x}) = \begin{cases} \min\{|\underline{x}|, |\overline{x}|\}, & \text{if } 0 \notin \boldsymbol{x} \\ 0 & \text{otherwise.} \end{cases} \tag{4.66}$$

However, even with pivoting, it is still possible to have a $\boldsymbol{U}_{ii}$ containing zero, causing the algorithm to break down. For example (Hargreaves, 2002), if the coefficient matrix is

$$\boldsymbol{A} = \begin{pmatrix} [0.95, 1.05] & [1.95, 2.05] & [2.95, 3.05] \\ [1.95, 2.05] & [3.95, 4.05] & [6.95, 7.05] \\ [1.95, 2.05] & [-0.05, 0.05] & [0.95, 1.05] \end{pmatrix},$$

then the upper triangular matrix $\boldsymbol{U}$ using column pivoting is given by

$$\boldsymbol{U} = \begin{pmatrix} [1.95, 2.05] & [3.95, 4.05] & [6.95, 7.05] \\ [0, 0] & [-4.31, -3.71] & [-6.46, -5.56] \\ [0, 0] & [0, 0] & [-1.23, 0.23] \end{pmatrix}.$$

$\boldsymbol{U}_{33}$ contains zero so that the back-substitution cannot be continued due to division by zero.

4.2.5.3 Interval Gauss-Seidel iteration

If an initial enclosure $\boldsymbol{x}$ of $\boldsymbol{A}^H\boldsymbol{b}$ is already known, a better enclosure may be obtained by interval Gauss-Seidel iteration. Consider a deterministic equation $Ax = b$, $A \in \boldsymbol{A}$ and $b \in \boldsymbol{b}$, the equation is written explicitly in components as

$$\sum_{k=1}^{n} A_{ik}x_k = b_i, \quad \text{for } i = 1, \ldots, n. \tag{4.67}$$

Assuming that $A_{ii} \neq 0$, the i-th variable can be solved from the i-th equation as

$$x_i = (b_i - \sum_{k \neq i} A_{ik}x_k)/A_{ii}. \tag{4.68}$$

Therefore, if an initial enclosure $\boldsymbol{x}$ is known and $0 \notin \boldsymbol{A}_{ii}$,

$$x_i \in \boldsymbol{x}_i' = (\boldsymbol{b}_i - \sum_{k \neq i} \boldsymbol{A}_{ik}\boldsymbol{x}_k)/\boldsymbol{A}_{ii}. \tag{4.69}$$

Since Eq. (4.69) holds for all x with $Ax = b$, $A \in \boldsymbol{A}$ and $b \in \boldsymbol{b}$, $\boldsymbol{x}'$ is an enclosure of the solution set for $\boldsymbol{Ax} = \boldsymbol{b}$. Moreover,

$$\Sigma(\boldsymbol{A}, \boldsymbol{b}) \subseteq \boldsymbol{x}' \cap \boldsymbol{x}, \tag{4.70}$$

thus a new enclosure which is at least as good as the initial one is obtained. The method can be improved by using the already obtained new enclosures for $\boldsymbol{x}_1, \ldots, \boldsymbol{x}_{n-1}$ to compute $\boldsymbol{x}_n$. This leads to the interval Gauss-Seidel iteration:

$$\boldsymbol{x}_i^{(l+1)} = (\boldsymbol{b}_i - \sum_{k<i} \boldsymbol{A}_{ik}\boldsymbol{x}_k^{(l+1)} - \sum_{k>i} \boldsymbol{A}_{ik}\boldsymbol{x}_k^{(l)})/\boldsymbol{A}_{ii} \cap \boldsymbol{x}_i^{(l)}, \quad \text{for } l = 1, 2, \ldots \tag{4.71}$$

The iterations can be terminated if the radii of the components of $\boldsymbol{x}^{(i)}$ are no longer rapidly decreasing (Hargreaves, 2002). The sum of these radii can be calculated after each iteration and compared with the previous sum.

Interval Gauss-Seidel iteration does not work all the time for general $\boldsymbol{A} \in \mathbb{IR}^{n\times n}$. It may happen that some initial enclosure $\boldsymbol{x}$ is not improved at all by the interval Gauss-Seidel iteration (Neumaier, 1990).

4.2.5.4 Fixed point iteration

Fixed point iteration is one of the most used methods for the solution of linear interval equations. This method has been discussed in the works of Gay (1982), Neumaier (1987), Neumaier (1990), Jansson (1991), Rump (1983), Rump (1992) and Rump (2001).

One typical approach to find the solution of a linear system $Ax = b$ is to transform it into a fixed point equation $g(x) = x$, in which

$$g(x) = x - R(Ax - b) = Rb + (I - RA)x, \tag{4.72}$$

where R is a nonsingular matrix. It can be seen R serves as a preconditioning matrix. Eq. (4.72) is the *Krawczyk operator* (Neumaier and Shen, 1990). From Brouwer's fixed point theorem (Brouwer, 1912), it follows that for some interval vector $\boldsymbol{x} \in \mathbb{IR}^n$

$$Rb + (I - RA)x \in \boldsymbol{x} \quad \forall x \in \boldsymbol{x} \tag{4.73}$$

implies

$$\exists x \in \boldsymbol{x} : Ax = b. \tag{4.74}$$

To apply this theorem, one has to verify that the range $Rb+(I-RA)x$ for each $x \in \boldsymbol{x}$ indeed belongs to $\boldsymbol{x}$. This is a range determination problem and can be handled by using interval arithmetic. If an interval vector $\boldsymbol{x}$ can be found satisfying the following condition:

$$Rb + (I - RA)\boldsymbol{x} \subseteq \boldsymbol{x}, \tag{4.75}$$

then $\boldsymbol{x}$ contains the solution of $Ax = b$. The result can be extended to find the enclosure of the solution set of linear interval equation $\boldsymbol{A}\boldsymbol{x} = \boldsymbol{b}$. The following theorem can be presented.

Theorem 4.2 (Rump, 1990) *Let* $\boldsymbol{A} \in \mathbb{IR}^{n\times n}$, $R \in \mathbb{R}^{n\times n}, \boldsymbol{b}, \boldsymbol{x} \in \mathbb{IR}^n$ *be given, if*

$$R\boldsymbol{b} + (I - R\boldsymbol{A})\boldsymbol{x} \subseteq \text{int}(\boldsymbol{x}), \tag{4.76}$$

then R *and every matrix* $A \in \boldsymbol{A}$ *is nonsingular, and*

$$\Sigma(\boldsymbol{A}, \boldsymbol{b}) = \{x \in \mathbb{R}^n \mid \exists A \in \boldsymbol{A},\ \exists b \in \boldsymbol{b} : Ax = b\} \subseteq \boldsymbol{x}, \tag{4.77}$$

where $\text{int}(\boldsymbol{x})$ denotes the interior of $\boldsymbol{x}$. Theorem 4.2 can be presented in a residual form (Neumaier, 1990): if $\boldsymbol{x}^* \in \mathbb{IR}^n$ satisfies

$$R\boldsymbol{b} - R\boldsymbol{A}x_0 + (I - R\boldsymbol{A})\boldsymbol{x}^* \subseteq \text{int}(\boldsymbol{x}^*), \tag{4.78}$$

then

$$\Sigma(\boldsymbol{A}, \boldsymbol{b}) \subseteq \boldsymbol{x}^* + x_0, \tag{4.79}$$

where x_0 is a deterministic vector.

Theorem 4.2 provides an outer estimation of the hull of the solution set. An inner estimation of the hull of the solution set can be obtained based on the following theorem.

Theorem 4.3 (Rump, 1990) *Let* $\boldsymbol{A} \in \mathbb{IR}^{n\times n}$, $R \in \mathbb{R}^{n\times n}, \boldsymbol{b} \in \mathbb{IR}^n$, $x_0 \in \mathbb{R}^n$ *be given, assume* R *is nonsingular and* $\boldsymbol{A}$ *is regular. Define*

$$\begin{aligned} \boldsymbol{q} &= x_0 + R\boldsymbol{b} - R\boldsymbol{A}x_0, \\ \boldsymbol{\Delta} &= (I - R\boldsymbol{A})\left(\Sigma(\boldsymbol{A},\boldsymbol{b}) - x_0\right). \end{aligned} \tag{4.80}$$

Then

$$\inf\left(\Sigma(\boldsymbol{A},\boldsymbol{b})\right) \le \inf(\boldsymbol{q}) + \sup(\boldsymbol{\Delta}), \tag{4.81}$$

$$\sup\left(\Sigma(\boldsymbol{A},\boldsymbol{b})\right) \ge \sup(\boldsymbol{q}) + \inf(\boldsymbol{\Delta}). \tag{4.82}$$

Since $\boldsymbol{\Delta}$ involves $\Sigma(\boldsymbol{A},\boldsymbol{b})$, the right hand sides of Eqs. (4.81) and (4.82) cannot be calculated directly to form an inner estimation. Using an outer estimation $\boldsymbol{x}$ of $\Sigma(\boldsymbol{A},\boldsymbol{b})$, e.g., some outer estimation computed by using Theorem 4.2, and defining

$$\boldsymbol{\Delta}^* = (I - R\boldsymbol{A})\left(\boldsymbol{x} - x_0\right), \tag{4.83}$$

one has

$$\boldsymbol{\Delta} = (I - R\boldsymbol{A})\left(\Sigma(\boldsymbol{A},\boldsymbol{b}) - x_0\right) \subseteq \boldsymbol{\Delta}^*, \tag{4.84}$$

which implies

$$\inf\left(\Sigma(\boldsymbol{A},\boldsymbol{b})\right) \le \inf(\boldsymbol{q}) + \sup(\boldsymbol{\Delta}^*), \tag{4.85}$$

$$\sup\left(\Sigma(\boldsymbol{A},\boldsymbol{b})\right) \ge \sup(\boldsymbol{q}) + \inf(\boldsymbol{\Delta}^*). \tag{4.86}$$

Hence, an inner estimation can be obtained with Δ replaced by Δ^* in Eqs. (4.81) and (4.82):

$$[\inf(\boldsymbol{q}) + \sup(\boldsymbol{\Delta}^*),\ \sup(\boldsymbol{q}) + \inf(\boldsymbol{\Delta}^*)] \subseteq \boldsymbol{A}^H\boldsymbol{b} \tag{4.87}$$

Based on Theorem 4.2 and Theorem 4.3, fixed point iteration can be constructed to obtain outer and inner estimations of the hull of the solution set for a linear interval equation $\boldsymbol{A}\boldsymbol{x} = \boldsymbol{b}$. The procedure is summarized in the following algorithm (Rump, 1992).

Step 1: Calculate the midpoint solution x_0, i.e., use the midpoint $\check{A}$ and $\check{b}$ of $\boldsymbol{A}$ and $\boldsymbol{b}$, solve $\check{A}x_0 = \check{b}$.

Step 2: Calculate the inverse of the midpoint of $\boldsymbol{A}$. Assign $R = (\text{mid}(\boldsymbol{A}))^{-1} = \check{A}^{-1}$, $\boldsymbol{z} = R\boldsymbol{b} - R\boldsymbol{A}x_0$, $\boldsymbol{G} = I - R\boldsymbol{A}$. Initialize $\boldsymbol{x}^* = 0,\ l = 0$.

Step 3: Calculate

$$\boldsymbol{x}^{*(l+1)} = \boldsymbol{z} + \boldsymbol{G}(\boldsymbol{\varepsilon}\boldsymbol{x}^{*(l)}). \tag{4.88}$$

$\boldsymbol{G}$ is the iterative matrix, and $\boldsymbol{z}$ the residual term.

Step 4: If $\boldsymbol{x}^{*(l+1)} \subseteq \text{int}(\boldsymbol{x}^{*(l)})$ or $l >$ maximum number of iterations allowed: stop. Otherwise, update $l = l + 1$, repeat Step 3.

Step 5: If $\boldsymbol{x}^{*(l+1)} \subseteq \text{int}(\boldsymbol{x}^{*(l)})$, then

- $\boldsymbol{A}^H\boldsymbol{b} \subseteq x_0 + \boldsymbol{x}^{*(l+1)} = \boldsymbol{x}$.
- By defining $\boldsymbol{y} = [\inf(\boldsymbol{z}) + \sup(\boldsymbol{G}\boldsymbol{x}^{*(l+1)}), \sup(\boldsymbol{z}) + \inf(\boldsymbol{G}\boldsymbol{x}^{*(l+1)})]$, an inner bound is obtained as $x_0 + \boldsymbol{y} \subseteq \boldsymbol{A}^H\boldsymbol{b}$.

else: no bounds can be computed.

Rohn and Rex (1998) have shown that the algorithm converges if and only if $\rho(|\boldsymbol{G}|) < 1$, where $\rho(|\boldsymbol{G}|)$ is the spectral radius of the absolute value of $\boldsymbol{G}$. The convergence will be discussed in more detail in Sec. 4.2.5.7. The $\boldsymbol{\varepsilon}$ used in the above algorithm is an interval number, serving as an "inflation parameter" to enforce finite termination of the algorithm. $\boldsymbol{\varepsilon}$ has a form of $[1 - \beta, 1 + \beta]$, $\beta \in [0,\ 1]$. Using a small β usually yields a sharper result, but requires more iterations. In general, β is chosen between 0.1 and 0.001.

4.2.5.5 Parametric linear interval equations

It must be noted that the interval Gauss elimination, interval Gauss-Seidel iteration, and fixed point iteration discussed previously do not consider the dependence between

the interval coefficients of the system matrix. In these methods, the interval coefficients in the system matrix are assumed to vary independently between their bounds. This assumption is no longer valid for the interval structural equations that arise in the interval FEA. The structural equations of an interval finite element system are a system of *parametric* linear interval equations. The term "parametric" emphasizes the fact that the interval coefficients in the equation are functions of some physical parameters (e.g., modulus of elasticity), which are uncertain and take interval values. Therefore, Eq. (4.49) is in fact of the form

$$\boldsymbol{A}(\boldsymbol{\alpha})\boldsymbol{x} = \boldsymbol{b}(\boldsymbol{\alpha}), \quad \text{with } \boldsymbol{\alpha} = (\boldsymbol{\alpha}_1, \ldots, \boldsymbol{\alpha}_m)^T, \tag{4.89}$$

where $\boldsymbol{\alpha}_i$, $i = 1, \ldots, m$, are system parameters varying over certain intervals. For every $\alpha \in \boldsymbol{\alpha}$, there is a corresponding real matrix $A(\alpha)$ and a real vector $b(\alpha)$. All the solutions of the deterministic equations $A(\alpha)x = b(\alpha)$ for all $\alpha \in \boldsymbol{\alpha}$ form the solution set of the parametric interval equation, denoted as

$$\Sigma(\boldsymbol{A}(\boldsymbol{\alpha}), \boldsymbol{b}(\boldsymbol{\alpha})) = \{x \in \mathbb{R}^n \mid \exists \alpha \in \boldsymbol{\alpha} : A(\alpha)x = b(\alpha)\}. \tag{4.90}$$

The solution set is connected and bounded if the interval matrix $\boldsymbol{A}(\boldsymbol{\alpha})$ is regular; i.e., $A(\alpha)$ is nonsingular for all $\alpha \in \boldsymbol{\alpha}$. This regularity condition is satisfied for the structural equations of the interval FEA. The solution set $\Sigma(\boldsymbol{A}(\boldsymbol{\alpha}), \boldsymbol{b}(\boldsymbol{\alpha}))$ is usually not an interval vector, and can be of quite complicated shape. The narrowest (tightest) interval vector enclosing $\Sigma(\boldsymbol{A}(\boldsymbol{\alpha}), \boldsymbol{b}(\boldsymbol{\alpha}))$ is referred to as the *hull* of the solution set, denoted as

$$\boldsymbol{A}(\boldsymbol{\alpha})^H \boldsymbol{b}(\boldsymbol{\alpha}) = \Diamond\Sigma(\boldsymbol{A}(\boldsymbol{\alpha}), \boldsymbol{b}(\boldsymbol{\alpha})). \tag{4.91}$$

For each $\alpha \in \boldsymbol{\alpha}$, there is a corresponding $A(\alpha)$ and $b(\alpha)$, and the associated solution is $x = A(\alpha)^{-1}b(\alpha)$. Hence, $\boldsymbol{A}(\boldsymbol{\alpha})^H \boldsymbol{b}(\boldsymbol{\alpha})$ can be expressed as

$$\boldsymbol{A}(\boldsymbol{\alpha})^H \boldsymbol{b}(\boldsymbol{\alpha}) = \Diamond\{A(\alpha)^{-1}b(\alpha) |\ \alpha \in \boldsymbol{\alpha}\}. \tag{4.92}$$

Computing the solution set or the hull of the solution set is difficult in a general case of parametric linear interval equations. For many practical purposes, it is of interest to seek an outer estimation (enclosure), i.e., an interval vector $\boldsymbol{x}$ enclosing the solution set $\Sigma(\boldsymbol{A}(\boldsymbol{\alpha}), \boldsymbol{b}(\boldsymbol{\alpha}))$, while still sharp enough to be practically useful. Within the context of the interval FEA, the enclosure of the system equation represents an outer bound of the ranges of the nodal displacements.

For the solution of parametric linear interval equations, it is essential to handle the dependence problem. At present, however, no methods have been devised for the general case of parametric linear interval equations. A number of algorithms, based on the standard fixed point iteration discussed in Sec. 4.2.5.4, have been proposed for certain types of parametric linear interval equations.

Jansson (1991) proposed an algorithm for computing sharp bounds for the solution sets of linear systems with symmetric matrices with interval coefficients. Using the same symbols as in Sec. 4.2.5.4, the residual term $\boldsymbol{z}$ in Eq. (4.88) is rewritten as

$$\boldsymbol{z}_i = \sum_{\mu=1}^{n} R_{i\mu}(b_\mu - \boldsymbol{A}_{\mu\mu} x_{0\mu}) - \sum_{\substack{\mu,\nu=1 \\ \mu<\nu}}^{n} (R_{i\mu} x_{0\nu} + R_{i\nu} x_{0\mu}) \boldsymbol{A}_{\mu\nu}, \tag{4.93}$$

thus only the upper triangular part of $\boldsymbol{A}$ appear in the formulation. The parametric interval equation developed in interval FEA, however, involves more dependencies than in a symmetric interval equation. Hence, applying this algorithm to the interval FEA leads to results of the same nature of the naïve interval FEA.

Rump (1994) generalized the method for any linear dependence of the system coefficients on interval parameters. The dependence was partially accounted for in this method. Consider the parametric linear interval equation $\boldsymbol{A}(\boldsymbol{\alpha})\boldsymbol{x} = \boldsymbol{b}(\boldsymbol{\alpha})$, where $\boldsymbol{A}(\boldsymbol{\alpha}) \in \mathbb{IR}^{n\times n}$ and $\boldsymbol{b}(\boldsymbol{\alpha}) \in \mathbb{IR}^n$ depend on an interval parameter vector $\boldsymbol{\alpha} \in \mathbb{IR}^m$. Each components $\boldsymbol{A}(\boldsymbol{\alpha})_{ij}$ and $\boldsymbol{b}(\boldsymbol{\alpha})_j$ depends linearly on $\boldsymbol{\alpha}$ means that there are vectors $w(i,j) \in \mathbb{R}^m$ for $0 \le i \le n$, $1 \le j \le n$ with

$$\boldsymbol{A}(\boldsymbol{\alpha})_{ij} = w(i,j)^T \boldsymbol{\alpha}, \quad \boldsymbol{b}(\boldsymbol{\alpha})_j = w(0,j)^T \boldsymbol{\alpha}. \tag{4.94}$$

Using Eq. (4.94), the residual term $\boldsymbol{z}$ in Eq. (4.88) is rewritten as

$$\boldsymbol{z}_i = (\sum_{j,\ v=1}^{n} R_{ij} \cdot (w(0,j) - x_{0v}) \cdot w(j,v))^T \cdot \boldsymbol{\alpha} \tag{4.95}$$

This method accounts for the dependence in the residual term $\boldsymbol{z}$ by factoring out the interval parameter vector $\boldsymbol{\alpha}$. However, the dependence in the iterative matrix $\boldsymbol{G}$ is not considered. This method was used in Popova et al. (2003) for static analysis of linear elastic composite material with interval modulus of elasticity. The example shows that this method gives sharp enclosure for narrow interval parameters, but the accuracy deteriorates with increase of the parameter uncertainties and the number of interval parameters. Moreover, Eq. (4.94) requires the explicit expressions of the dependence relations of the matrix coefficients on each interval parameter, which makes this method difficult to implement in FE formulation.

Dessombz et al. (2001) introduced a modified fixed point iteration for solving the parametric linear interval equations $\boldsymbol{K}\boldsymbol{u} = \boldsymbol{p}$ in the interval FEA. The stiffness matrix $\boldsymbol{K}$ and the load vector $\boldsymbol{p}$ are expressed as:

$$\boldsymbol{K} = K_0 + \sum_{i=1}^{m} \boldsymbol{\alpha}_i K_i, \tag{4.96}$$

$$\boldsymbol{p} = p_0 + \sum_{i=1}^{m} \boldsymbol{\alpha}_i p_i, \tag{4.97}$$

in which $\boldsymbol{\alpha}_1, \ldots, \boldsymbol{\alpha}_m$ are the interval parameters, and all other quantities are deterministic. Applying Eqs. (4.96) and (4.97) to the fixed point iteration, the residual term $\boldsymbol{z}$ is obtained as

$$\boldsymbol{z} = R\boldsymbol{p} - R\boldsymbol{K}x_0 = R(p_0 - K_0 x_0) + \sum_{i=1}^{m} \boldsymbol{\alpha}_i (R(p_i - K_i x_0)), \tag{4.98}$$

and the iterative matrix $\boldsymbol{G}$ is

$$\boldsymbol{G} = I - R\boldsymbol{K} = I - RK_0 - \sum_{i=1}^{m} \boldsymbol{\alpha}_i (RK_i). \tag{4.99}$$

This algorithm has been tested on simple mechanical systems, and leads to a conservative envelope of the transfer functions of the dynamic problems. The same method

was also presented in the work of Popova (2004). In this method, the dependence control becomes less effective with an increase of the number of interval parameters, therefore this algorithm can only handle a limited number of interval parameters.

4.2.5.6 Present algorithm

To incorporate the equation solver with dependence control, it is critical to exploit the special structures of the system equilibrium equations obtained using the EBE technique. In this thesis, the interval Gauss elimination and interval Gauss-Seidel iteration have been tested, but they failed to produce a sharp result. Dependence control is very difficult to implement in the interval Gauss elimination, and the over-estimation accumulated in the elimination process is often significant. The interval Gauss-Seidel iteration requires an initial enclosure to start with, and it does not always yield an improved solution.

The equation-solver developed in this thesis is based on the standard fixed point iteration introduced in Sec. 4.2.5.4. Recall that the structural equations of an interval finite element system formulated using the EBE technique and the penalty method is

$$(\boldsymbol{K} + Q)\boldsymbol{u} = \boldsymbol{p} \tag{4.100}$$

or

$$\boldsymbol{A}\boldsymbol{u} = \boldsymbol{p} \tag{4.101}$$

in which $\boldsymbol{K} \in \mathbb{IR}^{n\times n}$, $\boldsymbol{p} \in \mathbb{IR}^n$, $Q \in \mathbb{R}^{n\times n}$, and $\boldsymbol{A} = \boldsymbol{K} + Q$. Define R as the inverse of the midpoint of $\boldsymbol{A}$,

$$R = (\mathrm{mid}(\boldsymbol{A}))^{-1} = \check{A}^{-1} = (\check{K} + Q)^{-1}, \tag{4.102}$$

and u_0 the midpoint solution of Eq. (4.101),

$$u_0 = \check{A}^{-1}\check{p} = R\check{p}. \tag{4.103}$$

Applying the fixed point iteration to Eq. (4.101) yields

$$\begin{aligned} \boldsymbol{u}^{*(l+1)} &= \boldsymbol{z} + \boldsymbol{G}(\boldsymbol{\varepsilon}\boldsymbol{u}^{*(l)}) \\ &= (R\boldsymbol{p} - R\boldsymbol{A}u_0) + (I - R\boldsymbol{A})(\boldsymbol{\varepsilon}\boldsymbol{u}^{*(l)}). \end{aligned} \tag{4.104}$$

Due to the coefficient-dependence, evaluating Eq. (4.104) directly overestimates the results. To track the involvement of interval parameters in the computations, Eq. (4.18) is used to express $\boldsymbol{K}$ as

$$\boldsymbol{K} = \check{K}(I + \boldsymbol{D}) = \check{K} + \check{K}\boldsymbol{D}.$$

Combining Eqs. (4.18) and (4.104) yields

$$\begin{aligned} \boldsymbol{u}^{*(l+1)} &= (R\boldsymbol{p} - R(\check{K} + Q + \check{K}\boldsymbol{D})u_0) + (I - R(\check{K} + Q + \check{K}\boldsymbol{D}))(\boldsymbol{\varepsilon}\boldsymbol{u}^{*(l)}) \\ &= R\boldsymbol{p} - u_0 - R\check{K}\boldsymbol{D}u_0 - R\check{K}\boldsymbol{D}(\boldsymbol{\varepsilon}\boldsymbol{u}^{*(l)}) \\ &= R\boldsymbol{p} - u_0 - R\check{K}\boldsymbol{D}(u_0 + \boldsymbol{\varepsilon}\boldsymbol{u}^{*(l)}) \\ &= R\boldsymbol{p} - u_0 - R\check{K}\boldsymbol{M}^{(l)}\boldsymbol{\Delta}. \end{aligned} \tag{4.105}$$

As discussed in Sec. 4.2.3, the interval load vector $\boldsymbol{p}$ is obtained as

$$\boldsymbol{p} = \boldsymbol{p}_c + \boldsymbol{p}_b = \boldsymbol{p}_c + W\boldsymbol{F}, \tag{4.106}$$

in which W and $\boldsymbol{F}$ are respectively calculated according to Eqs (4.31) and (4.32). Substitution of Eq. (4.106) into Eq. (4.105) yields

$$\boldsymbol{u}^{*(l+1)} = R\boldsymbol{p}_c + (RW)\boldsymbol{F} - u_0 - R\check{K}\boldsymbol{M}^{(l)}\boldsymbol{\Delta}. \tag{4.107}$$

In the above expression the parentheses ( ) in $(RW)\boldsymbol{F}$ emphasize that the noninterval operation RW should be carried out first, followed by the multiplication of the interval vector $\boldsymbol{F}$. In the following discussions, the expression $R\boldsymbol{p}$ will be used for simplicity. In practice, however, $R\boldsymbol{p}$ should be calculated as $R\boldsymbol{p}_c + (RW)\boldsymbol{F}$.

For the case of deterministic loads, one has $\boldsymbol{p} = \check{p}$, and Eq. (4.105) reduces to a even simpler form

$$\boldsymbol{u}^{*(l+1)} = -R\check{K}\boldsymbol{M}^{(l)}\boldsymbol{\Delta}. \tag{4.108}$$

The iterations are terminated if

$$\boldsymbol{u}^{*(l+1)} \subseteq \text{int}(\boldsymbol{u}^{*(l)}), \tag{4.109}$$

and one has the solution

$$\boldsymbol{u} = u_0 + \boldsymbol{u}^{*(l+1)} = R\boldsymbol{p} - R\check{K}\boldsymbol{M}^{(l)}\boldsymbol{\Delta}. \tag{4.110}$$

Note that in Eqs. (4.105) and (4.108), $R\check{K}\boldsymbol{D}(u_0+\boldsymbol{\varepsilon u}^*)$ is transformed to $R\check{K}\boldsymbol{M}\boldsymbol{\Delta}$. This symbolic manipulation eliminates the dependence problem in $R\check{K}\boldsymbol{D}(u_0+\boldsymbol{\varepsilon u}^*)$. $\boldsymbol{M}$ is an interval matrix with dimension of $n \times N_e$. $\boldsymbol{M}$ contains the components of $u_0 + \boldsymbol{\varepsilon u}^{*(l)}$, and is updated with $\boldsymbol{u}^*$ in each iteration. $\boldsymbol{\Delta}$ is an interval vector with dimension of N_e. It contains the diagonal entries of $\boldsymbol{D}$, but every interval multiplier occurs only once. In general, when $\boldsymbol{D}$ is multiplied by an interval vector $\boldsymbol{u}$, the multiplication can be reformulated as $\boldsymbol{M}\boldsymbol{\Delta}$, in which $\boldsymbol{M}$ is obtained as

$$\boldsymbol{M} = \begin{pmatrix} (\boldsymbol{u}_e)_1 & & & \\ & (\boldsymbol{u}_e)_2 & & \\ & & \ddots & \\ & & & (\boldsymbol{u}_e)_{N_e} \end{pmatrix} \tag{4.111}$$

where $(\boldsymbol{u}_e)_i$ is the displacement vector of i-th element. This technique can be illustrated using the example of the EBE two-bar structure of Fig. 4.4. For this particular example,

$$\boldsymbol{D} = \begin{pmatrix} \boldsymbol{\delta_1} & 0 & 0 & 0 \\ 0 & \boldsymbol{\delta_1} & 0 & 0 \\ 0 & 0 & \boldsymbol{\delta_2} & 0 \\ 0 & 0 & 0 & \boldsymbol{\delta_2} \end{pmatrix}, \quad \boldsymbol{M} = \begin{pmatrix} \boldsymbol{u}_1 & 0 \\ \boldsymbol{u}_2 & 0 \\ 0 & \boldsymbol{u}_3 \\ 0 & \boldsymbol{u}_4 \end{pmatrix}, \quad \boldsymbol{\Delta} = \begin{pmatrix} \boldsymbol{\delta_1} \\ \boldsymbol{\delta_2} \end{pmatrix}.$$

Thus

$$\begin{pmatrix} \boldsymbol{\delta_1} & 0 & 0 & 0 \\ 0 & \boldsymbol{\delta_1} & 0 & 0 \\ 0 & 0 & \boldsymbol{\delta_2} & 0 \\ 0 & 0 & 0 & \boldsymbol{\delta_2} \end{pmatrix} \begin{pmatrix} \boldsymbol{u}_1 \\ \boldsymbol{u}_2 \\ \boldsymbol{u}_3 \\ \boldsymbol{u}_4 \end{pmatrix} = \begin{pmatrix} \boldsymbol{u}_1 & 0 \\ \boldsymbol{u}_2 & 0 \\ 0 & \boldsymbol{u}_3 \\ 0 & \boldsymbol{u}_4 \end{pmatrix} \begin{pmatrix} \boldsymbol{\delta_1} \\ \boldsymbol{\delta_2} \end{pmatrix}. \tag{4.112}$$

The interval quantities $\boldsymbol{\delta}_1$ and $\boldsymbol{\delta}_2$ each occur twice on the left-hand side of Eq. (4.112). This dependence will cause widening of the computed result. By rewriting $\boldsymbol{Du}$ as $\boldsymbol{M\Delta}$, $\boldsymbol{\delta}_1$ and $\boldsymbol{\delta}_2$ only occur once and the dependence is absent.

The equation solving procedure is summarized in the following algorithm:

Step 1: Calculate the midpoint solution $\check{A}u_0 = \check{p}$.

Step 2: Calculate the inverse of the midpoint of $\boldsymbol{A}$. and assign $R = (\mathrm{mid}(\boldsymbol{A}))^{-1} = \check{A}^{-1}$. Initialize $\boldsymbol{u}^* = 0,\ l = 0$.

Step 3: Calculate $\boldsymbol{M}^{(l)}$ according to Eq. (4.111), and $\boldsymbol{u}^{*(l+1)} = R\boldsymbol{p} - u_0 - R\check{K}\boldsymbol{M}^{(l)}\boldsymbol{\Delta}$.

Step 4: If $\boldsymbol{u}^{*(l+1)} \subseteq \mathrm{int}(\boldsymbol{u}^{*(l)})$ or $l >$ maximum number of iterations allowed: stop. Otherwise, update $l = l + 1$, repeat Step 3.

Step 5: If $\boldsymbol{u}^{*(l+1)} \subseteq \mathrm{int}(\boldsymbol{u}^{*(l)})$, then

- $\boldsymbol{A}^H\boldsymbol{p} \subseteq u_0 + \boldsymbol{u}^{*(l+1)} = R\boldsymbol{p} - R\check{K}\boldsymbol{M}^{(l)}\boldsymbol{\Delta} = \boldsymbol{u}$.
- By defining $\boldsymbol{y} = [\inf(\boldsymbol{z}) + \sup(\boldsymbol{G}\boldsymbol{u}^{*(l+1)}), \sup(\boldsymbol{z}) + \inf(\boldsymbol{G}\boldsymbol{u}^{*(l+1)})]$, an inner bound is obtained as $u_0 + \boldsymbol{y} \subseteq \boldsymbol{A}^H\boldsymbol{p}$.

else: no bounds can be computed.

The developed equation-solver has controlled the occurrences of the dependent interval quantities inside the iteration, thus avoiding the drastic overestimation in the naïve interval FEA.

4.2.5.7 Convergence of the fixed point iteration

For the fixed point iteration, Rohn and Rex (1998) have shown that the algorithm converges if and only if

$$\rho(|\boldsymbol{G}|) < 1, \tag{4.113}$$

where $\rho(|\boldsymbol{G}|)$ is the spectral radius of the absolute value of $\boldsymbol{G}$. For this reason, the choice $R = \check{A}^{-1}$ is made so that $\boldsymbol{G} = I - R\boldsymbol{A}$ has a small spectral radius, and the condition Eq. (4.113) is more likely to be satisfied. In general, the spectral radius of $\boldsymbol{G}$ is influenced by two factors: (a) the width of the interval parameters, and (b) the overestimation in $\boldsymbol{G}$ due to dependence problem. The first factor is determined by the physics of the problem. The formulation should minimize the effect of the second factor. If not handled properly, the dependence problem may result in significant overestimation in the value of $\boldsymbol{G}$, even for narrow interval parameters. As a consequence of the overestimation, Eq. (4.113) may not hold, and no enclosure can be found. It is of vital importance to keep the overestimation in $\boldsymbol{G}$ as minimum as possible. In general, the smaller the spectral radius of $|\boldsymbol{G}|$, the faster the convergence of the algorithm, and the smaller the overestimation of the solution. In the proposed iteration of Eq. (4.105), the iterative matrix $\boldsymbol{G}$ takes the form:

$$\begin{aligned} \boldsymbol{G} &= I - R\boldsymbol{A} \\ &= I - R(\check{K} + Q + \check{K}\boldsymbol{D}) \\ &= -R\check{K}\boldsymbol{D}. \end{aligned} \tag{4.114}$$

Hence, all noninterval values are multiplied first and the last multiplication involves the interval quantities. This treatment drastically reduces the overestimation in $\boldsymbol{G}$, and ensures the algorithm will converge for even relatively wide interval parameters.

4.2.6 Stresses and element nodal forces calculation

Once the nodal displacement u is calculated, stresses in each element can be calculated according to Eq. (3.6). If there are no initial stresses or initial strains, the stresses are obtained from

$$\sigma = C\varepsilon, \quad \text{with} \quad \varepsilon = Bu_e.$$

where B is the strain-displacement matrix. Thus,

$$\sigma = CBu_e. \tag{4.115}$$

In deterministic FEA, Eq. (4.115) is evaluated by extracting u_e from u and multiplying by EB. In the interval FEA, $\boldsymbol{u}_e$ and $\boldsymbol{C}$ are interval quantities. Following the same computation practice will bring in significant overestimation, making the bounds of the stresses unnecessarily wide. The reason behind this is that the components of $\boldsymbol{u}_e$ are related with each other through the interval parameters. It is desirable to avoid the direct involvement of $\boldsymbol{u}_e$ in the computations. Recall that the two critical issues in interval computations are: (a) reduce multiple occurrences of the same interval variables, and (b) make the use of interval arithmetic as late as possible in the process.

Suppose the interval nodal displacement $\boldsymbol{u}$ has been calculated after l iterations. According to Eq. (4.110),

$$\boldsymbol{u} = u_0 + \boldsymbol{u}^{*(l+1)} = R\boldsymbol{p} - R\check{K}\boldsymbol{M}^{(l)}\boldsymbol{\Delta},$$

and the element nodal displacement $\boldsymbol{u}_e$ can be extracted from $\boldsymbol{u}$ by

$$\boldsymbol{u}_e = L\boldsymbol{u} = LR\boldsymbol{p} - LR\check{K}\boldsymbol{M}^{(l)}\boldsymbol{\Delta}, \tag{4.116}$$

in which L is the element Boolean connectivity matrix. The interval element elasticity matrix $\boldsymbol{C}$ can be expressed as

$$\boldsymbol{C} = (1 + \boldsymbol{\delta})\check{C}, \tag{4.117}$$

in which $\boldsymbol{\delta}$ is the interval multiplier of the element's interval modulus of elasticity. Substituting Eqs. (4.116) and (4.117) in Eq. (4.115), the interval stress is obtained as

$$\begin{aligned}\boldsymbol{\sigma} &= \boldsymbol{C}B\boldsymbol{u}_e \\ &= \boldsymbol{C}(BLR\boldsymbol{p} - BLR\check{K}\boldsymbol{M}^{(l)}\boldsymbol{\Delta}) \\ &= (1+\boldsymbol{\delta})(\check{C}BLR\boldsymbol{p} - \check{C}BLR\check{K}\boldsymbol{M}^{(l)}\boldsymbol{\Delta}).\end{aligned} \tag{4.118}$$

Eq. (4.118) has minimized the occurrences of the interval quantities, and most sources of the overestimation are eliminated. When evaluating Eq. (4.118), all real operations have to be performed first, followed by the interval computations. If this order is not maintained, the results will not be sharp.

For truss, beam and frame elements, the interest often lies in calculating element internal forces. Take a frame element, for example, in which the axial force, shear force, and moment at the ends of the element can be determined by

$$f = T_e(ku_e - p_e), \tag{4.119}$$

where T_e is the coordinate transformation matrix, u_e is element nodal displacements and $-p_e$ represents the fixed-end reactions. In the present interval FEA, Eq. (4.119) must be calculated with consideration of the dependence problem, as in the stresses calculation. Since the system is assembled using the Element-By-Element technique, $\boldsymbol{K}\boldsymbol{u}$ yields

$$\boldsymbol{K}\boldsymbol{u} = \begin{pmatrix} \boldsymbol{k}_1(\boldsymbol{u}_e)_1 \\ \vdots \\ \boldsymbol{k}_{N_e}(\boldsymbol{u}_e)_{N_e} \end{pmatrix}, \tag{4.120}$$

and

$$\boldsymbol{p}_b = \begin{pmatrix} (\boldsymbol{p}_e)_1 \\ \vdots \\ (\boldsymbol{p}_e)_{N_e} \end{pmatrix}. \tag{4.121}$$

Combining Eqs (4.120) and (4.121), one finds that

$$\boldsymbol{K}\boldsymbol{u} - \boldsymbol{p}_b = \begin{pmatrix} \boldsymbol{k}_1(\boldsymbol{u}_e)_1 - (\boldsymbol{p}_e)_1 \\ \vdots \\ \boldsymbol{k}_{N_e}(\boldsymbol{u}_e)_{N_e} - (\boldsymbol{p}_e)_{N_e} \end{pmatrix}. \tag{4.122}$$

Defining matrix T as

$$T = \begin{pmatrix} (T_e)_1 & & \\ & \ddots & \\ & & (T_e)_{N_e} \end{pmatrix}, \tag{4.123}$$

and using Eqs (4.122) and (4.123), one obtains

$$T(\boldsymbol{K}\boldsymbol{u} - \boldsymbol{p}_b) = \begin{pmatrix} (T_e)_1(\boldsymbol{k}_1(\boldsymbol{u}_e)_1 - (\boldsymbol{p}_e)_1) \\ \vdots \\ (T_e)_{N_e}(\boldsymbol{k}_{N_e}(\boldsymbol{u}_e)_{N_e} - (\boldsymbol{p}_e)_{N_e}) \end{pmatrix}. \tag{4.124}$$

Comparing above with Eq. (4.119), it can be seen $T(\boldsymbol{K}\boldsymbol{u} - \boldsymbol{p}_b)$ gives the element internal forces at nodes for all elements. However, it is not advisable to compute Eq. (4.124) directly since $\boldsymbol{K}$ and $\boldsymbol{u}$ are dependent. From the structural equation $(\boldsymbol{K} + Q)\boldsymbol{u} = \boldsymbol{p}_c + \boldsymbol{p}_b$ we have

$$T(\boldsymbol{K}\boldsymbol{u} - \boldsymbol{p}_b) = T(\boldsymbol{p}_c - Q\boldsymbol{u}). \tag{4.125}$$

The right-hand side of Eq. (4.125) will be calculated to obtain $T(\boldsymbol{K}\boldsymbol{u} - \boldsymbol{p}_b)$. The

displacement $\boldsymbol{u}$ is given by Eq. (4.110) as

$$\boldsymbol{u} = R(\boldsymbol{p}_c + \boldsymbol{p}_b) - R\check{K}\boldsymbol{M}^{(l)}\boldsymbol{\Delta}.$$

Substitution of the expression of $\boldsymbol{u}$ in the right-hand side of Eq. (4.125) yields

$$\begin{aligned} T(\boldsymbol{p}_c - Q\boldsymbol{u}) &= T(\boldsymbol{p}_c - Q(R(\boldsymbol{p}_c + \boldsymbol{p}_b) - R\check{K}\boldsymbol{M}^{(l)}\boldsymbol{\Delta})) \\ &= T(I - QR)\boldsymbol{p}_c - TQR\boldsymbol{p}_b + TQR\check{K}\boldsymbol{M}^{(l)}\boldsymbol{\Delta}. \end{aligned} \tag{4.126}$$

In Eq. (4.126) the dependence of the interval quantities has been minimized and most sources of the overestimation are eliminated. The sharp bounds for element internal forces at nodes for all elements can be obtained.

4.2.7 Formulation using the Lagrange multipliers

The above discussions are based on the interval FEA formulated using the EBE technique and the penalty method. If the Lagrange multiplier method is used instead of the penalty method, the structural equation can be solved by using a similar procedure by the fixed point iteration. The procedure to be followed later to obtain the element stresses or element nodal forces also remains similar to the penalty method case.

Using the EBE technique and Lagrange multipliers one obtains the structural equation

$$\begin{pmatrix} \boldsymbol{K} & c^T \\ c & 0 \end{pmatrix} \begin{pmatrix} \boldsymbol{u} \\ \boldsymbol{\lambda} \end{pmatrix} = \begin{pmatrix} \boldsymbol{p} \\ 0 \end{pmatrix}. \tag{4.127}$$

Eq. (4.127) needs to be solved with dependence control in mind. Using Eq. (4.18), Eq. (4.127) is written as

$$\left(\begin{pmatrix} \check{K} & c^T \\ c & 0 \end{pmatrix} + \begin{pmatrix} \check{K}\boldsymbol{D} & 0 \\ 0 & 0 \end{pmatrix} \right) \begin{pmatrix} \boldsymbol{u} \\ \boldsymbol{\lambda} \end{pmatrix} = \begin{pmatrix} \boldsymbol{p} \\ 0 \end{pmatrix} \tag{4.128}$$

or

$$\boldsymbol{A}\boldsymbol{x} = \boldsymbol{b},$$

where

$$\boldsymbol{A} = \left(\begin{pmatrix} \check{K} & c^T \\ c & 0 \end{pmatrix} + \begin{pmatrix} \check{K}\boldsymbol{D} & 0 \\ 0 & 0 \end{pmatrix} \right), \quad \boldsymbol{x} = \begin{pmatrix} \boldsymbol{u} \\ \boldsymbol{\lambda} \end{pmatrix}, \quad \boldsymbol{b} = \begin{pmatrix} \boldsymbol{p} \\ 0 \end{pmatrix}. \tag{4.129}$$

Define

$$S = \begin{pmatrix} \check{K} & 0 \\ 0 & 0 \end{pmatrix}, \quad \boldsymbol{H} = \begin{pmatrix} \boldsymbol{D} & 0 \\ 0 & 0 \end{pmatrix}. \tag{4.130}$$

Thus

$$\boldsymbol{A} = \check{A} + S\boldsymbol{H}. \tag{4.131}$$

Calculate the inverse of $\check{A}$, and denote

$$R = \check{A}^{-1}, \; x_0 = \check{A}^{-1}\check{b} = R\check{b}. \tag{4.132}$$

Substitution of Eqs. (4.131) and (4.132) in the fixed point iteration yields

$$\begin{aligned} \boldsymbol{x}^{*(l+1)} &= (R\boldsymbol{b} - R\boldsymbol{A})x_0 + (I - R\boldsymbol{A})(\boldsymbol{\varepsilon}\boldsymbol{x}^{*(l)}) \\ &= (R\boldsymbol{b} - R(\check{A} + S\boldsymbol{H})x_0) + (I - R(\check{A} + S\boldsymbol{H}))(\boldsymbol{\varepsilon}\boldsymbol{x}^{*(l)}) \\ &= R\boldsymbol{b} - x_0 - RS\boldsymbol{H}x_0 - RS\boldsymbol{H}(\boldsymbol{\varepsilon}\boldsymbol{x}^{*(l)}) \\ &= R\boldsymbol{b} - x_0 - RS\boldsymbol{H}(x_0 + \boldsymbol{\varepsilon}\boldsymbol{x}^{*(l)}) \\ &= R\boldsymbol{b} - x_0 - RS\boldsymbol{M}^{(l)}\boldsymbol{\Delta}. \end{aligned} \tag{4.133}$$

Here $RS\boldsymbol{H}(x_0 + \boldsymbol{\varepsilon}\boldsymbol{x}^{*(l)})$ is transformed into $RS\boldsymbol{M}^{(l)}\boldsymbol{\Delta}$, so that the interval multipliers occur only once in the computations. The derivations of $\boldsymbol{M}$ and $\boldsymbol{\Delta}$ have been introduced in Sec. 4.2.5.6.

The iterations are terminated if

$$\boldsymbol{x}^{*(l+1)} \subseteq \text{int}(\boldsymbol{x}^{*(l)}), \tag{4.134}$$

and one has

$$\boldsymbol{x} = x_0 + \boldsymbol{x}^{*(l+1)} = R\boldsymbol{b} - RS\boldsymbol{M}^{(l)}\boldsymbol{\Delta}. \tag{4.135}$$

The displacement $\boldsymbol{u}$ can be extracted from $\boldsymbol{x}$ according to Eq. (4.129).

As for stresses, they can be calculated as

$$\begin{aligned} \boldsymbol{\sigma} &= \boldsymbol{C}B\boldsymbol{u}_e \\ &= \boldsymbol{C}BL\boldsymbol{x} \\ &= \boldsymbol{C}(BLR\boldsymbol{b} - BLRS\boldsymbol{M}^{(l)}\boldsymbol{\Delta}) \\ &= (1+\boldsymbol{\delta})(\check{C}BLR\boldsymbol{b} - \check{C}BLRS\boldsymbol{M}^{(l)}\boldsymbol{\Delta}), \end{aligned} \tag{4.136}$$

in which L is a Boolean matrix to extract $\boldsymbol{u}_e$ from $\boldsymbol{x}$.

For truss, beam and frame elements, the solved Lagrange multiplier vector $\boldsymbol{\lambda}$ can be used to calculate internal forces at element ends. As mentioned in Sec. 4.2.6, the term $T(\boldsymbol{K}\boldsymbol{u} - \boldsymbol{p}_b)$ in the EBE model gives the element internal forces at nodes for all elements. From Eq. (4.127) it follows

$$T(\boldsymbol{K}\boldsymbol{u} - \boldsymbol{p}_b) = T(\boldsymbol{p}_c - c^T\boldsymbol{\lambda}). \tag{4.137}$$

The right-hand side of Eq. (4.137) will be calculated. The Lagrange multiplier vector $\boldsymbol{\lambda}$ is extracted from $\boldsymbol{x}$ using a Boolean matrix L,

$$\boldsymbol{\lambda} = L\boldsymbol{x}. \tag{4.138}$$

For the interval vector $\boldsymbol{b} = (\boldsymbol{p} \quad 0)^T$, it can be expressed as

$$\boldsymbol{b} = \boldsymbol{b}_c + \boldsymbol{b}_b, \tag{4.139}$$

in which

$$\boldsymbol{b}_c = \begin{pmatrix} \boldsymbol{p}_c \\ 0 \end{pmatrix}, \quad \boldsymbol{b}_b = \begin{pmatrix} \boldsymbol{p}_b \\ 0 \end{pmatrix}. \tag{4.140}$$

The load $\boldsymbol{p}_c$ is extracted from $\boldsymbol{b}_c$ by a Boolean matrix L_c

$$\boldsymbol{p}_c = L_c \boldsymbol{b}_c, \tag{4.141}$$

and $\boldsymbol{p}_b$ is extracted from $\boldsymbol{b}_b$ by a Boolean matrix L_b

$$\boldsymbol{p}_b = L_b \boldsymbol{b}_b. \tag{4.142}$$

Substituting Eqs. (4.135), (4.138), (4.141) and (4.142) in the right-hand side of Eq. (4.137) yields

$$\begin{aligned} T(\boldsymbol{p}_c - c^T \boldsymbol{\lambda}) &= T(\boldsymbol{p}_c - c^T L(R\boldsymbol{b} - RS\boldsymbol{M}^{(l)}\boldsymbol{\Delta})) \\ &= T(L_c - c^T LR)\boldsymbol{b_c} - Tc^T LR\boldsymbol{b}_b + Tc^T LRS\boldsymbol{M}^{(l)}\boldsymbol{\Delta}. \end{aligned} \tag{4.143}$$

Eq. (4.143) has controlled the occurrences of the interval quantities in the computations. The sharp bounds for element internal forces at nodes are obtained.

4.2.8 Frame analysis under interval material, cross-sectional properties and loads

Frame analysis is very common in structural engineering. This section considers the analysis of two-dimensional frame structures under interval parameters. A frame element can have not only interval modulus of elasticity and interval loads, as usual, but also interval cross-sectional area and interval moment of inertia at the same time. For this case, the procedures introduced in Sec. 4.2.1 to Sec. 4.2.7 are still applicable and can be directly extended. The new technique used is that the coordinate transformation is delayed for the purpose of dependence control.

Figure 4.8: A frame element and its nodal d.o.f.

Consider a uniform frame element with a node at each end. For the case of planar deformation, each node has three d.o.f., namely axial and lateral translations, and rotation (Fig. 4.8). The elementary Euler-Bernoulli beam theory (Ugural and Fenster, 1995) is used. That is, the transverse shear deformation is ignored and only axial and bending deformations are considered. The stiffness matrix for such a frame element may thus be derived by combining the stiffness of a beam under pure bending and a truss element. The two-dimensional frame element stiffness matrix is

$$\boldsymbol{k}' = \begin{pmatrix} \frac{EA}{L} & 0 & 0 & -\frac{EA}{L} & 0 & 0 \\ 0 & \frac{12EI}{L^3} & \frac{6EI}{L^2} & 0 & -\frac{12EI}{L^3} & \frac{6EI}{L^2} \\ 0 & \frac{6EI}{L^2} & \frac{4EI}{L} & 0 & -\frac{6EI}{L^2} & \frac{2}{L} \\ -\frac{EA}{L} & 0 & 0 & \frac{EA}{L} & 0 & 0 \\ 0 & -\frac{12EI}{L^3} & -\frac{6EI}{L^2} & 0 & \frac{12EI}{L^3} & -\frac{6EI}{L^2} \\ 0 & \frac{6EI}{L^2} & \frac{2}{L} & 0 & -\frac{6EI}{L^2} & \frac{4EI}{L} \end{pmatrix}, \tag{4.144}$$

where E is the modulus of elasticity, I is the moment of inertia, and A is the cross-sectional area. Now consider a frame element with interval $\boldsymbol{E}$, $\boldsymbol{I}$ and $\boldsymbol{A}$. By factoring out the interval parameters, $\boldsymbol{k}'$ can be written as

$$\boldsymbol{k}' = \begin{pmatrix} \frac{1}{L} & 0 & 0 & -\frac{1}{L} & 0 & 0 \\ 0 & \frac{12}{L^3} & \frac{6}{L^2} & 0 & -\frac{12}{L^3} & \frac{6}{L^2} \\ 0 & \frac{6}{L^2} & \frac{4}{L} & 0 & -\frac{6}{L^2} & \frac{2}{L} \\ -\frac{1}{L} & 0 & 0 & \frac{1}{L} & 0 & 0 \\ 0 & -\frac{12}{L^3} & -\frac{6}{L^2} & 0 & \frac{12}{L^3} & -\frac{6}{L^2} \\ 0 & \frac{6}{L^2} & \frac{2}{L} & 0 & -\frac{6}{L^2} & \frac{4}{L} \end{pmatrix} \cdot \begin{pmatrix} \boldsymbol{EA} & 0 & 0 & 0 & 0 & 0 \\ 0 & \boldsymbol{EI} & 0 & 0 & 0 & 0 \\ 0 & 0 & \boldsymbol{EI} & 0 & 0 & 0 \\ 0 & 0 & 0 & \boldsymbol{EA} & 0 & 0 \\ 0 & 0 & 0 & 0 & \boldsymbol{EI} & 0 \\ 0 & 0 & 0 & 0 & 0 & \boldsymbol{EI} \end{pmatrix}, \tag{4.145}$$

or

$$\boldsymbol{k}' = s\boldsymbol{d}. \tag{4.146}$$

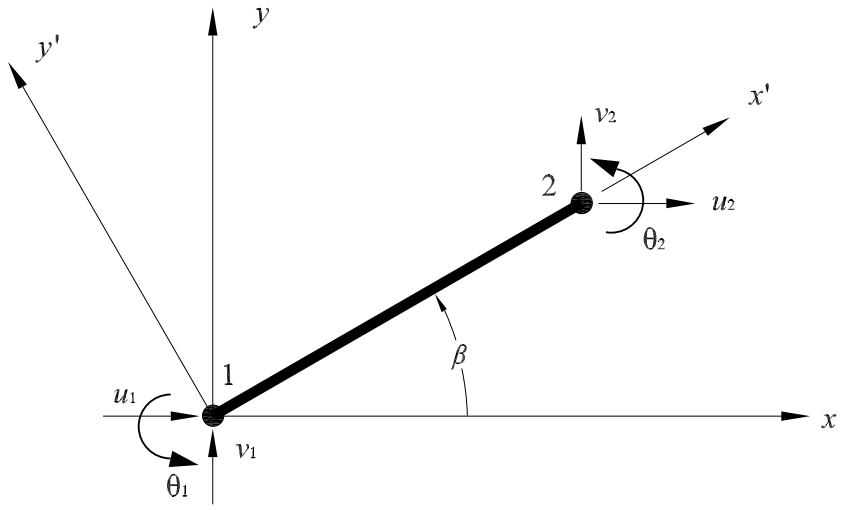

Figure 4.9: A frame element in the global coordinate system xy.

For a frame element of arbitrary orientation (Fig. 4.9), a coordinate transformation needs to be applied to $\boldsymbol{k}'$ to obtain the element stiffness matrix in global coordinates,

$$\boldsymbol{k} = T_e^T \boldsymbol{k}' T_e \tag{4.147}$$

in which T_e is the coordinate transformation matrix, given by

$$T_e = \begin{pmatrix} c & s & 0 & 0 & 0 & 0 \\ -s & c & 0 & 0 & 0 & 0 \\ 0 & 0 & 1 & 0 & 0 & 0 \\ 0 & 0 & 0 & c & s & 0 \\ 0 & 0 & 0 & -s & c & 0 \\ 0 & 0 & 0 & 0 & 0 & 1 \end{pmatrix}, \tag{4.148}$$

where

$$c = \cos\beta, \quad s = \sin\beta.$$

Note that $T_e^T T_e = T_e T_e^T = I$. The coordinate transformation will result in the overlapping of $\boldsymbol{EA}$ and $\boldsymbol{EI}$. Thus, the decomposition of $\boldsymbol{k}$ into a real matrix and an interval diagonal matrix is not possible in this case. To overcome this difficulty, the coordinate transformation will be delayed so that the interval equation can still be solved using the techniques discussed in Sec. 4.2.5.6.

Using Eq. (4.147), the structure stiffness matrix $\boldsymbol{K}$ in the EBE model can be expressed as

$$\boldsymbol{K} = \begin{pmatrix} \boldsymbol{k}_1 & & \\ & \ddots & \\ & & \boldsymbol{k}_{N_e} \end{pmatrix} = \begin{pmatrix} (T_e)_1^T s_1 \boldsymbol{d}_1 (T_e)_1 & & \\ & \ddots & \\ & & (T_e)_{N_e}^T s_{N_e} \boldsymbol{d}_{N_e} (T_e)_{N_e} \end{pmatrix}, \tag{4.149}$$

or

$$\boldsymbol{K} = T^T S \boldsymbol{D} T, \tag{4.150}$$

in which

$$T = \begin{pmatrix} (T_e)_1 & & \\ & \ddots & \\ & & (T_e)_{N_e} \end{pmatrix}, \quad S = \begin{pmatrix} s_1 & & \\ & \ddots & \\ & & s_{N_e} \end{pmatrix}, \quad \boldsymbol{D} = \begin{pmatrix} \boldsymbol{d}_1 & & \\ & \ddots & \\ & & \boldsymbol{d}_{N_e} \end{pmatrix}. \tag{4.151}$$

As mentioned in Sec. 4.2.4, constraints must be imposed to make the EBE model equivalent to the original structure. The penalty method or the Lagrange multiplier method can be used for this purpose. Let us consider the case in which the penalty method is used. Substituting Eq. (4.150) in the structural equation $(\boldsymbol{K} + Q)\boldsymbol{u} = \boldsymbol{p}$ results in

$$(T^T(S\boldsymbol{D})T + Q)\boldsymbol{u} = \boldsymbol{p}. \tag{4.152}$$

Using $TT^T = T^TT = I$, Eq. (4.152) can be transformed into

$$(S\boldsymbol{D} + Q')\boldsymbol{u}' = \boldsymbol{p}' \tag{4.153}$$

where $Q' = TQT^T$, $\boldsymbol{p}' = T\boldsymbol{p}$ and $\boldsymbol{u}' = T\boldsymbol{u}$. Eq. (4.153) can be solved by using the fixed point iteration procedure with dependence control, as discussed in Sec. 4.2.5.6. Let $\boldsymbol{A} = S\boldsymbol{D} + Q'$, $R = (S + Q')^{-1}$, and $u'_0 = R\check{p}'$, the fixed point iteration is constructed as

$$\boldsymbol{u}'^{*(l+1)} = \boldsymbol{z} + \boldsymbol{G}(\boldsymbol{\varepsilon}\boldsymbol{u}'^{*(l)}). \tag{4.154}$$

For the iterative matrix $\boldsymbol{G}$, by substituting $\boldsymbol{A}$ by its equivalent matrix $(S\boldsymbol{D} + Q')$, the following result can be obtained:

$$\begin{aligned} \boldsymbol{G} &= I - R\boldsymbol{A} \\ &= I - RQ' - RS\boldsymbol{D} \\ &= I - RQ' - RS - RS(\boldsymbol{D} - I) \\ &= -RS(\boldsymbol{D} - I) \end{aligned} \tag{4.155}$$

The residual term $\boldsymbol{z}$ is expressed as:

$$\begin{aligned}
\boldsymbol{z} &= R\boldsymbol{p}' - R\boldsymbol{A}u_0' \\
&= R\boldsymbol{p}' - R(S\boldsymbol{D} + Q')u_0' \\
&= R\boldsymbol{p}' - RQ'u_0' - RS\boldsymbol{D}u_0' \\
&= R\boldsymbol{p}' - RQ'u_0' - RSM\boldsymbol{\Upsilon}\boldsymbol{\Delta}. \qquad (4.156)
\end{aligned}$$

In Eq. (4.156), $RS\boldsymbol{D}u_0'$ is transformed into $RSM\boldsymbol{\Upsilon}\boldsymbol{\Delta}$. M is a deterministic matrix containing the components of u_0'. $\boldsymbol{\Upsilon}$ is an interval matrix containing the interval cross-sectional $\boldsymbol{A}$ and moment of inertia $\boldsymbol{I}$ of each element. It has the form

$$\boldsymbol{\Upsilon} = \begin{pmatrix}
\boldsymbol{A}_1 & & & & \\
\boldsymbol{I}_1 & & & & \\
& \boldsymbol{A}_2 & & & \\
& \boldsymbol{I}_2 & & & \\
& & \ddots & & \\
& & & \boldsymbol{A}_{N_e} & \\
& & & \boldsymbol{I}_{N_e} &
\end{pmatrix}. \qquad (4.157)$$

$\boldsymbol{\Delta}$ is an interval vector, whose components are the interval modulus of elasticity $\boldsymbol{E}$ of each element, that is,

$$\boldsymbol{\Delta} = (\boldsymbol{E}_1 \quad \boldsymbol{E}_2 \quad \ldots \boldsymbol{E}_{N_e})^T. \qquad (4.158)$$

The interval parameters ($\boldsymbol{A}, \boldsymbol{I}$ and $\boldsymbol{E}$) associated with each element occur only once in $\boldsymbol{\Upsilon}$ and $\boldsymbol{\Delta}$. This transformation eliminates the dependence problem in $RS\boldsymbol{D}u_0'$, and avoids the overestimation in $\boldsymbol{z}$. The transformation of $\boldsymbol{D}u_0'$ into $M\boldsymbol{\Upsilon}\boldsymbol{\Delta}$ can be illustrated by the following one-element example:

$$\begin{pmatrix} \boldsymbol{EA} & 0 & 0 & 0 & 0 & 0 \\ 0 & \boldsymbol{EI} & 0 & 0 & 0 & 0 \\ 0 & 0 & \boldsymbol{EI} & 0 & 0 & 0 \\ 0 & 0 & 0 & \boldsymbol{EA} & 0 & 0 \\ 0 & 0 & 0 & 0 & \boldsymbol{EI} & 0 \\ 0 & 0 & 0 & 0 & 0 & \boldsymbol{EI} \end{pmatrix} \cdot \begin{pmatrix} u'_{01} \\ u'_{02} \\ u'_{03} \\ u'_{04} \\ u'_{05} \\ u'_{06} \end{pmatrix} = \begin{pmatrix} u'_{01} & 0 \\ 0 & u'_{02} \\ 0 & u'_{03} \\ u'_{04} & 0 \\ 0 & u'_{05} \\ 0 & u'_{06} \end{pmatrix} \cdot \begin{pmatrix} \boldsymbol{A} \\ \boldsymbol{I} \end{pmatrix} \cdot (\boldsymbol{E})$$

Suppose $\boldsymbol{u}'$ has been calculated after l iterations,

$$\boldsymbol{u}' = u_0 + \boldsymbol{z} + \boldsymbol{G}(\boldsymbol{\varepsilon}\boldsymbol{u}'^{*(l)}), \tag{4.159}$$

the displacement $\boldsymbol{u}$ can be recovered as

$$\boldsymbol{u} = T^T\boldsymbol{u}' \ . \tag{4.160}$$

The above is the formal expression for $\boldsymbol{u}$. In practice, to obtain a sharp result for $\boldsymbol{u}$, all noninterval computations should be performed first. Thus, $\boldsymbol{u}$ is obtained by substituting Eq. (4.159) into Eq. (4.160), yielding

$$\begin{aligned} \boldsymbol{u} &= T^T\boldsymbol{u}' \\ &= T^Tu_0 + T^T\boldsymbol{z} + T^T\boldsymbol{G}(\boldsymbol{\varepsilon}\boldsymbol{u}'^{*(l)}), \end{aligned} \tag{4.161}$$

in which $T^T\boldsymbol{z}$ and $T^T\boldsymbol{G}(\boldsymbol{\varepsilon}\boldsymbol{u}'^{*(l)})$ must be calculated, respectively, as

$$T^T\boldsymbol{z} = (T^TR)\boldsymbol{p} - T^TRQ'u'_0 - (T^TRSM)\boldsymbol{\Upsilon}\boldsymbol{\Delta}, \tag{4.162}$$

$$T^T\boldsymbol{G}(\boldsymbol{\varepsilon}\boldsymbol{u}'^{*(l)}) = -((T^TRS)(\boldsymbol{D} - I))(\boldsymbol{\varepsilon}\boldsymbol{u}'^{*(l)}). \tag{4.163}$$

4.2.9 Plane stress and plane strain finite elements with interval material property and loads

The computational procedures presented in Sec. 4.2.1 to 4.2.7 can be applied straightforward on plane stress and plane strain problems of isotropic material with interval

material property and interval loads. According to Eq. (3.12), the element stiffness matrix is

$$k = \iint_{\text{Area}} B^T C B t \; dxdy \tag{4.164}$$

in which B is the strain-displacement matrix, t is the element thickness, C is the elasticity matrix. For the case of isotropic material, the elasticity matrix C in the state of plane stress is of the form

$$C = \frac{E}{1-\mu^2} \begin{pmatrix} 1 & \mu & 0 \\ \mu & 1 & 0 \\ 0 & 0 & (1-\mu)/2 \end{pmatrix}, \tag{4.165}$$

or in the state of plane strain

$$C = \frac{E}{(1-\mu)(1-2\mu)} \begin{pmatrix} 1-\mu & \mu & 0 \\ \mu & 1-\mu & 0 \\ 0 & 0 & (1-2\mu)/2 \end{pmatrix}, \tag{4.166}$$

where μ is the Poisson's ratio, and E is the modulus of elasticity. We assume that the modulus of elasticity in C is uncertain and described by an interval variable $\boldsymbol{E}$. The interval element stiffness matrix can be expressed as Eq. (4.6):

$$\boldsymbol{k} = \check{k}(I + \boldsymbol{d})$$

where $\check{k}$ is the deterministic element stiffness matrix evaluated using the midpoint of $\boldsymbol{E}$, I is the identity matrix, and $\boldsymbol{d}$ is an interval diagonal matrix, whose entries are the interval multiplier $\boldsymbol{\delta}$ associated with $\boldsymbol{E}$. The midpoint element stiffness matrix $\check{k}$ is obtained using the conventional FE formulation. Using Eq. (4.6), uncertain modulus of elasticity can be considered in any isotropic plane stress and plane strain finite elements such as linear triangle element.

To track the involvement of interval variables in the computations, the elements are assembled using the EBE technique (see Sec. 4.2.2). The interval structure stiffness matrix $\boldsymbol{K}$ has a block-diagonal form, and it can be expressed as Eq. (4.18):

$$\boldsymbol{K} = \check{K}(I + \boldsymbol{D})$$

in which $\boldsymbol{D}$ is an interval block diagonal matrix, whose submatrices are the $\boldsymbol{d}$ matrices of each element. If the loads are also uncertain, the procedures presented in Sec. 4.2.3 are used to eliminate the dependence problems in calculating the interval load vector.

Since the elements are detached in the EBE model, the continuity of the structure has to be recovered by imposing proper constraints. The penalty method or Lagrange multiplier method can be used to impose constraints (see Sec. 4.2.4). The resulting interval structural equations are solved using the fixed point iterations with considerations of the dependence problem of interval arithmetic, discussed in Sec. 4.2.5.4 to 4.2.5.6. After the nodal displacements are solved, the element stresses can be calculated using the procedures discussed in Sec. 4.2.6.

4.3 Computer Implementation

This section discusses the computer implementation of the interval FEA. The computer programs were developed using standard C++/C, in both the Windows operation system and Unix system. The computational procedures involve many interval and real matrix operations. Two libraries, namely PROFIL/BIAS and NEWMAT (Davies, 1991), are used to facilitate the development. PROFIL/BIAS (see Sec. 2.7) is a C++ class library supporting real and interval arithmetic matrix operations. The supported data types include REAL (double precision is used for the REAL type), VECTOR, MATRIX, INTEGER_MATRIX, INTERVAL, INTERVAL_VECTOR, and INTERVAL_MATRIX. The indexing of all vector and matrix types starts with 1. PROFIL/BIAS provides basic vector and matrix operations

for real and interval arithmetic, such as matrix addition, matrix-vector-product and matrix product.

PROFIL/BIAS is mainly used for the operations involving interval quantities. For the real matrix operations, the library NEWMAT is preferred. NEWMAT (Davies, 1991) is a C++ library supporting real matrix operations. The supported matrix types include: Matrix, UpperTriangularMatrix, LowerTriangularMatrix, DiagonalMatrix, SymmetricMatrix, BandMatrx, SymmetricBandMatrix, RowVector and ColumnVector. The library includes the basic matrix operations, inverse, transpose, submatrix, determinant, Cholesky decomposition, eigenvalues of a symmetric matrix, and sorting.

Both PROFIL/BIAS and NEWMAT are freely available through the Internet.

4.3.1 Implementation of the conventional interval FEA

Three conventional methods for interval finite element analysis were developed as part of this work, namely the combinatorial method, the Monte Carlo sampling method, and the naïve interval FEA. These methods are introduced in Sec. 3.2.2, 3.2.6 and 4.1, respectively. They are mainly used in this work for the evaluation of the developed interval FEA.

4.3.1.1 Combinatorial method

The computations involved in the combinatorial method are purely deterministic. The combinatorial method introduces every possible combination of the bounds of the interval parameters into analysis.

In computer implementation, the interval parameters are stored in a matrix

$$\alpha = \begin{pmatrix} \underline{\alpha}_1, & \overline{\alpha}_1 \\ \vdots & \vdots \\ \underline{\alpha}_m, & \overline{\alpha}_m \end{pmatrix}$$

in which $\underline{\alpha}_i$ and $\overline{\alpha}_i$ are the lower and upper bounds of the interval parameter $\boldsymbol{\alpha}_i$, respectively. The total number of interval parameters is m. The relevant C++ code implementing the combinatorial method would be something like this

```
for (int i_1 = 1; i_1 <= 2; i_1 + +){
    α_1 = α(1, i_1);
    ......
    for (int i_m = 1; i_m <= 2; i_m + +){
        α_m = α(m, i_m);
        FEA(α_1, ..., α_m);
        UpdateBounds;
    }
    ......
}
```

in which FEA$(\alpha_1, \ldots, \alpha_m)$ represents a deterministic finite element analysis routine with the input data $(\alpha_1, \ldots, \alpha_m)$. According to the results given by FEA$(\alpha_1, \ldots, \alpha_m)$, the routine UpdateBounds updates the minimal and the maximal responses.

4.3.1.2 Monte Carlo sampling method

The Monte Carlo sampling method involves the following steps: (a) obtaining uniform samples in the interval ranges of the uncertain parameters, (b) performing deterministic FEA for the combination of the sampled parameters, and (c) obtaing the bounds of the solution set of the simulation results. A straightforward implementation is

```
for (int i = 1; i <=numMC; i++){
    for (int j = 1; j <= m; j++)
        α_j =uniformRV(α̲_j, ᾱ_j);
    FEA(α_1, ..., α_m);
    UpdateBounds;
}
```

in which numMC is the total number of Monte Carlo simulations; uniformRV is a routine producing uniform samples in the range $(\underline{\alpha}_j,\ \overline{\alpha}_j)$. FEA$(\alpha_1, \ldots, \alpha_m)$ is a deterministic finite element analysis routine with the input data $(\alpha_1, \ldots, \alpha_m)$. Based on the results given by FEA$(\alpha_1, \ldots, \alpha_m)$, the routine UpdateBounds updates the minimal and the maximal responses.

4.3.1.3 Naïve interval FEA

For the naïve interval FEA, a straightforward implementation is to convert the deterministic finite element formulation by replacing each real parameters with interval parameters and each real operation by its corresponding interval arithmetic operation. The program structure remains the same as the deterministic finite element program. The differences are mainly in two aspects:

- data type, namely change from "real" to "interval,"
- equation solution technique.

The conversion was accomplished by using the interval arithmetic library PROFIL/BIAS, which provides interval (matrix) data types and interval operations. The resulting interval structural equation is solved by the routine ILSS provided in PROFIL/BIAS, which is based on the standard fixed point iteration (see Sec. 4.2.5.4).

4.3.2 Implementation of the present interval FEA

Based on the computational procedures presented in Sec. 4.2.1 to 4.2.6, planar truss and frame analysis programs have been developed for analyzing trusses and frames (beams) with interval material parameter (modulus of elasticity), interval cross-sectional parameters (cross-sectional area, moment of inertia) and interval load parameters. Interval modulus of elasticity and interval load parameters have also been incorporated in the six-node isoparametric quadratic triangle element for solid mechanics problems.

The interval FEA is implemented in the following C++ routines:

- A routine to read data.
- A routine for element analysis: calculate the midpoint element stiffness matrix $\check{k}$, the interval multiplier matrix $\boldsymbol{d}$, and the matrix w if the element is subjected to interval surface traction or interval body force.
- A routine to assemble elements by the Element-By-Element technique. Generate the midpoint structure stiffness matrix $\check{K}$, the structure interval multiplier matrix $\boldsymbol{D}$, and the matrix W associated with surface tractions or body force.
- A routine to generate the load vector $\boldsymbol{p}_c$ for external concentrated loads applied to structure nodes.
- A routine to impose constraints. Generate the penalty matrix Q for the penalty method, or the matrix c for the Lagrange multipliers method.
- A routine to use fixed point iteration to solve the resulting interval structural equations.
- A routine to calculate stresses, or element nodal internal forces for frame, beam and truss elements.

- A routine to output results.

Sparsity has been exploited in the solution of the interval structural equations. The midpoint of the interval coefficient matrix is stored using the skyline method.

In the program, the computation is based on the EBE model, while the input data is based on the original structure. Compared with the original structure, the EBE model has different node numbering and element connectivity. Thus the structure needs to be converted into the EBE model. We use the following example to show how the conversion is implemented.

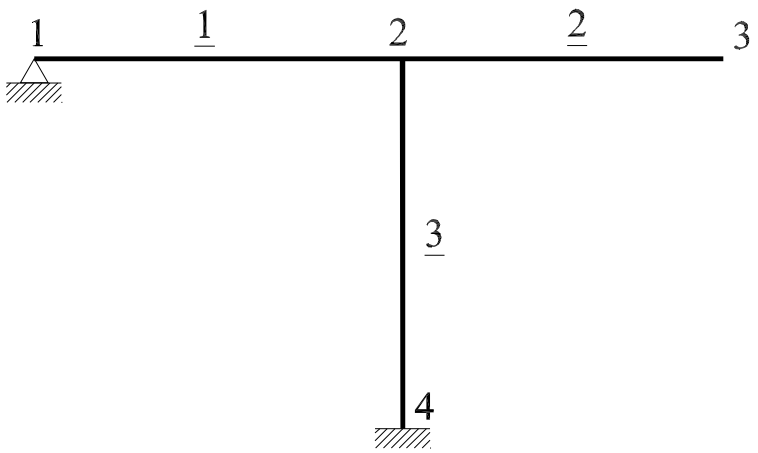

Figure 4.10: A frame structure with three elements.

Consider the frame shown in Fig. 4.10. There are four nodes and three elements. The element connectivity is:

Element 1: node numbers: 1, 2

Element 2: node numbers: 2, 3

Element 3: node numbers: 2, 4

The element connectivity information can be described using a vector

$$\text{CN} = (1 \quad 2 \quad 2 \quad 3 \quad 2 \quad 4).$$

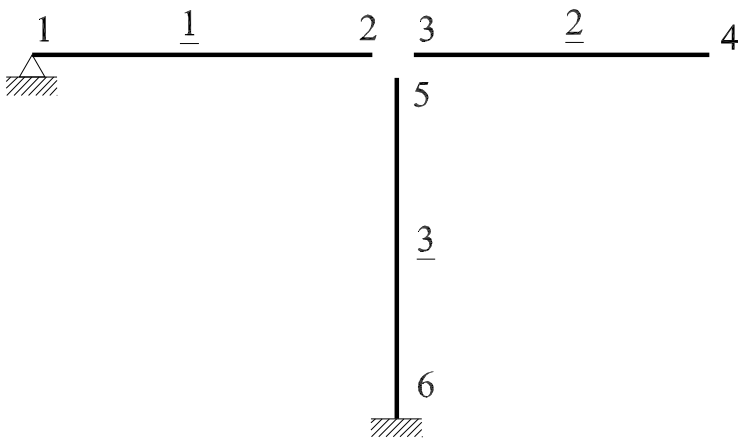

Figure 4.11: A frame structure with three elements: the Element-By-Element model.

The EBE model of the frame structure is shown in Fig. 4.11. In the EBE model, the nodes are renumbered according to the elements which they belong to. For element i, the node numbers are:

$$(i-1)*\mathrm{NNE}+1,\ldots,(i-1)*\mathrm{NNE}+\mathrm{NNE}$$

where NNE is the number of nodes per element. For this particular example, the element connectivity is

Element 1: node numbers: 1, 2

Element 2: node numbers: 3, 4

Element 3: node numbers: 5, 6

The element connectivity information of the EBE model can simply be represented by a vector

$$\mathrm{CE} = (1 \quad 2 \quad 3 \quad 4 \quad 5 \quad 6).$$

By using the two vectors CN and CE, it is easy to map node numbers between original structure and its corresponding EBE model. For node number i in the original structure, the procedure is to simply scan the vector CN, record the indexes of CN where i appears, and find the corresponding entries in the vector CE. Take the

example of node 2 in the original structure; it appears three times in CN, and the corresponding entries in CE are: 2, 3 and 5. This means that the nodes 2, 3 and 5 in the EBE model are shared nodes, and they must have the same displacements. This information is used in the routine which imposes constraints. The above mapping of node numbers between original structure and the EBE model can be illustrated in Fig. 4.12.

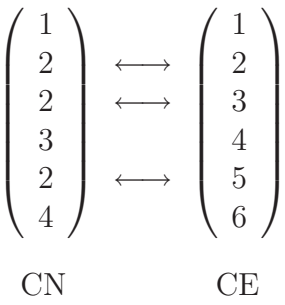

Figure 4.12: Node number mapping between original structure and its EBE model.

Note that the vector CE does not need to be generated in practice. Its entries are equivalent to its indexes, that is

$$\mathrm{CE}(i) = i.$$

In the output file the results are presented according to the node numbering and element connectivity of the actual structure. If a node is shared by several elements (like node 2 in the above frame example), its displacements obtained in all these elements are presented. The output file for nodal displacements will be something like this

. . . . . .

node 2:

in element 1: u_x $[-1.4221, 1.3166]$ u_y $[-6.7660, -6.1485]$ theta $[-1.8130, -1.5215]$

in element 2: u_x $[-1.4221, 1.3166]$ u_y $[-6.7660, -6.1485]$ theta $[-1.8130, -1.5215]$

in element 3: u_x $[-1.4221, 1.3166]$ u_y $[-6.7660, -6.1485]$ theta $[-1.8130, -1.5215]$

. . . . . .

This provides a check for the displacement compatibility and the appropriateness of the penalty number.

CHAPTER 5

NUMERICAL EXAMPLES

This chapter presents a series of numerical examples to evaluate the analysis capabilities of the developed interval FEA. The examples include truss, beam, frame structures, as well as a continuum problem. The first example is a planar truss structure with interval axial stiffness. We examine the rigorousness and accuracy of the presented method, and how its performance varies with the increase of the uncertainty in the parameters. The second example considers a two-span continuous beam with interval loads and interval bending stiffness. The third example considers a two-bay two-story planar frame under interval load, interval cross-sectional area, interval moment of inertia and interval modulus of elasticity. This example illustrates the capability of the developed method to handle frames with combined uncertain axial and bending stiffness. In the fourth example, a series of truss structures with a large number of interval variables are analyzed. The scalability and computational efficiency of the present method are examined. The fifth example considers a steel plate with uncertain modulus of elasticity. This example demonstrates the application of the present interval FEA in continuum problems.

For each problem, the quality of the solution obtained by the present interval FEA is evaluated through comparison with the solutions from some alternative methods (e.g., the combinatorial method, the sensitivity analysis method, the Monte Carlo sampling method). These alternative methods yield inner bounds of the response ranges, while the present method yields outer bounds. By comparing inner and outer bounds, one can get an approximation for the overestimation of the results obtained by the present interval FEA.

5.1 Truss Structure

A planar truss, shown in Fig. 5.1, is considered in this example. The structure consists of fifteen elements. A combination of horizontal and vertical loads are applied at nodes 2, 3, 5 and 6, as shown in the figure. The cross-sectional area of each element is uncertain and introduced as interval variable.

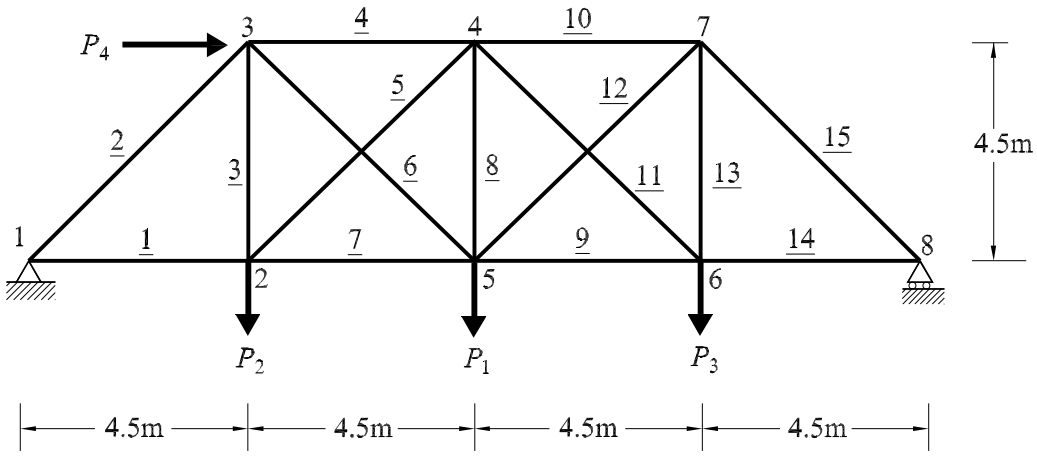

Figure 5.1: Truss structure with 15 elements.

First, two cases are studied to evaluate the rigorousness and the accuracy of the present method:

Case 1: 1% uncertainty in the cross-sectional areas, and loads are deterministic .

Case 2: 1% uncertainty in the cross-sectional areas, and 10% uncertainty in the loads.

Fifteen interval variables are present in case 1 ($\boldsymbol{A}_i$, $i = 1, \ldots, 15$), and nineteen in case 2 ($\boldsymbol{A}_i$, $i = 1, \ldots, 15$; $\boldsymbol{p}_j$, $j = 1, \ldots, 4$). $\boldsymbol{A}$ denotes cross-sectional area and i denotes element number.

Next, the performance of the present method is further tested through a series of analyses in which the uncertainty in the cross-sectional areas increases gradually, namely 3%, 5%, 7% and 10% of the midpoint value.

It is assumed that all interval variables vary independently within their bounds. The deterministic and interval variables used are listed in Table 5.1. For each case, three methods are applied to find the solution: (1) the combinatorial method, (2) the naïve interval FEA, and (3) the present interval FEA. These three methods are denoted as combinatorial, naïve IFEA and present IFEA in this chapter, respectively.

Table 5.1: Parameters in the truss of Fig. 5.1.

Parameter	Midpoint	1% Uncertainty	5% Uncertainty	10% Uncertainty
Cross-sectional area A_1, A_2, A_3, A_{13}, A_{14}, A_{15} (cm^2)	10	[9.95, 10.05]	[9.75, 10.25]	[9.5, 10.5]
Cross-sectional area of all other elements (cm^2)	6	[5.97, 6.03]	[5.85, 6.15]	[5.7, 6.3]
P_1 (kN)	200			[190, 210]
P_2, P_3 (kN)	100			[95, 105]
P_4 (kN)	90			[85.5, 94.5]
Modulus of elasticity of all elements (MPa)	200000	N/A	N/A	N/A

5.1.1 Deterministic analysis

Before carrying out the interval analysis, the deterministic model of this truss is analyzed using the developed interval finite element program. The midpoint (nominal) values of the interval variables are used as the input data. For example, the cross-sectional area of element 1 ($\boldsymbol{A}_1$) is specified as a thin interval [10, 10] in the input file. The objective of this deterministic analysis is to compare the result with the one obtained from conventional deterministic FEA, illustrate the compatibility of displacements at nodes, and determine the range of the penalty number.

In the present interval finite element formulation, the penalty matrix Q in Eq. (4.40) is calculated as

$$Q = \eta k_{max} c^T c, \tag{5.1}$$

Table 5.2: Vertical displacement at node 5 of the truss in Fig. 5.1 with deterministic parameters. El. = element. (unit: meter)

penalty number η	v_5 in El. 6	v_5 in El. 7	v_5 in El. 8	v_5 in El. 9	v_5 in El. 12
10^2	-0.0664548	-0.0664548	-0.0664392	-0.0664548	-0.0664346
10^4	-0.0659943	-0.0659943	-0.0659941	-0.0659943	-0.0659941
10^6	-0.0659897	-0.0659897	-0.0659897	-0.0659897	-0.0659897
10^8	-0.0659892	-0.0659892	-0.0659892	-0.0659892	-0.0659892
10^{10}	-0.0659474	-0.0659474	-0.0659474	-0.0659474	-0.0659474
10^{12}	-0.0623489	-0.0623489	-0.0623489	-0.0623489	-0.0623489

where η is the penalty number, k_{max} is the maximum diagonal entry of the midpoint structure stiffness matrix, and the matrix c contains only zeros and ones. To investigate the influence of η on the result, different values of η were used for analysis. Table 5.2 shows the vertical displacement of node 5 (v_5) obtained using different values of η. Node 5 is shared by five elements, namely element 6, 7, 8, 9, and 12. Each of these elements gives a value for v_5 in the Element-By-Element model. Thus for each analysis, five values of v_5 are presented in Table 5.2. The displacement compatibility condition requires that the five values of v_5 are equal to each other. As seen in Table 5.2, the compatibility condition is ensured when η is equal or greater than 10^6.

To evaluate the results in Table 5.2, the "exact" value of v_5 is obtained by using a conventional finite element program, GTSTRUDL (2002). The value obtained from GTSTRUDL is

$$v_5^{'} = -0.0659896 \text{ m}.$$

According to the data in Table 5.2 and the exact solution $v_5^{'}$, the displacement error vs. penalty number relationship is plotted in Fig 5.2. The relative error of v_5 is measured as

$$e = \frac{|v_5^* - v_5^{'}|}{v_5^{'}}$$

where v_5^* denotes the value of v_5 given by element 6 (any other element can be chosen).

As seen in Fig. 5.2, substantial errors are introduced when η is below 10^4 and larger than 10^9. The range of $10^6 \sim 10^8$ for η gives satisfactory results: the penalty number is large enough to ensure the compatibility, but not so large to provoke numerical error. In the following interval analyses, $\eta = 10^7$ was used.

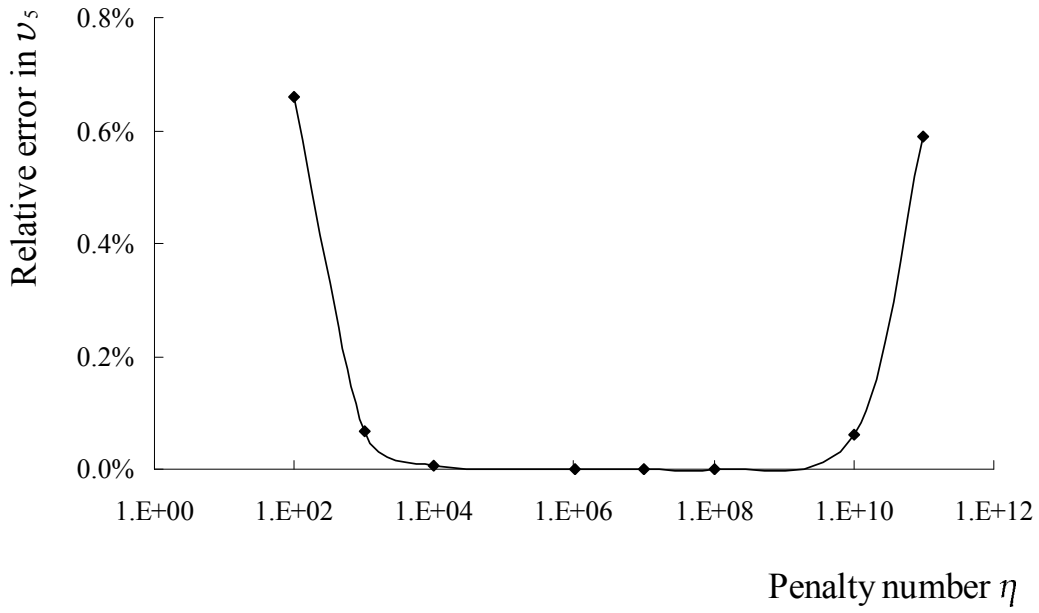

Figure 5.2: Behavior of the relative error in the vertical displacement of node 5 in the truss of Fig. 5.1 (deterministic model).

5.1.2 Interval analysis

5.1.2.1 1% uncertainty in cross-sectional areas

Table 5.3 compares the results of calculated displacement bounds of a typical node (node 5) using the combinatorial method, naïve interval FEA and the present interval FEA. An informative measurement of accuracy for the present method is its relative difference with the combinatorial solution. By its nature, the combinatorial solution is an inner bound, while the present interval FEA gives outer bounds. By comparing these two solutions, one can estimate the overestimations in the results of the present method. In Table 5.3, the relative difference between these two solutions are

calculated as

$$\left| \frac{\underline{\boldsymbol{x}}_{\text{IFEA}} - \underline{\boldsymbol{x}}_{\text{comb}}}{\underline{\boldsymbol{x}}_{\text{comb}}} \right| \quad \text{for lower bound,} \tag{5.2}$$

and

$$\left| \frac{\overline{\boldsymbol{x}}_{\text{IFEA}} - \overline{\boldsymbol{x}}_{\text{comb}}}{\overline{\boldsymbol{x}}_{\text{comb}}} \right| \quad \text{for upper bound,} \tag{5.3}$$

where $\boldsymbol{x}_{\text{comb}}$ denotes the combinatorial solution, and $\boldsymbol{x}_{\text{IFEA}}$ the solution obtained from the present method.

As shown in Table 5.3, the displacement bounds obtained by the present interval FEA contain the combinatorial solutions, as expected, with relative difference within a range of 0.01% to 0.03%. This shows the rigorousness and high accuracy of the present method in calculating the bounds of the displacement range. The naïve interval FEA, however, gives severe conservative bounds. A comparison with the combinatorial solution shows that the naïve solution overestimates the bounds by 90.6% to 147.8%. The naïve interval FEA could not even get the sign (i.e., direction) correct for some responses (e.g., the lower bound of $\boldsymbol{u}_5$). The interval results obtained from the naïve interval FEA are so wide that actually no useful information is obtained. In Table 5.3, an inner bound is also provided by the present method, based on the calculated outer bound (see Sec. 4.2.5.6). Compared with the combinatorial solution, the inner bound of the present method is slightly narrower, with relative differences within a range of 0.01% to 0.03%. Although the combinatorial method yields a slightly better inner bound in this case, it is much more computationally expensive. The combinatorial method has exponential complexity, which makes it feasible only for rather small problems. The results for all nodal displacements, computed with the combinatorial method, naïve interval FEA, and the present interval FEA, are listed in Table 5.11.

Table 5.4 gives the results for the axial forces of two representative elements, namely element 7 and 12. As seen from the table, the same observation can be made as in the case of nodal displacements: the results from the present method sharply enclose the one obtained by the combinatorial method, and the naïve interval FEA

yields severe conservative results. The relative difference between the present interval FEA solution and the combinatorial solution is within a range of 0.02% to 0.07%. The naïve interval FEA, however, yields results whose relative difference with the combinatorial solution ranges from 322% to 1596%. Table 5.12 lists the axial force for all elements, computed with the combinatorial method, the naïve interval FEA, and the present interval FEA.

Table 5.3: Bounds of displacement at Node 5 of the truss in Fig. 5.1, with 1% uncertainty in cross-sectional areas. (unit: meter)

Method	$\underline{\boldsymbol{u}}_5$	$\overline{\boldsymbol{u}}_5$	$\underline{\boldsymbol{v}}_5$	$\overline{\boldsymbol{v}}_5$
Combinatorial	0.018606	0.018815	−0.066321	−0.065661
Naïve IFEA	−0.008894	0.046314	−0.126405	−0.005574
δ	147.80%	146.15%	90.60%	91.51%
Present IFEA (inner)	0.018608	0.018812	−0.066304	−0.065675
δ	0.01%	0.02%	0.03%	0.02%
Present IFEA	0.018603	0.018818	−0.066335	−0.065644
δ	0.02%	0.01%	0.02%	0.03%

δ: relative difference with respect to combinatorial solution.

Table 5.4: Bounds of axial force of element 7 and 12 in the truss of Fig. 5.1, with 1% uncertainty in cross-sectional areas. (unit: kN)

Method	$\underline{\boldsymbol{N}}_7$	$\overline{\boldsymbol{N}}_7$	$\underline{\boldsymbol{N}}_{12}$	$\overline{\boldsymbol{N}}_{12}$
Combinatorial	287.960	289.127	113.082	114.865
Naïve IFEA	−639.828	1219.800	−1691.587	1920.101
δ	322.19%	321.89%	1595.89%	1571.62%
Present IFEA	287.910	289.176	113.009	114.939
δ	0.02%	0.02%	0.07%	0.06%

δ: relative difference with respect to combinatorial solution.

It should be noted that the truss in Fig. 5.1 is internally indeterminate but externally determinate. The support reactions and the axial forces in element 1, 2, 14

and 15 are independent of the structural stiffness. Thus, these axial forces are deterministic although the structural stiffness is uncertain. This phenomenon is correctly captured by the present interval FEA. The bounds for axial forces in element 1, 2, 14 and 15 are obtained as thin intervals

$$\boldsymbol{N}_1 = [267.5,\ 267.5]\ \text{kN}, \quad \boldsymbol{N}_2 = [-251.023,\ -251.023],$$
$$\boldsymbol{N}_{14} = [222.5,\ 222.5]\ \text{kN}, \quad \boldsymbol{N}_{15} = [-314.663,\ -314.663],$$

as listed in Table 5.12.

5.1.2.2 1% uncertainty in cross-sectional areas and 10% uncertainty in loads

This case illustrates the capability of the present method to handle uncertain stiffness and uncertain loads simultaneously. The results for the displacement of node 5 and axial forces in element 7 and 12 are given in Tables 5.5 and 5.6, respectively. The results in the tables indicate that the solutions from the present interval FEA sharply enclose the corresponding combinatorial solutions. For the bounds of displacements, the relative difference between the combinatorial solutions and the present interval FEA solutions is within a range of 0.11% to 0.25%. For the bounds of axial forces, the relative difference between these two solutions is within a range of 0.15% to 0.67%. The rigorousness and the accuracy of the present method are thus demonstrated.

From Tables 5.5 and 5.6, it is also observed that the results obtained by the naïve interval FEA are very wide. A comparison with the combinatorial solutions indicates that the naïve solution overestimates the bounds of the axial force by 327.27% to 1850.52%. This highlights the importance of accounting for dependence problem in the interval FEA.

The results for all nodal displacements, obtained by the combinatorial method, naïve interval FEA, and the present interval FEA, are presented in Table 5.13. The axial force for all elements are summarized in Table 5.14.

Table 5.5: Bounds of displacement at Node 5 of the truss in Fig. 5.1 with 1% uncertainty in cross-sectional areas and 10% uncertainty in loads. (unit: meter)

Method	$\underline{\boldsymbol{u}}_5$	$\overline{\boldsymbol{u}}_5$	$\underline{\boldsymbol{v}}_5$	$\overline{\boldsymbol{v}}_5$
Combinatorial	0.017676	0.019756	−0.069637	−0.062378
Naïve IFEA	−0.011216	0.048636	−0.132739	0.000760
δ	163.45%	146.18%	90.62%	101.22%
Present IFEA (inner)	0.017687	0.019723	−0.069483	−0.062496
δ	0.12%	0.17%	0.22%	0.19%
Present IFEA	0.017642	0.019778	−0.069755	−0.062224
δ	0.19%	0.11%	0.17%	0.25%

δ: relative difference with respect to combinatorial solution.

Table 5.6: Bounds of axial force of element 7 and 12 in the truss of Fig. 5.1, with 1% uncertainty in cross-sectional areas and 10% uncertainty in loads. (unit: kN)

Method	$\underline{\boldsymbol{N}}_7$	$\overline{\boldsymbol{N}}_7$	$\underline{\boldsymbol{N}}_{12}$	$\overline{\boldsymbol{N}}_{12}$
Combinatorial	273.562	303.584	106.451	121.568
Naïve IFEA	−717.152	1297.124	−1863.438	2092.526
δ	362.15%	327.27%	1850.52%	1621.28%
Present IFEA	273.049	304.037	105.733	122.215
δ	0.19%	0.15%	0.67%	0.53%

δ: relative difference with respect to combinatorial solution.

5.1.2.3 Performance of the present method

To further test how the performance of the present method varies with increasing uncertainty in the parameters, a series of analyses are carried out with the uncertainty in cross-sectional areas being 1% (discussed in Sec. 5.1.2.1), 3%, 5%, 7% and 10% of the midpoint value. The loads are considered deterministic. The results for the cases of 5% and 10% uncertainty are presented in detail here.

For the case when the cross-sectional area of each element has 5% uncertainty, the results for selected nodal displacements and element axial forces are given in

Tables 5.7 and 5.8, respectively. As seen from the tables, the solutions obtained by the present method contain the combinatorial solutions. The relative difference between these two solutions is less than 0.8% for the displacement, and less than 1.9% for the axial forces. It illustrates that the solutions from the present interval FEA remain very sharp, as the uncertainty increases to 5%. The results for all nodal displacements and element axial forces are presented in Tables 5.15 and 5.16. As for the naïve interval FEA, the increased uncertainty adds the overestimations in the computations due to the dependence problem. Consequently, the resulting interval structural equation cannot be solved due to the failure of the fixed point iteration to converge.

Table 5.7: Bounds of displacement at Node 5 of the truss in Fig. 5.1, with 5% uncertainty in cross-sectional areas. (unit: meter)

Method	$\underline{\boldsymbol{u}}_5$	$\overline{\boldsymbol{u}}_5$	$\underline{\boldsymbol{v}}_5$	$\overline{\boldsymbol{v}}_5$
Combinatorial	0.018199	0.019247	−0.067682	−0.064380
Present IFEA (inner)	0.018267	0.019153	−0.067185	−0.064794
δ	0.38%	0.49%	0.73%	0.64%
Present IFEA	0.018105	0.019315	−0.068094	−0.063886
δ	0.51%	0.35%	0.61%	0.77%
Naïve IFEA	No convergence			

δ: relative difference with respect to combinatorial solution.

Table 5.8: Bounds of axial force of element 7 and 12 in the truss of Fig. 5.1, with 5% uncertainty in cross-sectional areas. (unit: kN)

Method	$\underline{\boldsymbol{N}}_7$	$\overline{\boldsymbol{N}}_7$	$\underline{\boldsymbol{N}}_{12}$	$\overline{\boldsymbol{N}}_{12}$
Combinatorial	285.628	291.467	109.510	118.421
Present IFEA	284.148	292.938	107.293	120.654
δ	0.52%	0.50%	2.02%	1.89%
Naïve IFEA	No convergence			

δ: relative difference with respect to combinatorial solution.

For the case of 10% uncertainty, Tables 5.9 and 5.10 compare the results of selected nodal displacements and element forces calculated using the present method and the combinatorial method. The naïve interval FEA could not converge at this level of uncertainty. It may be seen from the tables that as the uncertainty increases to 10%, the discrepancy between the present interval FEA solution and the combinatorial solution increases accordingly, but still within a reasonable range. Useful information about the response ranges can still be obtained by the present method. For example, according to Table 5.10 the axial force in element 7 is guaranteed to lie between 274.962 kN and 302.124 kN. The results for all nodal displacements and element axial forces are summarized in Tables 5.17 and 5.18, respectively.

Table 5.9: Bounds of displacement at Node 5 of the truss in Fig. 5.1, with 10% uncertainty in cross-sectional areas. (unit: meter)

Method	$\underline{\boldsymbol{u}}_5$	$\overline{\boldsymbol{u}}_5$	$\underline{\boldsymbol{v}}_5$	$\overline{\boldsymbol{v}}_5$
Combinatorial	0.017711	0.019811	−0.069463	−0.062847
Present IFEA (inner)	0.018074	0.019347	−0.066927	−0.065052
δ	2.05%	2.34%	3.65%	3.51%
Present IFEA	0.017252	0.020168	−0.071652	−0.060328
δ	2.59%	1.80%	3.15%	4.01%
Naïve IFEA	No converge			

δ: relative difference with respect to combinatorial solution.

Table 5.10: Bounds of axial force of element 7 and 12 in the truss of Fig. 5.1, with 10% uncertainty in cross-sectional areas. (unit: kN)

Method	$\underline{\boldsymbol{N}}_7$	$\overline{\boldsymbol{N}}_7$	$\underline{\boldsymbol{N}}_{12}$	$\overline{\boldsymbol{N}}_{12}$
Combinatorial	282.722	294.400	105.028	122.852
Present IFEA	274.962	302.124	93.297	134.651
δ	2.74%	2.62%	11.17%	9.60%
Naïve IFEA	No convergence			

δ: relative difference with respect to combinatorial solution.

To illustrate the effects of the uncertainty level on the obtained solutions, the vertical displacement at node 5 and the axial force in element 7 are plotted as a function of the uncertainty level, shown in Fig. 5.3 and 5.4, respectively. The solutions obtained by the present method and the combinatorial method are plotted in the same figure for comparison. As seen clearly in the figures, the solution from the present method always encloses the one from the combinatorial method.

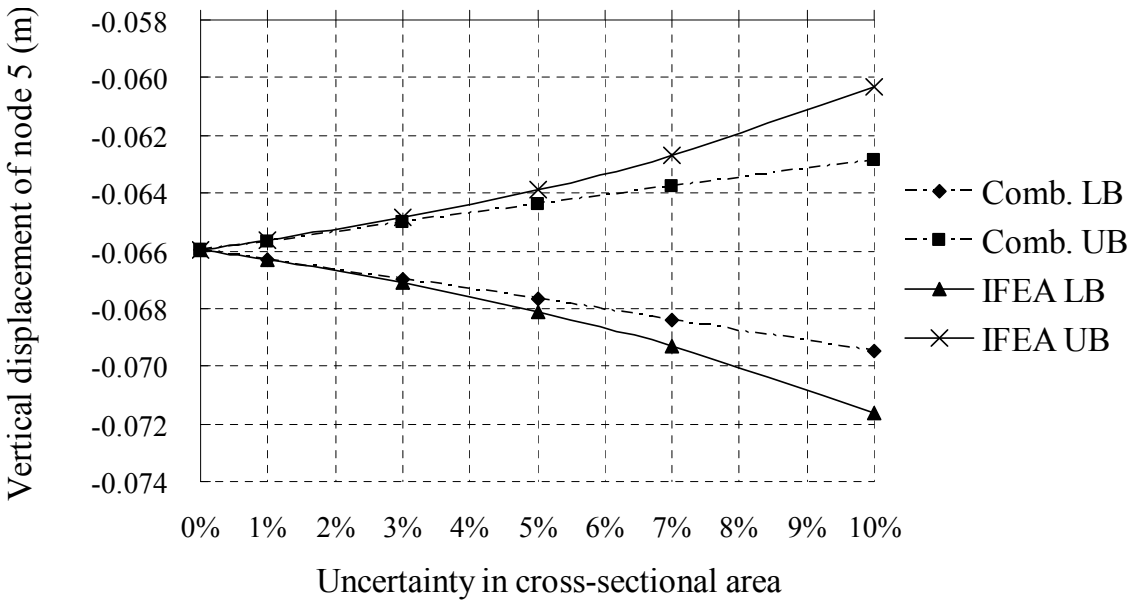

Figure 5.3: Vertical displacement at node 5 in the truss of Fig. 5.1: comparison of combinatorial method and present method. (LB=lower bound, UB=upper bound).

5.1.2.4 Discussions

Based on the results presented in Sec. 5.1.2.1 to 5.1.2.3, some conclusions can be drawn:

1. In all the cases analyzed, the bounds of the response quantities (displacement and axial force) obtained by the present interval FEA enclose those obtained by the combinatorial method.

2. For moderate uncertainty (no more than 5%), the present interval FEA yields

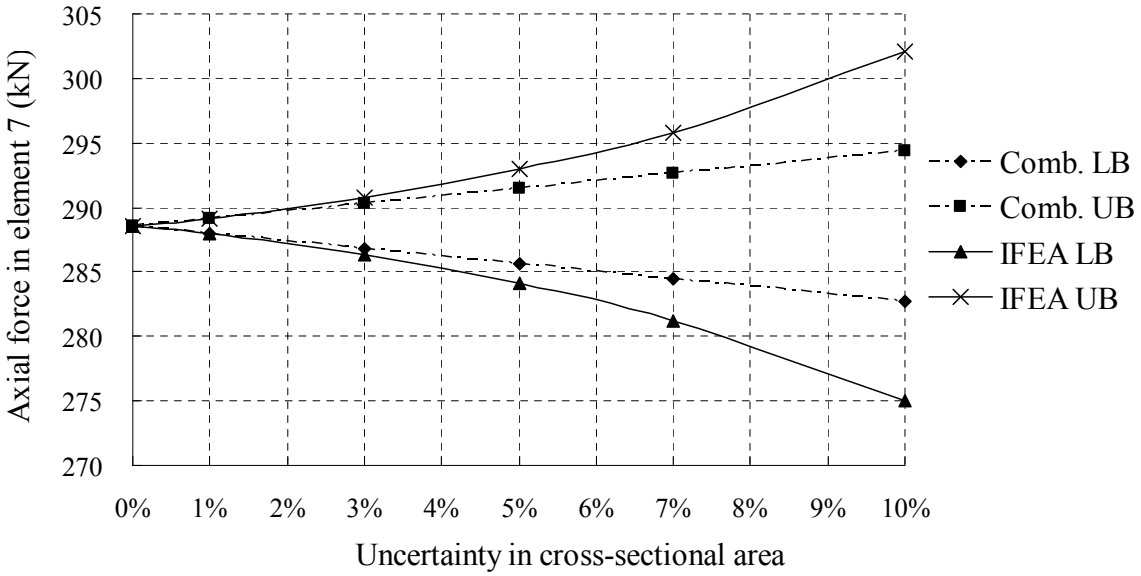

Figure 5.4: Axial force of element 7 in the truss of Fig. 5.1: comparison of combinatorial method and present method. (LB=lower bound, UB=upper bound).

very sharp bounds for the responses.

3. For relatively large uncertainty (within the range of 5% to 10%), the present interval FEA yields reasonable bounds for the responses.

4. Even for small uncertainty (e.g., 1%), the naïve interval FEA gives overly conservative results. No useful information can be obtained. The naïve interval FEA fails to converge as the uncertainty exceeds 5%.

Table 5.11: Bounds of displacement of the truss in Fig. 5.1, with 1% uncertainty in cross-sectional areas. (unit: meter)

	Combinatorial		Naïve IFEA		Present IFEA	
Displ.	LB	UB	LB	UB	LB	UB
$\boldsymbol{u}_2$	0.006654	0.006721	−0.004258	0.017633	0.006654	0.006721
$\boldsymbol{v}_2$	−0.048578	−0.048074	−0.095735	−0.000914	−0.048588	−0.048061
$\boldsymbol{u}_3$	0.032538	0.032959	−0.003961	0.069457	0.032529	0.032966
$\boldsymbol{v}_3$	−0.045542	−0.045058	−0.091831	0.001233	−0.045549	−0.045048
$\boldsymbol{u}_4$	0.019068	0.019431	−0.008331	0.046830	0.019060	0.019438
$\boldsymbol{v}_4$	−0.063696	−0.063040	−0.125689	−0.001044	−0.063711	−0.063023
$\boldsymbol{u}_5$	0.018606	0.018815	−0.008894	0.046314	0.018603	0.018818
$\boldsymbol{v}_5$	−0.066321	−0.065661	−0.126405	−0.005574	−0.066335	−0.065644
$\boldsymbol{u}_6$	0.029561	0.029895	−0.011640	0.071094	0.029554	0.029900
$\boldsymbol{v}_6$	−0.048208	−0.047694	−0.093462	−0.002438	−0.048219	−0.047681
$\boldsymbol{u}_7$	0.006433	0.006809	−0.011464	0.024705	0.006425	0.006816
$\boldsymbol{v}_7$	−0.044648	−0.044159	−0.088005	−0.000800	−0.044657	−0.044147
$\boldsymbol{u}_8$	0.035095	0.035486	−0.012211	0.082790	0.035087	0.035492

$\boldsymbol{u}$: horizontal displacement. $\boldsymbol{v}$: vertical displacement.

Subscripts indicate node number. LB denotes lower bound, and UB upper bound.

Table 5.12: Bounds of axial force of the truss in Fig. 5.1 with 1% uncertainty in cross-sectional areas. (unit: kN)

	Combinatorial		Naïve IFEA		Present IFEA	
Element	LB	UB	LB	UB	LB	UB
1	267.500	267.500	−171.167	708.842	267.500	267.500
2	−251.023	−251.023	−1925.425	1420.869	−251.023	−251.023
3	120.460	121.627	−3655.217	3898.148	120.410	121.677
4	−324.540	−323.373	−1876.232	1225.079	−324.590	−323.323
5	−30.586	−28.934	−1818.021	1758.219	−30.655	−28.864
6	79.016	80.667	−1985.834	2145.647	78.946	80.737
7	287.960	289.127	−639.828	1219.800	287.910	289.176
8	61.964	63.942	−2898.519	3023.965	61.877	64.026
9	263.778	265.039	−1397.856	1929.317	263.726	265.091
10	−303.722	−302.461	−1406.033	796.819	−303.774	−302.409
11	−60.159	−58.377	−2191.846	2072.551	−60.232	−58.302
12	113.082	114.865	−1691.587	1920.101	113.009	114.939
13	141.278	142.539	−3440.760	3725.340	141.226	142.591
14	222.500	222.500	−3348.870	3796.095	222.500	222.500
15	−314.663	−314.663	−2510.903	1878.592	−314.663	−314.663

LB denotes lower bound, and UB upper bound.

Table 5.13: Bounds of displacement of the truss in Fig. 5.1 with 1% uncertainty in cross-sectional areas and 10% uncertainty in loads. (unit: meter)

	Combinatorial		Naïve IFEA		Present IFEA	
Displ.	LB	UB	LB	UB	LB	UB
$\boldsymbol{u}_2$	0.006322	0.007057	−0.005142	0.018517	0.006318	0.007057
$\boldsymbol{v}_2$	−0.051007	−0.045670	−0.100533	0.003883	−0.051095	−0.045555
$\boldsymbol{u}_3$	0.030911	0.034607	−0.007442	0.072938	0.030831	0.034664
$\boldsymbol{v}_3$	−0.047819	−0.042805	−0.096433	0.005836	−0.047885	−0.042712
$\boldsymbol{u}_4$	0.018115	0.020403	−0.010678	0.049177	0.018037	0.020462
$\boldsymbol{v}_4$	−0.066881	−0.059888	−0.131988	0.005255	−0.067006	−0.059727
$\boldsymbol{u}_5$	0.017676	0.019756	−0.011216	0.048636	0.017642	0.019778
$\boldsymbol{v}_5$	−0.069637	−0.062378	−0.132739	0.000760	−0.069755	−0.062224
$\boldsymbol{u}_6$	0.028083	0.031390	−0.015204	0.074658	0.028021	0.031433
$\boldsymbol{v}_6$	−0.050618	−0.045310	−0.098145	0.002245	−0.050716	−0.045184
$\boldsymbol{u}_7$	0.006111	0.007149	−0.012703	0.025944	0.006033	0.007208
$\boldsymbol{v}_7$	−0.046880	−0.041951	−0.092415	0.003611	−0.046957	−0.041847
$\boldsymbol{u}_8$	0.033341	0.037260	−0.016361	0.086940	0.033259	0.037321

$\boldsymbol{u}$: horizontal displacement. $\boldsymbol{v}$: vertical displacement.

Subscripts indicate node number. LB denotes lower bound, and UB upper bound.

Table 5.14: Bounds of axial force of the truss in Fig. 5.1 with 1% uncertainty in cross-sectional areas and 10% uncertainty in loads. (unit: kN)

	Combinatorial		Naïve IFEA		Present IFEA	
Element	LB	UB	LB	UB	LB	UB
1	254.125	280.875	−206.705	744.380	254.125	280.875
2	−266.756	−235.290	−2087.898	1583.342	−266.756	−235.290
3	113.390	128.749	−4032.722	4276.019	112.881	129.206
4	−340.767	−307.204	−2016.817	1365.664	−341.221	−306.692
5	−36.144	−23.432	−1990.705	1930.888	−36.799	−22.721
6	72.376	87.363	−2187.039	2347.521	71.665	88.018
7	273.562	303.584	−717.152	1297.124	273.049	304.037
8	57.663	68.285	−3201.886	3328.419	56.834	69.069
9	250.590	278.291	−1539.817	2071.278	250.075	278.741
10	−318.908	−287.338	−1492.541	883.327	−319.359	−286.824
11	−65.725	−52.882	−2395.291	2276.163	−66.371	−52.164
12	106.451	121.568	−1863.438	2092.526	105.733	122.215
13	134.215	149.666	−3805.355	4090.591	133.700	150.116
14	211.375	233.625	−3658.966	4106.191	211.375	233.625
15	−330.396	−298.929	−2707.870	2075.398	−330.396	−298.929

LB denotes lower bound, and UB upper bound.

Table 5.15: Bounds of displacement of the truss in Fig. 5.1 with 5% uncertainty in cross-sectional areas. (unit: meter)

	Combinatorial		Present IFEA (inner)		Present IFEA	
Displ.	LB	UB	LB	UB	LB	UB
$\boldsymbol{u}_2$	0.006524	0.006859	0.006525	0.006850	0.006516	0.006859
$\boldsymbol{v}_2$	−0.049617	−0.047093	−0.04926	−0.047391	−0.049914	−0.046736
$\boldsymbol{u}_3$	0.031715	0.033821	0.031926	0.033569	0.031464	0.034031
$\boldsymbol{v}_3$	−0.046537	−0.044117	−0.04624	−0.044355	−0.046773	−0.043824
$\boldsymbol{u}_4$	0.018353	0.020167	0.018569	0.019930	0.018116	0.020383
$\boldsymbol{v}_4$	−0.065049	−0.061765	−0.06454	−0.062196	−0.065477	−0.061256
$\boldsymbol{u}_5$	0.018199	0.019247	0.018267	0.019153	0.018105	0.019315
$\boldsymbol{v}_5$	−0.067682	−0.064380	−0.06719	−0.064794	−0.068094	−0.063886
$\boldsymbol{u}_6$	0.028911	0.030586	0.029048	0.030406	0.028732	0.030723
$\boldsymbol{v}_6$	−0.049264	−0.046695	−0.04886	−0.047040	−0.049608	−0.046292
$\boldsymbol{u}_7$	0.005684	0.007564	0.005912	0.007329	0.005450	0.007791
$\boldsymbol{v}_7$	−0.045654	−0.043206	−0.04532	−0.043489	−0.045935	−0.042869
$\boldsymbol{u}_8$	0.034338	0.036291	0.034526	0.036053	0.034101	0.036479

$\boldsymbol{u}$: horizontal displacement. $\boldsymbol{v}$: vertical displacement.

Subscripts indicate node number. LB denotes lower bound, and UB upper bound.

Table 5.16: Bounds of axial force of the truss in Fig. 5.1 with 5% uncertainty in cross-sectional areas. (unit: kN)

	Combinatorial		Present IFEA	
Element	LB	UB	LB	UB
1	267.500	267.500	267.500	267.500
2	−251.023	−251.023	−251.023	−251.023
3	118.128	123.967	116.649	125.438
4	−326.872	−321.033	−328.351	−319.562
5	−33.895	−25.637	−35.975	−23.545
6	75.707	83.964	73.627	86.057
7	285.628	291.467	284.148	292.938
8	58.036	67.930	55.455	70.448
9	261.264	267.565	259.684	269.132
10	−306.236	−299.935	−307.815	−298.368
11	−63.731	−54.820	−65.948	−52.587
12	109.510	118.421	107.293	120.654
13	138.764	145.065	137.184	146.632
14	222.500	222.500	222.500	222.500
15	−314.663	−314.663	−314.663	−314.663

LB denotes lower bound, and UB upper bound.

Table 5.17: Bounds of displacement of the truss in Fig. 5.1 with 10% uncertainty in cross-sectional areas. (unit: meter)

	Combinatorial		Present IFEA (inner)		Present IFEA	
Displ.	LB	UB	LB	UB	LB	UB
$\boldsymbol{u}_2$	0.006369	0.007039	0.006371	0.007004	0.006336	0.007039
$\boldsymbol{v}_2$	−0.050974	−0.045917	−0.049148	−0.047501	−0.052546	−0.044103
$\boldsymbol{u}_3$	0.030720	0.034939	0.031836	0.033659	0.029451	0.036045
$\boldsymbol{v}_3$	−0.047836	−0.042988	−0.046347	−0.044250	−0.049087	−0.041511
$\boldsymbol{u}_4$	0.017473	0.021108	0.018610	0.019888	0.016261	0.022237
$\boldsymbol{v}_4$	−0.066817	−0.060238	−0.064202	−0.062531	−0.069095	−0.057638
$\boldsymbol{u}_5$	0.017711	0.019811	0.018074	0.019347	0.017252	0.020168
$\boldsymbol{v}_5$	−0.069463	−0.062847	−0.066927	−0.065052	−0.071652	−0.060328
$\boldsymbol{u}_6$	0.028133	0.031490	0.028863	0.030592	0.027244	0.032211
$\boldsymbol{v}_6$	−0.050643	−0.045495	−0.048569	−0.047331	−0.052467	−0.043433
$\boldsymbol{u}_7$	0.004750	0.008517	0.005939	0.007302	0.003542	0.009699
$\boldsymbol{v}_7$	−0.046966	−0.042062	−0.045246	−0.043558	−0.048450	−0.040354
$\boldsymbol{u}_8$	0.033431	0.037345	0.034423	0.036156	0.032252	0.038328

$\boldsymbol{u}$: horizontal displacement. $\boldsymbol{v}$: vertical displacement.

Subscripts indicate node number. LB denotes lower bound, and UB upper bound.

Table 5.18: Bounds of axial force of the truss in Fig. 5.1 with 10% uncertainty in cross-sectional areas. (unit: kN)

	Combinatorial		Present IFEA	
Element	LB	UB	LB	UB
1	267.500	267.500	267.500	267.500
2	−251.023	−251.023	−251.023	−251.023
3	115.222	126.900	107.462	134.625
4	−329.778	−318.100	−337.538	−310.375
5	−38.043	−21.527	−48.967	−10.553
6	71.559	88.075	60.635	99.049
7	282.722	294.400	274.962	302.124
8	53.183	72.971	39.609	86.294
9	258.131	270.734	249.787	279.029
10	−309.369	−296.766	−317.713	−288.470
11	−68.213	−50.390	−79.945	−38.590
12	105.028	122.852	93.297	134.651
13	135.631	148.234	127.287	156.529
14	222.500	222.500	222.500	222.500
15	−314.663	−314.663	−314.663	−314.663

LB denotes lower bound, and UB upper bound.

5.2 Beam Structure

The second example is a two-span continuous beam as shown in Fig. 5.5. The beam is subjected to a uniform load $\boldsymbol{w}$ acting on the left span, and a concentrated load $\boldsymbol{p}$ in the middle of the right span. The modulus of elasticity of the beam is 200 GPa. The loads and the moment of inertia of the beam are uncertain and described by interval variables. The nominal (midpoint) value of the moment of inertia is $I_{\mathrm{AB}} = 120 \times 10^6$ mm^4 for the left span, and $I_{\mathrm{BC}} = 90 \times 10^6$ mm^4 for the right span. The uncertain parameters are described by the following intervals:

$$\mathbf{w} = [3, 4.5] \text{ kN/m}, \qquad \boldsymbol{p} = [30, 40] \text{ kN},$$
$$\boldsymbol{I}_{\mathrm{AB}} = [118.8, 121.2] \times 10^6 \text{ mm}^4, \quad \boldsymbol{I}_{\mathrm{BC}} = [89.1, 90.9] \times 10^6 \text{ mm}^4.$$

The uncertainty introduced is 2% for $\boldsymbol{I}_{\mathrm{AB}}$ and $\boldsymbol{I}_{\mathrm{BC}}$, 40% for $\mathbf{w}$, and 28.6% for $\boldsymbol{p}$.

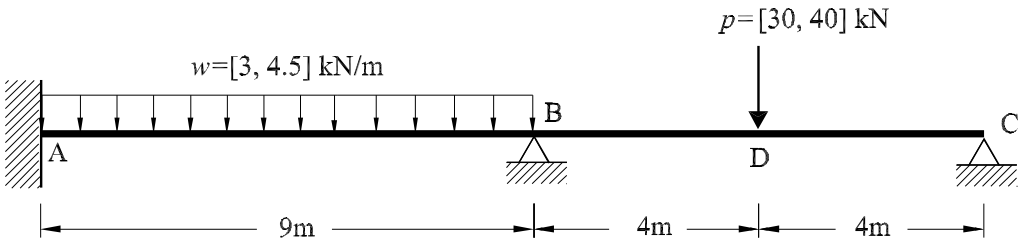

Figure 5.5: Two-span continuous beam.

Tables 5.19 and 5.20 compare the results of calculated typical displacement and internal moment using the combinatorial method, Monte Carlo sampling method, naïve interval FEA and present interval FEA. 10^7 samples are made in the Monte Carlo sampling method. The result from the combinatorial method is chose as a reference, and the relative differences between the combinatorial solution and other solutions are listed in the tables. It is observed that the combinatorial method, the Monte Carlo sampling method and the present method yield solutions very close to each other. Also, we have

$$\boldsymbol{x}_{\mathrm{MC}} \subseteq \boldsymbol{x}_{\mathrm{comb}} \subseteq \boldsymbol{x}_{\mathrm{IFEA}}$$

where $\boldsymbol{x}_{\mathrm{MC}}$ denotes the Monte Carlo sampling solution, $\boldsymbol{x}_{\mathrm{comb}}$ the combinatorial solution, and $\boldsymbol{x}_{\mathrm{IFEA}}$ the present interval FEA solution. The relative difference between $\boldsymbol{x}_{\mathrm{comb}}$ and $\boldsymbol{x}_{\mathrm{IFEA}}$ is within a range of 0.11% to 0.92% for the displacement, and 0.03% to 0.38% for the moment. The accuracy of the present method is thus highlighted. It is also observed that the naïve interval FEA yields overly conservative result. A comparison with the combinatorial solution illustrates that the naïve interval FEA overestimates the bounds of internal moment by 20.66% to 80.38%.

Table 5.19: Bounds of selected nodal displacement for the beam in Fig. 5.5 with uncertain loads and moment of inertia.

Method	$\underline{\boldsymbol{v}}_{\mathrm{D}}$ (m)	$\overline{\boldsymbol{v}}_{\mathrm{D}}$ (m)	$\underline{\boldsymbol{\theta}}_{\mathrm{C}}$ (rad)	$\overline{\boldsymbol{\theta}}_{\mathrm{C}}$ (rad)
Combinatorial	−0.013933	−0.008948	0.003716	0.005642
Monte Carlo	−0.013862	−0.008993	0.003735	0.005613
δ	0.51%	0.50%	0.50%	0.51%
Naïve IFEA	−0.015045	−0.007786	0.003066	0.006273
δ	7.98%	12.98%	17.50%	11.19%
Present IFEA	−0.013949	−0.008877	0.003682	0.005655
δ	0.11%	0.79%	0.92%	0.23%

δ: relative difference with respect to combinatorial solution.

Table 5.20: Bounds of bending moment of the beam in Fig. 5.5 with uncertain loads and moment of inertia. (unit: kN-m)

Method	$\underline{M}_{\mathrm{B}}$	$\overline{M}_{\mathrm{B}}$	$\underline{M}_{\mathrm{D}}$	$\overline{M}_{\mathrm{D}}$
Combinatorial	−48.6589	−35.2901	40.2994	57.7973
Monte Carlo	−48.5877	−35.3497	40.3168	57.7499
δ	0.15%	0.17%	0.04%	0.08%
Naïve IFEA	−58.7121	−25.4424	7.9059	90.3078
δ	20.66%	27.91%	80.38%	56.25%
Present IFEA	−48.7564	−35.1572	40.2041	57.8138
δ	0.20%	0.38%	0.24%	0.03%
δ: relative difference with respect to combinatorial solution.				

5.3 Frame Structure

In this example a two-bay two-story planar frame shown in Fig. 5.6 is considered. The frame is adopted from the work of Buonopane et al. (2003). In the figure the column is denoted as "C" and the beam as "B." Subscripts indicate member number. The frame is subjected to uniform loads acting on the member B_1, B_2, B_3 and B_4. The geometric and material properties of each member are summarized in Table 5.21.

Two cases are analyzed in this example. In the first case, the four uniform loads $\mathbf{w}_i$ $(i = 1, 2, 3, 4)$ are considered uncertain and described by the following interval variables:

$$\mathbf{w}_1 = [105.8,\ 113.1]\ \mathrm{kN/m}, \qquad \mathbf{w}_2 = [105.8,\ 113.1]\ \mathrm{kN/m},$$
$$\mathbf{w}_3 = [49.255,\ 52.905]\ \mathrm{kN/m}, \quad \mathbf{w}_4 = [49.255,\ 52.905]\ \mathrm{kN/m}.$$

All other parameters are deterministic. The nominal values (midpoint) of the cross-sectional properties of the members are used in analysis. The modulus of elasticity of each member is 200 GPa. In the second case, the loads are the same interval variables as in case 1. The cross-sectional area, moment of inertia and modulus of elasticity of each member are considered uncertain as well, and the variations are 1% of their

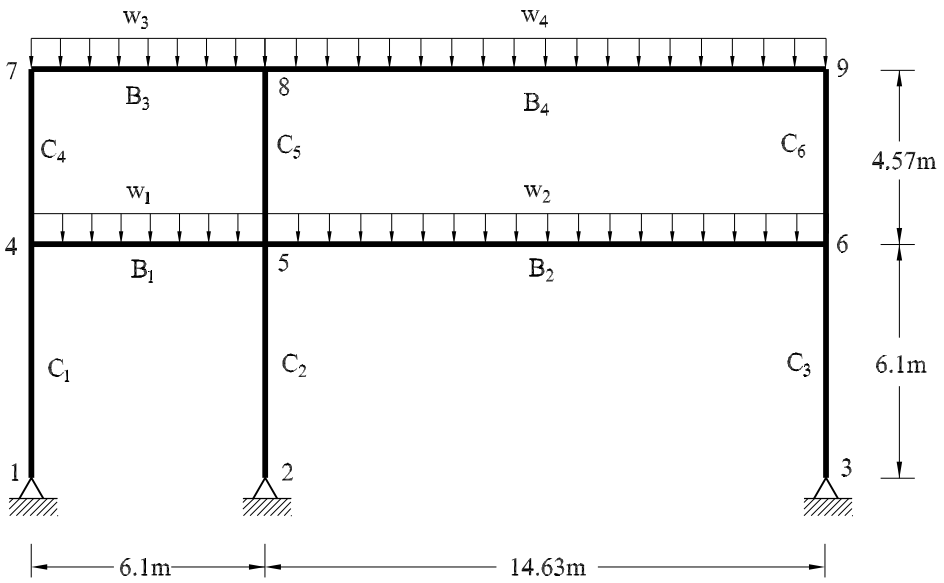

Figure 5.6: Two-bay two-story frame.

nominal values. The intervals used are summarized in Table 5.21. In both cases, it is assumed that all interval variables vary independently within their bounds.

Table 5.21: Interval properties for the members of the frame in Fig. 5.6.

Member	Shape	$\boldsymbol{A}$ (cm^2)	$\boldsymbol{I}$(cm^4)	$\boldsymbol{E}$(GPa)
C_1	W12×19	[35.76, 36.12]	[5383.95, 5438.06]	[199, 201]
C_2	W14×132	[249.07, 251.57]	[63364.99, 64001.83]	[199, 201]
C_3	W14×109	[205.42, 207.48]	[51354.63, 51870.76]	[199, 201]
C_4	W10×12	[22.72, 22.95]	[2228.13, 2250.52]	[199, 201]
C_5	W14×109	[205.42, 207.48]	[51354.63, 51870.76]	[199, 201]
C_6	W14×109	[205.42, 207.48]	[51354.63, 51870.76]	[199, 201]
B_1	W27×84	[159.20, 160.80]	[118032.83, 119219.09]	[199, 201]
B_2	W36×135	[254.85, 257.41]	[323037.21, 326283.81]	[199, 201]
B_3	W18×40	[75.75, 76.51]	[25346.00, 25600.73]	[199, 201]
B_4	W27×94	[177.82, 179.60]	[135427.14, 136788.21]	[199, 201]

5.3.1 Case with only load uncertainty

If only loads involve interval variables, the exact ranges of the system responses can be obtained, as discussed in Sec. 4.2.3.2. For comparison purpose the combinatorial method is also used. It should be noted that the combinatorial method yields the exact solution in this case. The reason for this is that the response quantities are linear functions of the loads.

Table 5.22 summarizes the displacement bounds at node 5 and node 9, obtained by the combinatorial method and the present interval FEA. Table 5.23 gives the member nodal forces of member B_2 (left node) and C_5 (bottom node). It is observed that the present interval FEA yields the same bounds as the combinatorial method. For other nodal displacements and member nodal forces obtained by the present method, a complete agreement with the exact solution (combinatorial solution) is also observed.

Table 5.22: Bounds of selected nodal displacement for the frame in Fig. 5.6 with only load uncertainty.

	Combinatorial		Present IFEA	
Displ.	LB	UB	LB	UB
$\boldsymbol{u}_5$ (cm)	−0.73386	−0.68373	−0.73386	−0.68373
$\boldsymbol{v}_5$ (cm)	−0.24502	−0.22888	−0.24502	−0.22888
$\boldsymbol{\theta}_5$ (rad)	−0.00411	−0.00354	−0.00411	−0.00354
$\boldsymbol{u}_9$ (cm)	−1.48008	−1.38317	−1.48008	−1.38317
$\boldsymbol{v}_9$ (cm)	−0.20772	−0.19300	−0.20772	−0.19300
$\boldsymbol{\theta}_9$ (rad)	0.00525	0.00598	0.00525	0.00598
LB denotes lower bound, and UB upper bound.				

5.3.2 Case with stiffness uncertainty and load uncertainty

In this case, in addition of load uncertainty, the cross-sectional area, moment of inertia, and modulus of elasticity of each member are also considered uncertain and

Table 5.23: Bounds of selected member nodal forces for the frame in Fig. 5.6 with only load uncertainty.

		Combinatorial		Present IFEA	
Member (node)	Nodal force	LB	UB	LB	UB
B_2	Axial (kN)	219.60	239.37	219.60	239.37
(left node)	Shear (kN)	833.61	891.90	833.61	891.90
	Moment (kN-m)	1847.21	1974.95	1847.21	1974.95
C_5	Axial (kN)	−618.28	−574.05	−618.28	−574.05
(bottom node)	Shear (kN)	−287.22	−262.45	−287.22	−262.45
	Moment (kN-m)	−680.06	−622.93	−680.06	−622.93

LB denotes lower bound, and UB upper bound.
Axial force: tension (+). Moment: counter clockwise (+).

introduced as interval variables. The descriptions of the interval material and geometry parameters are listed in 5.21. There are thirty-four interval variables involved in this case. The combinatorial method requires 2^{34} deterministic FEA, which is computationally infeasible. Monte Carlo sampling method is used instead to evaluate the quality of the results obtained by the present interval FEA. 10^6 samples are made.

The displacement at node 5 and node 9, and the member nodal force of member B_2 (left node) and C_5 (bottom node) are summarized in Tables 5.24 and 5.25, respectively. As seen from the tables, the solution obtained by the present method sharply encloses the one from Monte Carlo sampling method. This suggests that the overestimation of the bounds obtained by the present interval FEA is small, and sharp bounds are obtained.

Table 5.24: Bounds of selected nodal displacement for the frame in Fig. 5.6 with stiffness uncertainty and load uncertainty.

	Monte Carlo Sampling		Present IFEA	
Displ.	LB	UB	LB	UB
$\boldsymbol{u}_5$ (cm)	−0.76882	−0.65149	−0.78265	−0.62739
$\boldsymbol{v}_5$ (cm)	−0.24745	−0.22655	−0.24778	−0.22610
$\boldsymbol{\theta}_5$ (rad)	−0.00414	−0.00351	−0.00417	−0.00348
$\boldsymbol{u}_9$ (cm)	−1.52209	−1.34186	−1.56420	−1.29056
$\boldsymbol{v}_9$ (cm)	−0.20962	−0.19119	−0.21009	−0.19064
$\boldsymbol{\theta}_9$ (rad)	0.00519	0.00603	0.00515	0.00607

LB denotes lower bound, and UB upper bound.

Table 5.25: Bounds of selected member nodal forces for the frame in Fig. 5.6 with stiffness uncertainty and load uncertainty.

		Monte Carlo Sampling		Present IFEA	
Member (node)	Nodal force	LB	UB	LB	UB
B_2	Axial (kN)	218.23	240.98	216.35	242.67
(left node)	Shear (kN)	833.34	892.24	832.96	892.47
	Moment (kN-m)	1842.86	1979.32	1839.01	1982.63
C_5	Axial (kN)	−618.63	−573.34	−619.00	−573.29
(bottom node)	Shear (kN)	−288.69	−261.16	−289.84	−259.59
	Moment (kN-m)	−683.94	−619.79	−688.02	−614.90

LB denotes lower bound, and UB upper bound.

Axial force: tension (+). Moment: counter clockwise (+).

5.4 Trusses with a large number of interval variables

A series of truss structures are analyzed in this example. The goal of the analysis is to investigate the ability of the developed interval FEA to handle problems with a large number of interval variables, its scalability and computational efficiency. The trusses analyzed are based on those of Pownuk (2004a,b). The configuration of the truss structure is shown in Fig. 5.7. The truss consists of m bays and n stories. Concentrated nodal loads are applied in the horizontal direction at the left edge nodes and in the vertical direction at the top edge nodes, as illustrated in Fig. 5.7. The loads are deterministic with value of P for each concentrated nodal load. Each element is assigned two interval variables for its cross-sectional area and modulus of elasticity, respectively. Hence, the total number of interval variables is twice the number of elements in the structure. It is assumed that the midpoint of the cross-sectional area of all elements is A, and the midpoint of the modulus of elasticity of all elements is E. For all interval variables, the introduced uncertainty is 1% of their midpoint values. Therefore, for i-th element, the cross-sectional area is $\boldsymbol{A}_i = [0.995,\ 1.005]A$, and the modulus of elasticity is $\boldsymbol{E}_i = [0.995,\ 1.005]E$. All interval variables are assumed to vary independently within their bounds.

In most prior studies of the FEA dealing with interval variables, the number of interval variables considered is rather small ($<<$ 100). In this example, a total of ten trusses are analyzed with the number of interval variables ranging from 246 to 2576. In this sense, the problems considered here is "large" scale. Table 5.26 lists the combinations of story (n) and bay (m) for each truss, and the corresponding number of elements and interval variables.

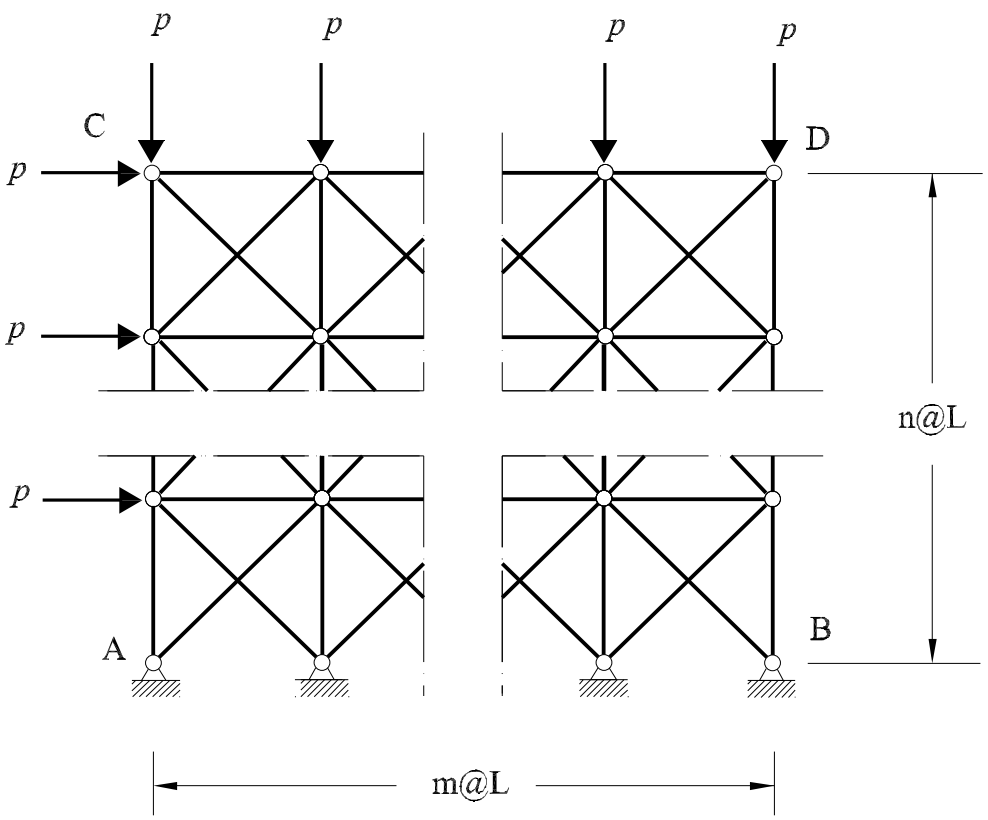

Figure 5.7: m bay - n story truss.

5.4.1 Scalability study

The scalability of the present method is examined through the study of how its performance varies with increasing number of interval variables. Due to the large number of interval variables in this example, the combinatorial method is infeasible, and the naïve interval FEA does not converge. The sensitivity analysis method (Pownuk, 2004a,b) is used for the evaluation of the present method. As discussed in Sec. 3.2.4, the sensitivity analysis method is based on the monotonicity assumption of the response quantities, and can provide a good inner bound when the parameter uncertainty is small.

The results for a typical displacement, namely the vertical displacement at the

Table 5.26: Truss structures analyzed.

Truss (story× bay)	Num. elements	Num. interval variables
3×10	123	246
4×12	196	392
4×20	324	648
5×22	445	890
5×30	605	1210
6×30	726	1452
6×35	846	1692
6×40	966	1932
7×40	1127	2254
8×40	1288	2576

right upper corner (node D) of the trusses are summarized in Table 5.27. The displacement $\boldsymbol{v}_D$ has a form as

$$\boldsymbol{v}_D = \boldsymbol{a}\frac{PL}{EA}.$$

Only the dimensionless part $\boldsymbol{a}$ is presented in the table. Table 5.27 compares the solutions obtained by the present method with those from the sensitivity analysis. The midpoint solution d_0 is also listed, i.e., the deterministic solution obtained when the parameters take their midpoint (nominal) values. For the solution from the present method, the ratio of its width to the midpoint solution is also listed in the table.

From Table 5.27, it is observed that the solutions from the present method are slightly wider than those from the sensitive analysis method in all problems. In the three-story ten-bay truss involving 246 interval variables, the relative difference between these two solutions is 0.12% and 0.1% for the lower bound and upper bound, respectively. As the problem scale increases to eight-story forty-bay with 2576 interval variables, the relative difference between these two solutions is 0.48% and 0.45% for the lower bound and upper bound, respectively. This comparison indicates that the

Table 5.27: Bounds for vertical displacement at node D of the trusses in Fig. 5.7, with 1% uncertainty in cross-sectional area and modulus of elasticity.

Truss	Midpoint	Sensitivity Anal.		Present IFEA				
story×bay	solution d_0	LB*	UB*	LB	UB	δ_{LB}	δ_{UB}	wid/d_0
3×10	2.5447	2.5143	2.5756	2.5112	2.5782	0.12%	0.10%	2.64%
4×12	3.4193	3.3782	3.4612	3.3723	3.4664	0.18%	0.15%	2.75%
4×20	3.3001	3.2592	3.3418	3.2532	3.3471	0.18%	0.16%	2.84%
5×22	4.1309	4.0791	4.1837	4.0690	4.1928	0.25%	0.22%	3.00%
5×30	4.1005	4.0486	4.1532	4.0386	4.1624	0.25%	0.22%	3.02%
6×30	4.9246	4.8617	4.9886	4.8462	5.0030	0.32%	0.29%	3.18%
6×35	4.9111	4.8482	4.9751	4.8326	4.9895	0.32%	0.29%	3.19%
6×40	4.9054	4.8425	4.9694	4.8270	4.9838	0.32%	0.29%	3.20%
7×40	5.7201	5.6461	5.7954	5.6236	5.8166	0.40%	0.37%	3.37%
8×40	6.5422	6.4570	6.6289	6.4259	6.6586	0.48%	0.45%	3.56%

LB denotes lower bound, and UB upper bound.
$\delta_{\text{LB}} = |\text{LB} - \text{LB}^*|/\text{LB}^*$. $\delta_{\text{UB}} = |\text{UB} - \text{UB}^*|/\text{UB}^*$. $\text{wid}/d_0 = (\text{UB} - \text{LB})/d_0$.

present method yields sharp results for large scale problems, and the accuracy remains at the same level with the increase of problem size. The scalability of the method is thus demonstrated.

Another useful information listed in Table 5.27 is the ratio of the present IFEA solution to the midpoint solution. This ratio gives an estimation of the uncertainty in the response resulting from the uncertainty in the parameter. The results show reasonable values of the displacement variations in all problems, ranging from 2.64% to 3.56%. For example, in the case of the eight-story forty-bay truss with 1288 elements, 1% uncertainty in the cross-sectional area and modulus of elasticity of each element will result in 3.56% uncertainty in the vertical displacement at node D.

5.4.2 Computational efficiency studies

Next, we investigate the computational efficiency of the present interval FEA. As mentioned in Sec. 4.2.5.6, solving a linear interval equation involves two major steps: (a) calculation of the preconditioning matrix; i.e., the inverse of the midpoint of the interval coefficient matrix, and (b) the iteration process. Table 5.28 summarizes the problem scale, iteration number and total computational time of each problem solved by the present method. The table also contains iteration time and matrix inversion time, as well as their ratios to the total computational time. All time measured is CPU time. The computations were carried out on a PC with Intel Pentium4 2.4 GHz CPU with 1GB RAM under Windows XP. According to the data in Table 5.28, the total computational time, the iteration time and the matrix inversion time are plotted as functions of the number of interval variables, shown in Fig. 5.8.

Table 5.28: CPU time for the truss analyses in example 4 with the present interval FEA. (unit: seconds)

Truss (story× bay)	n_v	Iterations	t_i	t_r	t	t_i/t	t_r/t
3×10	246	4	0.14	0.56	0.72	19.5%	78.4%
4×12	392	5	0.45	2.06	2.56	17.7%	80.5%
4×20	648	5	1.27	8.80	10.17	12.4%	86.5%
5×22	890	5	2.66	21.48	24.38	10.9%	88.1%
5×30	1210	6	6.09	53.17	59.70	10.2%	89.1%
6×30	1452	6	11.08	89.06	100.77	11.0%	88.4%
6×35	1692	6	15.11	140.23	156.27	9.7%	89.7%
6×40	1932	6	20.11	208.64	230.05	8.7%	90.7%
7×40	2254	6	32.53	323.14	358.76	9.1%	90.1%
8×40	2576	7	48.454	475.72	528.45	9.2%	90.0%

n_v: Number of interval variables. t_i: Total CPU time for iterations.
t_r: CPU time for matrix inverse calculation. t: Total computational CPU time.

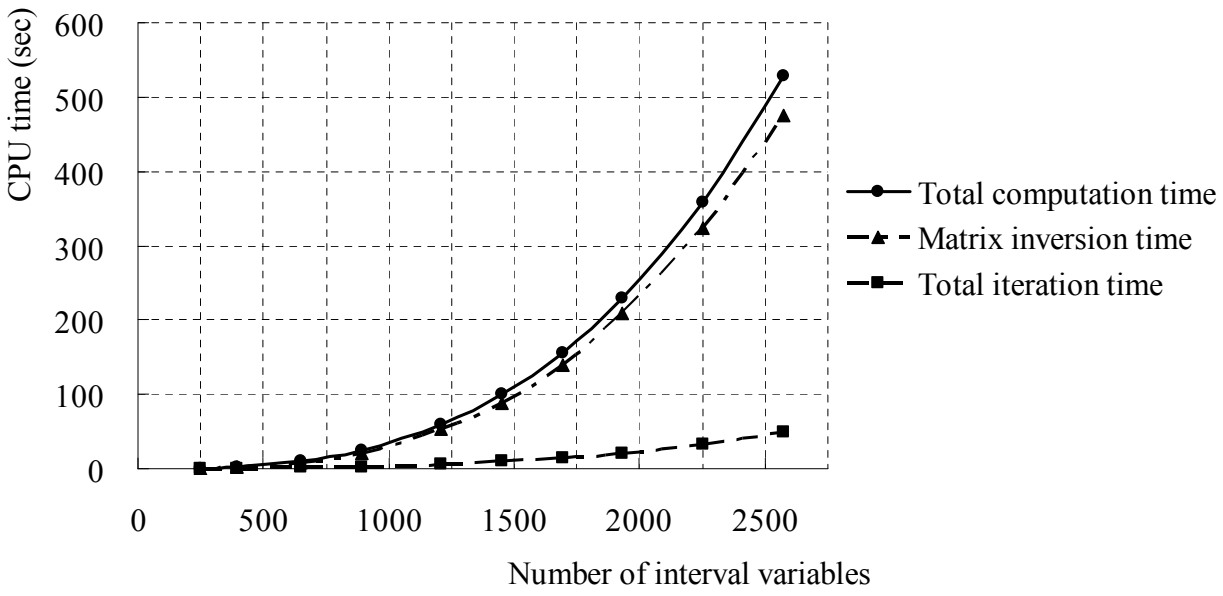

Figure 5.8: CPU time vs. problem scale for the present interval FEA.

It may be seen from Table 5.28 that the number of iterations needed to achieve convergence are comparable for all the problems. As compared to the matrix inversion, the iterations take much less time, ranging from 8.7% to 19.5% of total computational time. As discussed in Sec. 4.2.5.6, the iteration equation (4.107) involves very sparse matrices. The sparsity has been exploited in the implementation of the interval FEA for better efficiency.

The results in Table 5.28 also indicate that the percentage of the CPU time spent on calculating the matrix inverse ranges from 78.4% to 90.7%. For the majority of the problems, the percentage is around 90%. In the present interval finite element program, the inverse of the matrix is calculated by two steps: (a) perform Cholesky decomposition for the matrix, and (b) employ the columns of the identity matrix as multiple right hand sides (Press et al., 1992). The midpoint of the coefficient matrix is stored using the skyline method to exploit the sparsity.

It is observed that the computational time increases approximately cubically with the number of interval variables for the present interval FEA. A good fit to the data

in Table 5.28 can be found with

$$t = 8.5 \times 10^{-8} n_v^{2.8707}$$

where t is the total computational CPU time and n_v is the number of interval variables. Hence, the present interval FEA has an approximately cubic computational complexity.

Table 5.29: Computational CPU time: a comparison of sensitivity analysis method and the present interval FEA. (unit: seconds)

n_v	Sensitivity Analysis	Present IFEA
246	1.06	0.72
392	6.23	2.56
648	64.05	10.17
890	269.77	24.38
1210	965.86	59.70
1452	2204.43	100.77
1692	4099.70	156.27
1932	7718.17	230.05
2254	14449.60	358.76
2576	32401.50	528.45
n_v: numerber of interval variables		

Table 5.29 compares the total computational time of the sensitivity analysis method and the present method for this example. All analyses are carried out on the same machine, a PC with Intel Pentium4 2.4GHz CPU with 1GB RAM under Windows XP. According to the data in Table 5.29, Fig. 5.9 is plotted to show the relationship between the computational time and the number of interval variables for the two methods. Clearly, the present interval FEA is significantly superior to the sensitivity analysis method. The advantage of the present method becomes more obvious as the problem scale increases. For the example of the truss with 2576 interval variables, 32401.5 seconds (9 hours) CPU time are needed for the sensitivity analysis

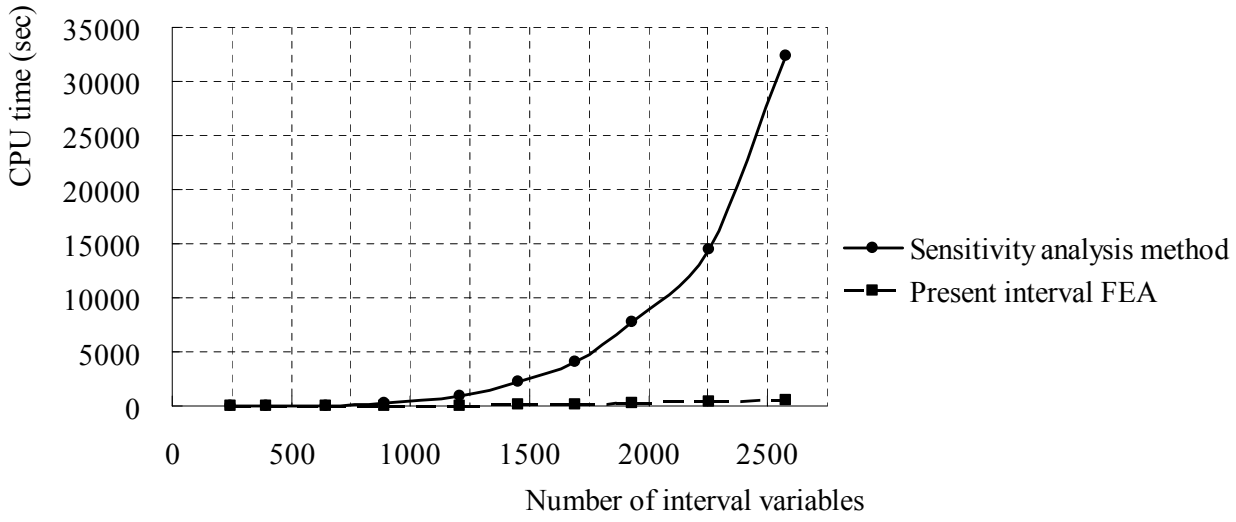

Figure 5.9: Computational CPU time vs. problem scale: a comparison of the sensitivity analysis method and the present interval FEA.

method. While for the present interval FEA, it can be solved for 528.45 seconds (8.8 minutes). The advantage and efficiency of the present method are thus obvious.

5.5 Plate with Quarter-Circle Cutout

Consider the plate with quarter-circle cutout shown in Fig. 5.10. The plate has a dimension of 0.1 m $\times$ 0.05 m with a thickness of 0.005 m, and the radius of the circular cutout is 0.02 m. Let the Poisson's ratio $\nu = 0.3$. Uniformly distributed load of 100 kN/m is applied to the right edge as shown in Fig. 5.10. The plate is analyzed as a plane-stress problem. The six-node isoparametric quadratic triangle element is used for the finite element analysis. There are three hundred and fifty-two elements in the finite element mesh. The uniformly distributed edge load is converted to consistent nodal loads in the analysis.

The modulus of elasticity of the plate is uncertain and varies over the whole area. Two cases are considered for modelling its variations within the plate:

1. The modulus of elasticity varies independently over each element. For element i, the modulus of elasticity is same within the element, but the value is unknown

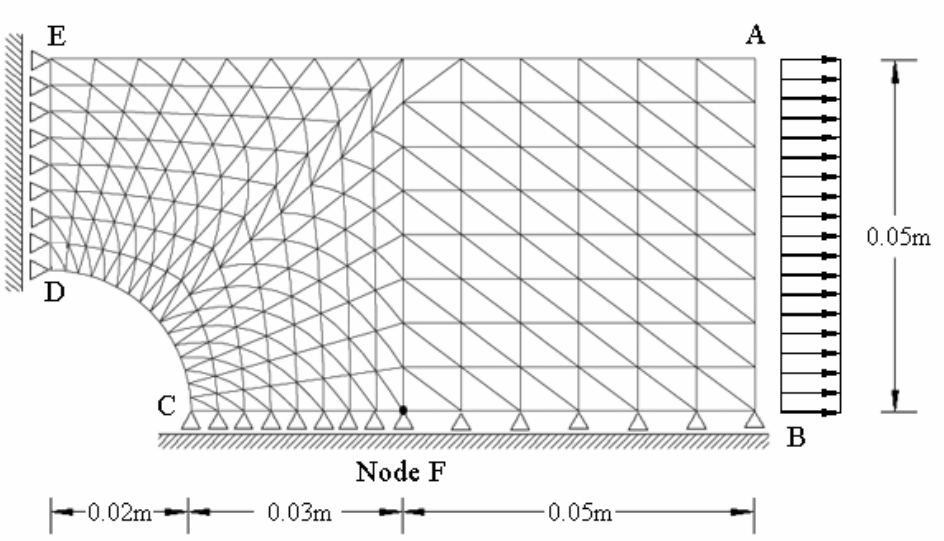

Figure 5.10: Plate with quarter-circle cutout.

and varies in an interval $\boldsymbol{E}_i$. The uncertainty is assumed to be 1% for all elements. That is, $\boldsymbol{E}_i = [199,\ 201]$ GPa, for $i = 1, \ldots, N_e$ where N_e is the number of elements. In this example, $N_e = 352$. Thus 352 interval variables are present in this case.

2. The plate has eight subdomains as shown in Fig. 5.11. The modulus of elasticity varies independently over each subdomain. The elements in the same subdomain have the same modulus of elasticity which is uncertain and varies in an interval. The interval values used are $\boldsymbol{E}_i = [199,\ 201]$ GPa, for $i = 1, \ldots, 8$. Hence, eight interval variables are present in this case.

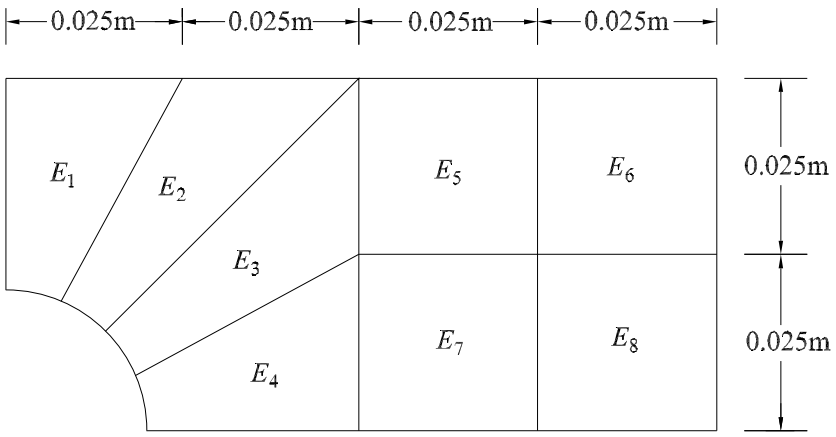

Figure 5.11: Eight subdomains of the plate. Each subdomain has an independent interval modulus of elasticity.

5.5.1 Case 1

In this case, the modulus of elasticity for each element varies independently in the interval [199, 201] GPa. The present interval FEA is evaluated through comparison with the results from a Monte Carlo sampling. 10^6 samples were made. Table 5.30 summarizes the results of selected displacements, the horizontal displacement at node A ($\boldsymbol{u}_A$) and B ($\boldsymbol{u}_B$), and the vertical displacement at node E ($\boldsymbol{v}_E$), obtained by the present interval FEA and the Monte Carlo sampling method. It can be seen that the results obtained by the present method enclose those obtained by the Monte Carlo sampling method. In fact, the Monte Carlo sampling method provides an inner estimate of the response ranges, whereas the present interval FEA yields the outer bounds of the response ranges. A comparison of the computed results by these two methods concludes that the present interval FEA yields a sharp bound for the displacements.

The bounds of stresses ($\boldsymbol{\sigma}_{xx}$, $\boldsymbol{\sigma}_{yy}$) of node F are given in Table 5.31. Node F is shared by three elements. The stresses listed are average stresses. As seen in the table, the interval FEA yields reasonable bounds for the stresses.

Table 5.30: Bounds of selected displacements for the plate in Fig. 5.10, with 1% uncertainty in each element's modulus of elasticity. (unit: $\times 10^{-5}$ meter)

Method	$\underline{\boldsymbol{u}}_A$	$\overline{\boldsymbol{u}}_A$	$\underline{\boldsymbol{u}}_B$	$\overline{\boldsymbol{u}}_B$	$\underline{\boldsymbol{v}}_E$	$\overline{\boldsymbol{v}}_E$
Monte Carlo	1.19094	1.20081	1.25203	1.26168	−0.42638	−0.42238
Present IFEA	1.18768	1.20387	1.24907	1.26511	−0.42894	−0.41940

Table 5.31: Bounds of stress at node F of the plate in Fig. 5.10, with 1% uncertainty in each element's modulus of elasticity. (unit: MP)

Method	$\underline{\boldsymbol{\sigma}}_{xx}$	$\overline{\boldsymbol{\sigma}}_{xx}$	$\underline{\boldsymbol{\sigma}}_{yy}$	$\overline{\boldsymbol{\sigma}}_{yy}$
Monte Carlo	13.164	13.223	1.803	1.882
Present IFEA	12.699	13.690	1.592	2.090

5.5.2 Case 2

For this case, the plate is discretized into eight subdomains, and each subdomain has an independent modulus of elasticity. Eight interval variables are present. For comparison purposes, the combinatorial method is also used. Table 5.32 gives the results of selected displacements, the horizontal displacement at node A ($\boldsymbol{u}_A$) and B ($\boldsymbol{u}_B$), and the vertical displacement at node E ($\boldsymbol{v}_E$), obtained by the present interval FEA and the combinatorial method. Table 5.33 lists the bounds of stresses ($\boldsymbol{\sigma}_{xx}$, $\boldsymbol{\sigma}_{yy}$) of node F. As seen from the tables, the results obtained by the present interval FEA sharply enclose those obtained by the combinatorial method.

Table 5.32: Bounds of selected displacements for the plate in Fig. 5.10, with 1% uncertainty in each subdomain's modulus of elasticity. (unit: $\times 10^{-5}$ meter)

Method	$\underline{\boldsymbol{u}}_A$	$\overline{\boldsymbol{u}}_A$	$\underline{\boldsymbol{u}}_B$	$\overline{\boldsymbol{u}}_B$	$\underline{\boldsymbol{v}}_E$	$\overline{\boldsymbol{v}}_E$
Combinatorial	1.19002	1.20197	1.25108	1.26365	−0.42689	−0.42183
Present IFEA	1.18819	1.20368	1.24952	1.26507	−0.42824	−0.42040

The displacement and stress results obtained by the present interval FEA in case 1 and case 2 are compared in Tables 5.34 and 5.35, respectively. As expected, wider bounds are obtained in case 1 than in case 2. The reason for this is that Case 1

Table 5.33: Bounds of stress at node F of the plate in Fig. 5.10, with 1% uncertainty in each subdomain's modulus of elasticity. (unit: MP)

Method	$\underline{\boldsymbol{\sigma}}_{xx}$	$\overline{\boldsymbol{\sigma}}_{xx}$	$\underline{\boldsymbol{\sigma}}_{yy}$	$\overline{\boldsymbol{\sigma}}_{yy}$
Combinatorial	13.158	13.230	1.797	1.885
Present IFEA	12.875	13.513	1.686	1.996

Table 5.34: Bounds of selected displacements for the plate in Fig. 5.10 . Comparison of case 1 and case 2. (unit: $\times 10^{-5}$ meter)

	$\underline{\boldsymbol{u}}_A$	$\overline{\boldsymbol{u}}_A$	$\underline{\boldsymbol{u}}_B$	$\overline{\boldsymbol{u}}_B$	$\underline{\boldsymbol{v}}_E$	$\overline{\boldsymbol{v}}_E$
Case 1	1.18768	1.20387	1.24907	1.26511	-0.42894	-0.41940
Case 2	1.18819	1.20368	1.24952	1.26507	-0.42824	-0.42040

Table 5.35: Bounds of stress at node F of the plate in Fig. 5.10. Comparison of case 1 and case 2. (unit: MP)

	$\underline{\boldsymbol{\sigma}}_{xx}$	$\overline{\boldsymbol{\sigma}}_{xx}$	$\underline{\boldsymbol{\sigma}}_{yy}$	$\overline{\boldsymbol{\sigma}}_{yy}$
Case 1	12.699	13.690	1.592	2.090
Case 2	12.875	13.513	1.686	1.996

describes higher level of variations in the modulus of elasticity over the plate.

5.6 Rectangular Plate

In this example a rectangular plate shown in Fig. 5.12 is considered. The plate has a dimension of 0.1 m $\times$ 0.05 m with a thickness of 0.005 m. The Poisson's ratio ν is 0.3. A uniformly distributed load of 100 kN/m is applied to the right edge. The plate is analyzed as a plane-stress problem. The six-node isoparametric quadratic triangle element is used for the finite element analysis. The modulus of elasticity of the plate is uncertain and varies in the interval [196, 204] GPa. Two cases are considered for modelling its space variations within the plate:

1. The modulus of elasticity varies independently in the interval [196, 204] GPa over each element. In this case, the material mesh is the same as the finite element mesh. To investigate the effect of the mesh on the result, six different meshes are used in which the number of elements ranges from 36 to 324.

2. The plate has four subdomains as shown in Fig. 5.13. The modulus of elasticity varies independently in the interval [196, 204] GPa over each subdomain. The elements in the same subdomain have the same modulus of elasticity which is uncertain and varies in an interval. In this case, the material mesh is different than the finite element mesh.

5.6.1 Case 1

In this case, the modulus of elasticity for each element varies independently in the interval [196, 204] GPa. The material mesh is the same as the finite element mesh. Apparently, the computed result will be affected by the mesh used. A finer mesh models a more inhomogeneous material property. Consequently, the uncertainty in the response will increase. To investigate the effect of the mesh on the result, six different meshes are considered in which the number of elements is 36, 100, 144, 196, 256, and 324, respectively. All the meshes are uniform. Table 5.36 summarizes the

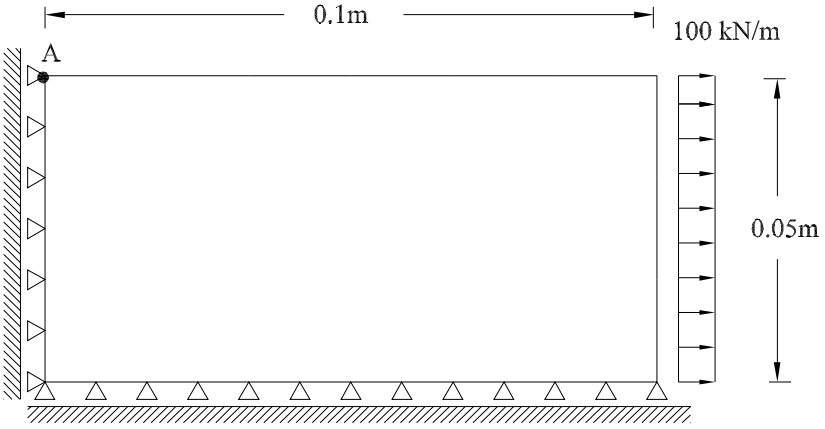

Figure 5.12: Rectangular plate.

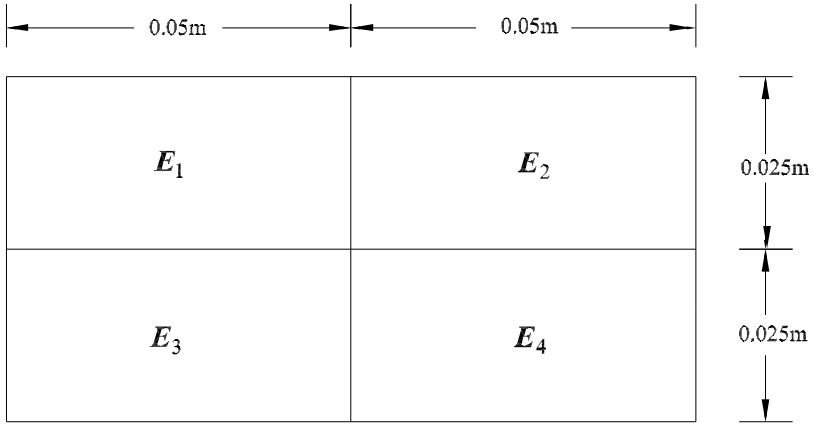

Figure 5.13: Four subdomains of the plate. Each subdomain has an independent interval modulus of elasticity.

vertical displacement at node A ($\boldsymbol{v}_A$). The table also lists the midpoint solution v_{A0}; i.e., the deterministic solution obtained using the midpoint (nominal) values of the interval parameters. The result is also plotted as a function of the number of elements, shown in Fig.5.14.

The result verifies that a finer mesh results in a wider response range. In fact, different meshes represent different problems. The analyst should carefully choose the appropriate mesh based on the information available.

Table 5.36: Vertical displacement at node A in the plate of Fig. 5.12 (unit: 10^{-6} m). Each element has an independent interval modulus of elasticity [196, 204] GPa.

Num. Ele.	v_{A0}	$\underline{\boldsymbol{v}}_A$	$\overline{\boldsymbol{v}}_A$
36	−1.4900	−1.5569	−1.4231
100	−1.4936	−1.5825	−1.4047
144	−1.4946	−1.6003	−1.3889
196	−1.4953	−1.6251	−1.3656
256	−1.4959	−1.6623	−1.3295
324	−1.4963	−1.7248	−1.2679

v_{A0}: midpoint solution.

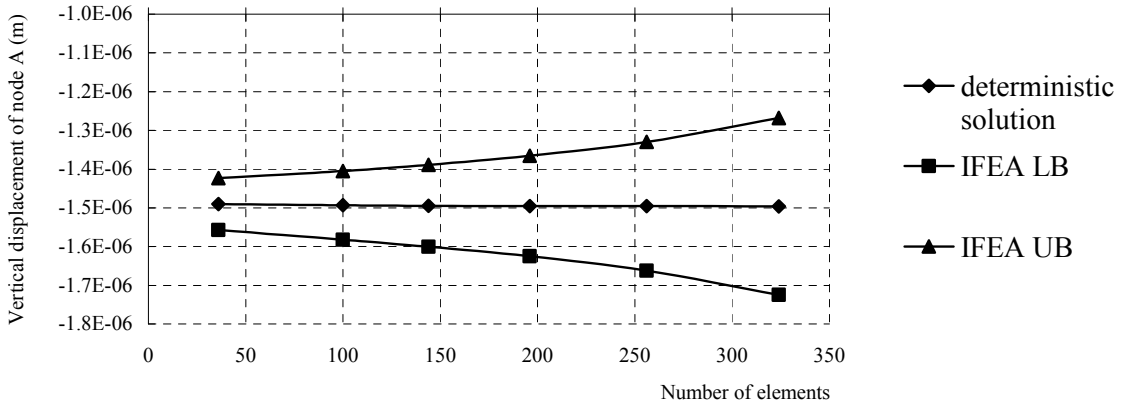

Figure 5.14: Vertical displacement at node A in the plate of Fig. 5.12. Each element has an independent interval modulus of elasticity [196, 204] GPa.

5.6.2 Case 2

In this case, the plate is discretized into four subdomains (Fig. 5.13), and each subdomain has an independent modulus of elasticity [196, 204] GPa. The material mesh is different than the finite element mesh. Two uniform meshes are considered with 144 and 256 elements, respectively. Table 5.37 summarizes the calculated vertical displacement at node A. It can be seen that the results from these two meshes are very close to each other. This illustrates that for the same material mesh, the interval result is relatively insensitive to the finite element mesh, as long as the finite element mesh is fine enough in the sense of the deterministic FEA.

Table 5.37: Vertical displacement at node A in the plate of Fig. 5.12 (unit: 10^{-6} m). Each subdomain has an interval modulus of elasticity [196, 204] GPa.

Num. Ele.	v_{A0}	$\underline{\boldsymbol{v}}_A$	$\overline{\boldsymbol{v}}_A$
144	-1.4946	-1.5722	-1.4170
256	-1.4959	-1.5777	-1.4141

v_{A0}: midpoint solution.

CHAPTER 6

CONCLUSIONS AND FUTURE WORK

6.1 Conclusions

In this study, the interval approach is used to account for uncertainties in the geometry, material and load parameters in finite element analysis for solid and structural mechanics problems. The objective of this study is to develop a computationally efficient method for interval FEA which yields rigorous and sharp bounds on the range of structural responses which may include nodal displacement, element nodal force, or stress. To achieve rigorous results, interval arithmetic is used in the formulation to guarantee an enclosure for the response ranges. The major difficulty associated with interval computation is the dependence problem, which results in severe overestimation of the system response range. Thus, in the development of the present method, particular attention is given to reduce the overestimation in the results due to the dependence problem in the interval computation. This goal has been achieved by developing an algorithm that consists of: (a) factorization of interval parameters out of element stiffness matrix, (b) the Element-By-Element technique for element assembly, (c) the penalty method and Lagrange multiplier method for imposition of constraints to ensure the continuity of the EBE model, (d) application and enhancement of the standard fixed point iteration for solution of the interval structural equations, and (e) symbolic manipulation of expressions to avoid dependence in the interval computation. Further, special algorithms have been developed to calculate sharp results for stresses and element nodal forces. In the developed method, most sources of overestimation due to dependence problem have been eliminated. This ensures the convergence of the fixed point iteration for problems with relatively large

uncertainties. The present method is generally applicable to linear static interval FEA, regardless of element type.

The present interval finite element formulation and the algorithm have been implemented in a newly developed C++ computer program which is capable of analyzing truss, beam and frame structures with interval material, geometry, and load parameters. Material uncertainty and load uncertainty have also been incorporated in the six-node isoparametric quadratic triangle element for plane stress and plane strain problems.

Numerical examples are presented to evaluate the performance of the developed method in the aspects of rigorousness, accuracy, scalability, and computational efficiency. The following problems are considered:

1. A planar truss structure with uncertain axial stiffness. This example studies how the accuracy of the present method is affected by the increase of uncertainty in the parameters.

2. A two-span continuous beam with interval loads and interval bending stiffness.

3. A two-bay two-story planar frame structure under interval load, interval modulus of elasticity, interval cross-sectional area, and interval moment of inertia. This example illustrates the capability of the present method to analyze frames under all these types of interval parameters.

4. A series of truss structures with the number of interval variables ranging from 246 to 2576. This example demonstrates the capability of the present method to handle problems with a large number of interval variables. The scalability and the computational efficiency of the present method are examined.

5. A steel plate with quarter-circle cutout. The modulus of elasticity of the plate is considered interval. This example demonstrates the application of the present method on continuum problems.

For each example, the performance of the present method is evaluated through comparison with some alternative methods (e.g., the combinatorial method, the sensitivity analysis method, the Monte Carlo sampling method). As discussed in Chapter 3, these alternative methods yield inner (nonrigorous) bounds of the response ranges. By comparing these inner bounds and the solution from the present method, one can get an approximation for the accuracy of the present method.

In all the examples, it is observed that the results (displacement, element nodal force, stress) obtained by the present interval FEA enclose those from the alternative methods. This illustrates that the present method yields rigorous results which are guaranteed to enclose the true response range.

Numerical examples demonstrate that the present method yields very sharp (accurate) results for problems involving moderate uncertainty (no more than 5%) in the material and geometry parameters. As the parameter uncertainty increases to a relatively large level (5% to 10%), reasonable bounds can still be achieved. In the first example when the truss has 1% uncertainty in each element's cross-sectional area, the relative difference between the displacement solution from the present method and the one from the combinatorial method is within a range of 0.01% to 0.03%. The relative difference of these two solutions is within a range of 0.35% to 0.77% when the parameter uncertainty increases to 5%. As the parameter uncertainty increases further to 10%, the relative difference of these two solutions is still within a reasonable range, namely 1.80% to 4.01%.

The high accuracy of the present method has also been observed in other examples, including in the fourth example which involves a large number of interval variables.

The scalability of the present method is demonstrated in the fourth example, in which the number of interval variables considered increases from 246 to 2576. It has been shown that the accuracy of the results remains at the same level with the increase of the problem scale.

Compared with the other methods (e.g., the combinatorial method, the sensitivity analysis method, the Monte Carlo sampling method), the advantage of the present method lies in not only its rigorousness, accuracy, and scalability, but also its computational efficiency. The combinatorial method has exponential complexity which limits its application to rather small problems. The Monte Carlo sampling method requires a large number of deterministic analyses. The sensitivity analysis method becomes increasingly inefficient as the number of interval variables increases. Also, these methods result in only inner bounds of the response ranges. The present method, however, can obtain the enclosures of the response ranges by just one interval analysis. For instance, for the truss with 2576 interval variables presented in the fourth example, 32401.5 seconds (9 hours) CPU time are needed for the sensitivity analysis method, while the present method can solve the problem in 528.45 seconds (8.8 minutes). Clearly, the efficiency of the present method is significantly superior to the sensitivity analysis method.

In summary, the development and implementation of the present interval FEA meets the need for fast, rigorous and accurate estimates of the system response ranges. The capability of the present method for analysis of structural and solid problems under interval uncertainty are illustrated. The present interval FEA represents an elegant and efficient method to be used in engineering applications.

6.2 Directions for Future Work

6.2.1 Improvement to the present interval FEA

The computational efficiency of the present interval FEA may be further improved. In the present form, the interval structural equation is solved by the fixed point iteration, with the preconditioning matrix chosen as the inverse of the midpoint matrix of the interval coefficient matrix. The process for inverting the midpoint matrix involves two steps: (a) perform Cholesky decomposition, and (b) employ the columns of the identity matrix as multiple right hand sides (forward and backward substitution). The interval coefficient matrix is very sparse, and so is its midpoint matrix. In the present implementation, the sparsity of the midpoint matrix has only been exploited in step (a) by using the skyline method. A high-efficiency algorithm has yet to be developed for the forward and backward substitution with consideration of the matrix sparsity.

Preconditioning a large sparse interval coefficient matrix with the inverse of its midpoint matrix gives the sharpest solution in a general case. However, even when the sparsity has been fully exploited, inverting a large sparse matrix involves a considerable amount of computing. It is of interest to explore some other form of preconditioning matrix which requires less computation. This study has not been addressed in the present work and its consideration in the future is strongly recommended.

The developed interval FEA, in its present form does not address the uncertain parameters described by interval functions. Implementation of this feature will improve its ability to characterize uncertainties. For example, the cross-sectional area of a non-prismatic bar is described by an interval function $\boldsymbol{A}(x)$ which is an n-th order polynomial

$$\boldsymbol{A}(x) = \boldsymbol{a}_0 + \boldsymbol{a}_1 x + \cdots + \boldsymbol{a}_n x^n$$

where the coefficients $\boldsymbol{a}_i$ are intervals. Future research could focus on extending the present interval FEA so that it can address uncertainties described by interval

functions.

6.2.2 Reliability assessment using the interval FEA

As discussed in Chapter 1, the probabilistic and the interval approaches are suitable for different types of uncertainties. Many practical problems, however, have to deal with interval uncertainty and probabilistic uncertainty at the same time (Penmetsa and Grandhi, 2002; Berleant et al., 2005). Thus the classic reliability analysis should be reformulated to accept interval information. Some approaches have been proposed to combine interval uncertainty and probabilistic uncertainty, such as the Dempster-Shafer theory of evidence (Dempster, 1967; Shafer, 1976), random set theory (Kendall, 1974), and the probability-bounds analysis (Berleant, 1993; Ferson and Ginzburg, 1996). The mathematical analysis of these uncertainty descriptions can be built up using a series of interval analyses. Future research could focus on combining these approaches with the interval FEA to perform reliability assessment. Such a work will broaden the objectivity of classic reliability analysis, and the interval uncertainty and probabilistic uncertainty can both be accommodated.

6.2.3 Consideration of discretization error

In addition to the uncertainties associated with parameters, another important source of error in FEA is the discretization error. This has not been addressed in the present study. Interval analysis has been used to compute rigorous bounds on the solution of ordinary and partial differential equations (Moore, 1979; Plum, 2001; Jackson and Nedialkov, 2002). Future work can explore interval analysis for its potential to rigorously bound the finite element discretization error.

REFERENCES

Akpan, U. O., Koko, T. S., Orisamolu, I. R., and Gallant, B. K. (2001a). "Fuzzy finite element analysis of smart structures." *Smart Mater. Struct.*, 10, 273–284.

Akpan, U. O., Koko, T. S., Orisamolu, I. R., and Gallant, B. K. (2001b). "Practical fuzzy finite element analysis of structures." *Finite Elem. Anal. Des.*, 38, 93–111.

Alefeld, G. and Herzberger, J. (1983). *Introduction to interval computations*. Academic Press, New York.

Ang, A. H.-S. and Tang, W. (1975). *Probability concepts in engineering planning and design, Vol.1-basic principes*. John Wiley.

Apostolatos, N. and Kulisch, U. (1968). "Grundzüge einer intervallrechtung für matrizen und einige anwwendungen." *Elektron. Rechenanlagen*, 10, 73–83. (in German).

b4m (1998). "b4m: a free interval arithmetic toolbox for matlab". http://www.ti3.tu-harburg.de/zemke/b4m/.

Bathe, K. (1996). *Finite element procedures*. Prentice-Hall, Upper Saddle River, NJ.

Ben-Haim, Y. (1994). "A non-probabilistic concept of reliability." *Struct. Saf.*, 14, 227–245.

Ben-Haim, Y. and Elishakoff, I. (1990). *Convex models of uncertainty in applied mechanics*. Elsevier Science, Amsterdam.

Berleant, D. (1993). "Automatically verified reasoning with both intervals and probability density functions." *Interval Computations*, (2), 48–70.

Berleant, D., Ferson, S., Kreinovich, V., and Lodwick, W. A. (2005). "Combining interval and probabilistic uncertainty: foundations, algorithms, challenges-an overview." *4th International Symposium on Imprecise Probabilities and Their Applications*, Pittsburgh, PA.

Bogle, D., Johnson, D., and Balendra, S. (2004). "Handling uncertainty in the development and design of chemical processes." *Proc. NSF workshop on reliable engineering computing*, R. L. Muhanna and R. L. Mullen, eds., Savannah, GA. http://www.gtsav.gatech.edu/rec/recworkshop/index.html.

Bojadziev, G. and Bojadziev, M. (1995). *Fuzzy sets, fuzzy logic, applications*. World Scientific Publishing Co. Pte. Ltd., Singapore.

Brouwer, L. E. J. (1912). "Uber abbildung von mannigfaltigkeiten." *Math. Ann.*, 71, 97–115.

Buonopane, S. G., Schafer, B. W., and Igusa, T. (2003). "Reliability implications of advanced analysis in design of steel frames." *Proc. ASSCCA'03*, Sydney, Australia.

Chen, L. and Rao, S. (1997). "Fuzzy finite element approach for the vibration analysis of imprecisely-defined systems." *Finite Elem. Anal. Des.*, 27, 69–83.

Chen, S. H. (1999). *Matrix perturbation theory in structural dynamics designs*. Science Press, Beijing, China.

Chen, S. H., Lian, H. D., and Yang, X. W. (2002). "Interval static displacement analysis for structures with interval parameters." *Int. J. Numer. Methods Engrg.*, 53, 393–407.

Chen, S. H. and Yang, X. W. (2000). "Interval finite element method for beam structures." *Finite Elem. Anal. Des.*, 34, 75–88.

Cook, R. D., Malkus, D. S., Plesha, M. E., and Witt, R. J. (2002). *Concepts and applications of finite element analysis*. John Wiley & Sons, 4 edition.

Corliss, G., Foley, C., and Kearfott, R. B. (2004). "Formulation for reliable analysis of structural frames." *Proc. NSF workshop on reliable engineering computing*, R. L. Muhanna and R. L. Mullen, eds., Savannah, GA. http://www.gtsav.gatech.edu/rec/recworkshop/index.html.

Corliss, G. F. (1990). "Industrial applications of interval techniques." *Computer Arithmetic and Self-Validating Numerical Methods*, C. Ullrich, ed., Notes and Reports in Mathematics in Science and Engineering, No. 7, Academic Press, New York, 91–113.

Corliss, G. F. and Kearfott, R. B. (1999). "Rigorous global search: Industrial applications." *Developments in reliable computing*, T. Csendes, ed. Kluwer Academic Publishers, 1–16.

Davies, R. (1991). "Newmat: a free matrix library in c++, version 10B". http://www.robertnz.net/nm_intro.htm.

Dempster, A. P. (1967). "Upper and lower probabilities induced by a multi-valued mapping." *Ann. Mat. Stat.*, 38, 325–339.

Dessombz, O., Thouverez, F., Laîné, J.-P., and Jézéquel, L. (2001). "Analysis of mechanical systems using interval computations applied to finite elements methods." *J. Sound. Vib.*, 238(5), 949–968.

Dongarra, J. J., Croz, J. D., Hammarling, S., and Hanson, R. J. (1988). "An extended set of fortran basic linear algebra subprograms." *ACM Trans. Math. Softw.*, 14, 1–17.

Elishakoff, I. (1995). "Essay on uncertainties in elastic and viscoelastic structures: from a. m. freudenthal's criticisms to modern convex modeling." *Comput. Struct.*, 56(6), 871–895.

Ferson, S. (1996). "What monte carlo methods cannot do." *Hum. Ecol. Risk Assess.*, 2, 990–1007.

Ferson, S. and Ginzburg, L. R. (1996). "Different methods are needed to propagate ignorance and variability." *Reliab. Engng. Syst. Saf.*, 54, 133–144.

Ferson, S. and Hajagos, J. G. (2004). "Arithmetic with uncertain numbers: rigorous and (often) best possible answers." *Reliab. Engng. Syst. Saf.*, 85, 135–152.

Ferson, S., Joslyn, C., Helton, J. C., Oberkampf, W. L., and Sentz, K. (2004). "Summary from the epistemic uncertainty workshop: consensus amid diversity." *Reliab. Engng. Syst. Saf.*, 85, 355–369.

Ferson, S., Kreinovich, V., Ginzburg, L., Myers, D. S., and Sentz, K. (2003). "Constructing probability boxes and Dempster-Shafer structures." *Report No. SAND2002-4015*, Sandia National Laboratories.

Fetz, T., Jäger, J., Köll, G., Lessmann, H., Oberguggenberger, M., and Stark, R. (1999). "Fuzzy models in geotechnical engineering and construction management." *Compu.-Aided Civ. Infrastruct. Engrg.*, 14, 93–106.

Freudenthal, A. M. (1972). "Introductory remarks." *Proc. Int. Conf. Structural Safety and Reliability*, A. M. Freudenthal, ed., Pergamon Press, Oxford. 5–6.

Gallagher, R. H. (1975). *Finite element analysis fundamentals*. Printice Hall, Englewood Cliffs, N.J.

Ganzerli, S. and Pantelides, C. P. (1999). "Load and resistance convex models for optimum design." *Struct. Optim.*, 17, 259–268.

Gay, D. M. (1982). "Solving interval linear equations." *SIAM J. Numer. Anal.*, 19(4), 858–870.

Gersem, H. D., Moens, D., desmet, W., and Vandepitte, D. (2004). "Interval and fuzzy finite element analysis of mechanical structures with uncertain parameters." *Proc. ISMA 2004, International Conference on Noise and Vibration Engineering*, Leuven, Belgium. 3009–3021.

Ghanem, R. G. and Spanos, P. D. (1991). *Stochastic finite elements: a spectral approach*. Springer-Verlag, New York.

GTSTRUDL (2002). *GSTRUDL User Guide*. Computer Aided Structural Engineering Center, Georgia Institute of Technology, Atlanta, GA.

Guan, Z. and Lu, J. P. (1998). *Numerical analysis*. Higher Education Press, Beijing, China.

Haldar, A. and Mahadevan, S. (2000). *Reliability assessment using stochastic finite element analysis*. John Wiley & Sons, Chichester.

Hall, J., Rubio, E., and Anderson, M. G. (2004). "Random sets of probability measures in slope hydrology and stability analysis." *J. Appl. Math. Mech.* in press.

Hansen, E. and Walster, G. W. (2003). *Global optimization using interval analysis.* Marcel Dekker, Inc., New York.

Hargreaves, G. I. (2002). "Interval analysis in matlab." *Report No. 416*, University of Manchester.

Hayter, A. J. (2002). *Probability and statistics for engineers and scientists.* Duxbury, 2 edition.

Helton, J. C. and Burmaster, D. E. (1996). "Guest editorial: treatment of aleatory and epistemic uncertainty in performance assessment for complex systems." *Reliab. Engng. Syst. Saf.*, 54, 91–94.

Hora, S. C. (1996). "Aleatory and epistemic uncertainty in probability elicitation with an example from hazardous waste management." *Reliab. Engng. Syst. Saf.*, 54, 217–223.

Jackson, K. R. and Nedialkov, N. S. (2002). "Some recent advances in validated methods for ivps for odes." *Appl. Numer. Math.*, 42, 269–284.

Jansson, C. (1991). "Interval linear system with symmetric matrices, skew-symmetric matrices, and dependencies in the right hand side." *Computing*, 46, 265–274.

Jasiński, M. and Pownuk, A. (2000). "Modelling of heat transfer in biological tissue by interval fem." *Compu. Assisted Mech. Engrg. Sci.*, 7(4), 699–705.

Jaulin, L., Kieffer, M., Didrit, O., and Walter, E. (2001). *Applied interval analysis.* Springer.

Joslyn, C. and Ferson, S. (2004). "Approximate representations of random intervals for hybrid uncertainty quantification." *4th Int. conf. on sensitivity analysis of model output.*

Kaufman, A. and Gupta, M. M. (1991). *Introduction to fuzzy arithmetic: theory and applications.* Van Nostrand Reinhohld, New York, N.Y.

Kearfott, R. B. (1995). "A fortran 90 environment for research and prototyping of enclosure algorithms for nonlinear equations and global optimization." *ACM Trans. Math. Softw.*, 21(1), 63–78.

Kearfott, R. B. (1996). "Interval computations: introduction, uses, and resources." *Euromath. Bull.*, 2(1), 95–112.

Kearfott, R. B., Dawande, M., Du, K., and Hu, C. (1994). "Algorithm 737: Intlib: a portable fortran 77 interval standard-function library." *ACM Trans. Math. Softw.*, 20(4), 447–459.

Keese, A. (2003). "A review of recent developements in the numerical solution of stochastic partial differential equations (stochastic finite elements)." *Report No. Informatikbericht 2003-6*, Technische Universitat Braunschweig, Braunschweig.

Kendall, D. G. (1974). "Foundations of a theory of random sets." *Stochastic Geometry*, E. Harding and D. Kendall, eds., New York. Wiley, 322–376.

Klatte, R., Kulisch, U., Lawo, C., Rauch, M., and Wiethoff, A. (1993). *C-XSC- a C++ class library for scientific computing*. Springer-Verlag, Berlin.

Klier, G. and Folger, T. (1998). *Fuzzy sets, uncertainty, and information*. Prentice Hall, Englewood Cliffs, NJ, 1 edition.

Knüppel, O. (1994a). "BIAS-basic interval arithmetic subroutines: documentation". http://www.ti3.tu-harburg.de/Software/PROFIL/Profil.texinfo_toc.html.

Knüppel, O. (1994b). "Profil/bias-a fast interval library." *Computing*, 53, 277–288.

Koyluoglu, H. U. and Elishakoff, I. (1998). "A comparison of stochastic and interval finite elements applied to shear frames with uncertain stiffness properties." *Comput. Struct.*, 67, 91–98.

Koyluoglu, U., Cakmak, S., Ahmet, N., and Soren, R. K. (1995). "Interval algebra to deal with pattern loading and structural uncertainty." *J. Engrg. Mech.*, 121(11), 1149–1157.

Krämer, W. and Geulig, I. (2001). "Interval calculus in maple: the extension intpakx to the package intpak of the share-library. http://www.math.uni-wuppertal.de/wrswt/software_en.html.

Kreinovich, V., Beck, J., Ferregut, C., Sanchez, A., Keller, G., Averill, M., and Starks, S. (2004). "Monte-carlo-type techniques for processing interval uncertainty, and their engineering applications." *Proc. NSF workshop on reliable engineering computing*, R. L. Muhanna and R. L. Mullen, eds., Savannah, GA. http://www.gtsav.gatech.edu/rec/recworkshop/index.html.

Kulpa, Z., Pownuk, A., and Skalna, I. (1998). "Analysis of linear mechanical structures with uncertainties by means of interval methods." *Compu. Assisted Mech. Engrg. Sci.*, 5(4), 443–477.

Lanford, O. E. (1984). "Computer-assisted proofs in analysis." *Physica. A.*, 124, 465–470.

Matthews, J., Broadwater, R., and Long, L. (1990). "The application of interval mathematics to utility economic analysis." *IEEE Trans. Power Syst.*, 5(1), 177–181.

Matthies, H., Brenner, C., Bucher, C., and Soares, C. G. (1997). "Uncertainties in probabilistic numerical analysis of structures and solids - stochastic finite elements." *Struct. Safety*, 19(3), 283–336.

Mayer, O. (1970). "Algebraische und metrische strukturen in der intervallrechung und eingine anwendungen." *Computing*, 5, 144–162. (in German).

McWilliam, S. (2000). "Anti-optimisation of uncertain structures using interval analysis." *Comput. Struct.*, 79, 421–430.

Melchers, R. E. (1999). *Structural reliability analysis and prediction*. John Wiley & Sons, West Sussex, England, 2 edition.

Modares, M., Mullen, R. L., Muhanna, R. L., and Zhang, H. (2004). "Buckling analysis of structures with uncertain properties and loads using an interval finite element method." *Proc. NSF workshop on reliable engineering computing*, R. L. Muhanna and R. L. Mullen, eds., Savannah, GA. http://www.gtsav.gatech.edu/rec/recworkshop/index.html.

Moens, D. and Vandepitte, D. (2002). "Fuzzy finite element method for frequency response function analysis of uncertain structures." *AIAA J.*, 40(1), 126–136.

Möller, B., Beer, M., Graf, W., and Hoffmann, A. (1999). "Possibility theory based safety assessment." *Compu.-Aided Civ. Infrastruct. Engrg.*, 14, 81–91.

Möller, B., Graf, W., and Beer, M. (2000). "Fuzzy structural analysis using level-optimization." *Comput. Mech.*, 26(6), 547–565.

Moore, R. E. (1966). *Interval Analysis*. Prentice-Hall, Inc., Englewood Cliffs, N. J.

Moore, R. E. (1979). *Methods and applications of interval analysis*. SIAM, Philadelphia.

Muhanna, R. L. and Mullen, R. L. (1995). "Development of interval based methods for fuzziness in continuum mechanics." *Proc. ISUMA-NAFIPS'95*. 23–45.

Muhanna, R. L. and Mullen, R. L. (1999). "Formulation of fuzzy finite element methods for mechanics problems." *Compu.-Aided Civ. Infrastruct. Engrg.*, 14, 107–117.

Muhanna, R. L. and Mullen, R. L. (2001). "Uncertainty in mechanics problems-interval-based approach." *J. Engrg. Mech.*, 127(6), 557–566.

Muhanna, R. L. and Mullen, R. L. (2004). "Interval methods for reliable computing." *Engineering design reliability handbook*, CRC Press LLC, chapter 12.

Muhanna, R. L. and Mullen, R. L., eds. (2004). *Proc. NSF workshop on reliable engineering computing*. Savannah, GA, USA.

Mullen, R. L. and Muhanna, R. L. (1996). "Structural analysis with fuzzy-based load uncertainty." *Proc. 7th ASCE EMD/STD Joint Spec. Conf. on Probabilistic Mech. and Struct. Reliability*, Mass. 310–313.

Mullen, R. L. and Muhanna, R. L. (1999). "Bounds of structural response for all possible loadings." *J. Struct. Engrg., ASCE*, 125(1), 98–106.

Nataraj, P. S. V. and Tharewal, S. (2004). "A computational approach to existence verification and construction of robust qft controllers." *Proc. NSF workshop on reliable engineering computing*, R. L. Muhanna and R. L. Mullen, eds., Savannah, GA. http://www.gtsav.gatech.edu/rec/recworkshop/index.html.

Neumaier, A. (1987). "Overestimation in linear interval equations." *SIAM J. Numer. Anal.*, 24(1), 207–214.

Neumaier, A. (1990). *Interval methods for systems of equations*. Cambridge University Press.

Neumaier, A. (2001). *Introduction to numerical analysis*. Cambridge University Press, Cambridge, United Kingdom.

Neumaier, A. and Shen, Z. (1990). "The krawczyk operator and kantorovich's theorem." *J. Math. Anal. Appl.*, 149(2), 437–443.

Oberkampf, W. L., DeLand, S. M., Rutherford, B. M., Diegert, K. V., and Alvin, K. F. (2002). "Error and uncertainty in modeling and simulation." *Reliab. Engng. Syst. Saf.*, 75, 335–357.

Oberkampf, W. L. and Helton, J. C. (2005). "Evidence theory for engineering applications." *Engineering design reliability handbook*, E. Nikolaidis, D. M. Ghiocel, and S. Singhal, eds. CRC Press.

Oettli, W. (1965). "On the solution set of a linear system with inaccurate coefficients." *J. SIAM Numer. Anal.*, 2(1), 115–118.

Pantelides, C. P. and Ganzerli, S. (2001). "Comparison of fuzzy set and convex model theories in structural design." *Mech. Systems Signal Process.*, 15(3), 499–511.

Paté-Cornell, M. E. (1996). "Uncertainties in risk analysis: six levels of treatment." *Reliab. Engng. Syst. Saf.*, 54, 95–111.

Penmetsa, R. C. and Grandhi, R. V. (2002). "Efficient estimation of structural reliability for problems with uncertain intervals." *Comput. Struct.*, 80, 1103–1112.

Pereira, S. C., Mello, U. T., Ebecken, N., and Muhanna, R. L. (2004). "uncertainty in thermal basin modeling: an interval finite element approach." *Proc. NSF workshop on reliable engineering computing*, R. L. Muhanna and R. L. Mullen, eds., Savannah, GA. http://www.gtsav.gatech.edu/rec/recworkshop/index.html.

Peschl, G. and Schweiger, H. (2003). "Reliability analysis in geotechnics with finite elements-comparison of probabilistic, stochastic and fuzzy set methods." *Proc. ISIPTA'03*, Lugano, Switzerland.

Plum, M. (2001). "Computer-assisted enclosure methods for elliptic differential equations." *Linear Algebra Appl.*, 324, 147–187.

Popova, E. D. (2004). "Generalizing the parametric fixed-point iteration." *Proc. Appl. Math. Mech.*, 4(1), 680–681.

Popova, E. D., Datcheva, M., Iankov, R., and Schanz, T. (2003). "Mechanical models with interval parameters." *Proc. 16th International Conference on the Applications of Computer Science and Mathematics in Architecture and Civil Engineering*, K. Guerlebeck, L. Hempel, and C. Koenke, eds.

Pownuk, A. (2004a). "Calculation of the extreme values of displacements in truss structures with interval parameters. http://s212.bud.polsl.gliwice.pl/ andrzej/php/apdl2interval/apdl2interval_ init.php.

Pownuk, A. (2004b). "Efficient method of solution of large scale engineering problems with interval parameters." *Proc. NSF workshop on reliable engineering computing*, R. L. Muhanna and R. L. Mullen, eds., Savannah, GA. http://www.gtsav.gatech.edu/rec/recworkshop/index.html.

Press, W. H., Teukolsky, S. A., Vetterling, W. T., and Flannery, B. P. (1992). *Numerical recipes in C*. Cambridge University Press, Cambridge, second edition. The art of scientific computing.

Qiu, Z. and Elishakoff, I. (1998). "Antioptimization of structures with large uncertain-but-non-rand parameters via interval analysis." *Compt. Meth. Appl. Mech. Engng.*, 152, 361–372.

Rao, S. and Liu, Q. (2004). "Fuzzy approach to the mechanics of fiber-reinforced composite materials." *AIAA J.*, 42(1), 159–167.

Rao, S. S. and Berke, L. (1997). "Analysis of uncertain structural systems using interval analysis." *AIAA J.*, 35(4), 727–735.

Rao, S. S. and Chen, L. (1998). "Numerical solution of fuzzy linear equations in engineering analysis." *Int. J. Numer. Meth. Engng.*, 43, 391–408.

Reddy, J. N. (1993). *An introduction to the finite element method*. McGraw-Hill, 2 edition.

Rohn, J. (1995). "Linear interval equations: computing sufficiently accurate enclosures is np-hard." *Report No. 621*, Institute of computer science, Academy of Sciences of the Czech Republic.

Rohn, J. and Rex, G. (1998). "Enclosing solutions of linear equations." *SIAM J. Numer. Anal.*, 35(2), 524–539.

Ross, T. (1995). *Fuzzy logic with engineering applications*. McGraw-Hill, New York, N.Y.

Rump, S. M. (1983). "Solving algebraic problems with high accuracy." *A new approach to scientific computation*, U. Kulisch and W. Miranker, eds., Academic Press, New York.

Rump, S. M. (1990). "Rigorous sensitivity analysis for systems of linear and nonlinear equations." *Math. Comp.*, 54(190), 721–736.

Rump, S. M. (1992). "On the solution of interval linear systems." *Computing*, 47, 337–353.

Rump, S. M. (1994). "Verification methods for dense and sparse systems of equations." *Topics in validated computations*, J. Herzberger, ed., Elsevier Science B. V., 63–135.

Rump, S. M. (2001). "Self-validating methods." *Linear Algebra Appl.*, 324, 3–13.

Rump, S. M. (2002). "INTLAB-interval laboratory, a matlab toolbox for verified computations, version 3.1". http://www.ti3.tu-harburg.de/rump/intlab/index.html.

Saxena, V. (2003). "Interval finite element analysis for load pattern & load combination". Master's thesis, Georgia Institute of Technology, Atlanta, GA.

Schuëller, G. (1997). "A state-of-the-art report on computational stochastic mechanics." *Probabilistic Engineering Mechanics*, 12(4), 197–321.

Sentz, K. and Ferson, S. (2002). "Combination of evidence in Dempster-Shafer theory." *Report No. SAND2002-0835*, Sandia National Laboratories.

Shafer, G. (1976). *A mathematical theory of evidence*. Princeton University Press, Princeton,N.J.

Sun microsystems (2002). *Interval arithmetic in high performance technical computing*. Sun microsystems. (A White Paper).

Tonon, F. (2004). "On the use of random set theory to bracket the results of monte carlo simulations." *Reliable Computing*, 10, 107–137.

Tonon, F., Bernardini, A., and Mammino, A. (2000). "Reliability analysis of rock mass response by means of random set theory." *Reliab. Engng. Syst. Saf.*, 70, 263–282.

Ugural, A. C. and Fenster, S. (1995). *Advanced strength and applied elasticity*. Prentice Hall, 3 edition.

Walley, P. (1991). *Statistical reasoning with imprecise probabilities*. Chapman and Hall, London.

Wang, Y. (2004). "Solving interval constraints in computer-aided design." *Proc. NSF workshop on reliable engineering computing*, R. L. Muhanna and R. L. Mullen, eds., Savannah, GA. http://www.gtsav.gatech.edu/rec/recworkshop/index.html.

Wilkinson, J. H. (1971). "Modern error analysis." *SIAM Rev.*, 13(4), 548–568.

Yen, J. (1999). "Fuzzy logic - a modern perspective." *IEEE Trans. Knowl. Data Eng*, 11(1), 153–165.

Yen, J., Langari, R., and Zadeh, L. A. (1995). *Industrial applications of fuzzy logic and intelligent systems*. IEEE Press, Piscataway, New Jersey.

Zadeh, L. A. (1965). "Fuzzy sets." *Information and Control*, 8, 338–353.

Zemke, J. (1998). "b4m-a free interval arithmetic toolbox for matlab based on BIAS, version 1.02.004". http://www.ti3.tu-harburg.de/zemke/b4m.

Zhang, H. and Muhanna, R. L. (2004). "Finite element analysis for structures with interval parameters." *Proc. 9th ASCE Joint Spec. Conf. on Probabilistic Mech. and Struct. Reliability*, Albuquerque, New Mexico, U.S.A.

Zienkiewicz, O. C. (1977). *The finite element method*. McGraw-Hill, 3 edition.

VITA

Hao Zhang was born in Changzhou, China on November 27, 1975. He received his Bachelor of Science degree and Master of Science degree in Civil Engineering in 1998 and 2001, respectively, from Department of Hydraulic and Hydropower Engineering of Tsinghua University, Beijing, China. He began his Ph.D. studies at the Georgia Institute of Technology in the fall of 2001. During his doctoral studies, he worked in the Center of Reliable Engineering Computing (CREC) as a Research Assistant under the guidance of Dr. Rafi L. Muhanna. He also worked as a Teaching Assistant for School of Civil and Environmental Engineering.